



The
University
Of
Sheffield.

Upper extremity electromyography signal feature extraction and classification

A thesis submitted to The University Of Sheffield
for the degree of Doctor of Philosophy

by

Wan Mohd Bukhari Bin Wan Daud

Supervisors

Prof. M. O. Tokhi & Prof. M. Mahfouf

Department of Automatic Control and Systems Engineering

The University of Sheffield

Mappin Street,
Sheffield, S1 3JD
United Kingdom

August 2019

Abstract

The human upper forearm (UFA) consists of several muscles. These muscles are used by researchers to identify the hand movements based on their acquired EMG signal. The precision of EMG signal features and parameters proportionally vary with muscle signal, features and fatigue. The major challenge for the study is to identify fundamental manifestation in the EMG signal in muscle localisation in the human UFA regions, so that EMG based control performance is improved. This can be achieved through improvement of data collection, features extraction and classification. Hence, a fundamental study is performed by investigating the signals acquired from the human UFA to discover muscle characteristics and to establish the inter-relationship between the forearm and upper arm muscles. The principal objective of this study is to investigate the research challenges stated earlier via non-invasive EMG acquisition. Therefore, experimental protocols for data collection are designed to achieve the study objectives. Using new features extracted from muscle inter-relationship, feature reductions and specific classifier, a linear discriminant analysis (LDA) is trained to detect possible errors in classification decisions. Non-stationary conditions in real life applications for normally limbed human are taken into account in the data collection strategy, such as different levels of maximum voluntary contraction (MVC) so that the classification is robust and accurate estimations are achieved. The proposed study contributes towards the enhancement of data collection strategy, extraction of best features and parameters, and optimal classification accuracy for the control strategy. Furthermore, it is established that the relationship between human UFA muscles is contributed from the movement with an accuracy of $>90\%$. This provides an additional insight into the inter-relationship between both muscle regions (forearm and upper arm), which is unique in this study.

Acknowledgement

All praise be to Allah, the Most Merciful and Beneficent. There is no God but Allah, and Prophet Muhammad (Peace be upon him) is the Messenger of Allah. With His wills and gracious, this thesis is completed.

My gracious thanks to the soul who have helped and encouraged myself for this study. The soul that have aided myself from the beginning of the study to the end. My appreciation to supervisor Prof. Dr Mohamed Osman Tokhi and second supervisor Prof. Dr Mahdi Mahfouf, for the aid and support during the study. I want to express personal thankfulness to Norafizah Abas, Abdullah Khaled Alshatti and all group members for their generosity and guidance through the thrilling stages of my doctoral studies.

Finally, I want to express my heartfelt honour to my family, particularly my mothers, Hjh Sabariah Bt Mat Taib, and my lovely family for their affection, help and understanding in those years far away from home. Finally, I yearn to thank my lovely wife Nurul Rusydiah, for her kindness, respect and trust. Moreover, last but not least, my precious little boys Wan Muhammad Fayyadh, Wan Abdul Fattah, and Wan Umar Fahd who forever with me all the time.

Contents

Abstract	i
Acknowledgement	ii
Contents	vi
List of figures	xii
List of tables	xv
Acronyms	xvi
1 Introduction	1
1.1 Background of EMG	2
1.2 Motivation of the study and its significance	3
1.3 Hypothesis	4
1.4 Research questions	5
1.5 Study objectives	6
1.6 Scope of the study	7
1.7 Contributions	8
1.8 Thesis structure	9
2 Literature review	12
2.1 Introduction	12
2.2 The model of EMG signal	12
2.2.1 EMG characteristics	18
2.2.2 Muscle fatigue manifestation	19
2.2.3 Human upper forearm	21
2.3 Review of surface EMG assessment of the forearm and upper arm	26
2.4 Relationship between surface EMG of forearm and upper arm muscles, force, %MVC and wrist angle	26
2.5 Surface EMG features extraction and classification	30

2.5.1	Features extraction	30
2.5.2	Classification	33
2.6	Summary	34
3	Research methodology	35
3.1	Introduction	35
3.2	Surface EMG under European recommendations	37
3.3	Development of new EMG data acquisition protocol	40
3.4	Introduction to data collection	48
3.4.1	Pre-task protocols	49
3.4.2	Muscle Selection Protocol	52
3.5	Experiment 1: Extraction of EMG signals on human upper forearm muscles contributing to the finger(s) pinching at various wrist movements	52
3.5.1	Experimental protocols	53
3.6	Experiment 2: Extraction of EMG signals on human upper forearm muscles contributing to the hand grasping, wrist movements and curl exercise	54
3.6.1	Experimental protocols	54
3.7	Experiment 3: Extraction of EMG signals on human upper forearm muscles contributing to pronation and supination of hand with curl exercise	55
3.7.1	Experimental protocols	55
3.8	Experiment 4: Extraction of EMG signals on human upper forearm muscles contributing to curl exercise	56
3.8.1	Experimental protocols	56
3.9	Summary	57
4	Pre-processing, feature and classification based methods	58
4.1	Introduction	58
4.2	EMG pre-processing	58
4.2.1	EMG signal conditioning	59
4.3	Feature extraction	61
4.3.1	Time domain features	61
4.3.2	Frequency domain features	66
4.4	Statistical analysis	69
4.4.1	Descriptive statistic	69
4.4.2	Correlation coefficients	69
4.5	Time-frequency domain	70
4.5.1	Fourier transform	70
4.5.2	Wavelet transform	72
4.6	Feature dimensionality reduction	75

4.6.1	Principal component analysis	76
4.6.2	Uncorrelated linear discriminant analysis	77
4.7	Pattern classification strategy	79
4.7.1	Artificial neural network	81
4.7.2	Linear discriminant analysis	82
4.8	Classification performance evaluation	84
4.8.1	Classification accuracy	84
4.8.2	Classification plot	85
4.9	Summary	86
5	Assessment strategy of human upper forearm	87
5.1	Introduction	87
5.2	The assessment strategy for subject muscles and EMG site selection	88
5.2.1	Data acquisition system and protocol	89
5.2.2	Electrode placement and muscle channels	90
5.2.3	Assessing muscle fatigue	90
5.2.4	Muscle selection	94
5.3	Feature performance analysis	97
5.3.1	Data collection	99
5.3.2	Pre-processing	101
5.3.3	Feature Extraction	108
5.3.4	Feature reduction technique	109
5.3.5	Descriptive statistical strategy	117
5.4	Summary	121
6	Fuzzy entropy mutual information based on wavelet EMG fusion	123
6.1	Introduction	123
6.2	Data fusion techniques	124
6.3	Fusion strategy	125
6.4	Wavelet analysis	126
6.4.1	Continuous wavelet transform	126
6.5	Mutual information based on wavelet fusion	129
6.6	Feature extraction method	133
6.7	Results	134
6.7.1	Mother wavelet determination	135
6.8	Correlation of EMG fusion with wavelet	143
6.9	Fuzzy mutual information	150
6.10	Summary	155

7 Conclusion and future works 156
7.1 Discussions and conclusions 156
7.2 Contributions 158
7.3 Limitations 159
7.4 Suggestions for future works 160
7.5 Conclusions 160

Appendices 171

A Ethical Approval 172

B Tables 182

List of Figures

2.1	MUAPs developed from individual muscle fibre action potential composition Kamen and Caldwell (1996)	14
2.2	The raw EMG signals and its power spectrum for references. This details can be found in Appendix B	14
2.3	Example of power spectrum recorded from the fresh muscle (solid line) and fatigue (broken line) Petrofsky and Lind (1980)	22
2.4	The human upper forearm regions and muscles; A) Upper arm and forearm, B) Upper arm muscles; Biceps Brachii (BB), Triceps Brachii (TB), Coracobrachialis (CB), and Brachialis(Br), C) Forearm muscles; Pronator Teres (PT), Flexor Carpi Radialis (FCR), Flexor carpi Ulnaris (FCU), Palmaris Longus (PL), Flexor Digitorum Superficialis (FDS), Flexor Pollicis Longus (FPL), Flexor Digitorum Profundus (FDP), and Pronator Quadratus (PQ).	23
2.5	Cross section of forearm showing the muscles available for the study . . .	23
3.1	Block diagram of the research methodology proposed in this study	36
3.2	Illustrations of electrodes setup and its configurations as recommended by SENIAM used in this study. The details of these muscle selection can be found in Appendix A.	38
3.3	Subjects at their preferable positioning before EMG data collection begin. Experimental protocol revealing the wrist inserted by pillow aid that stopped the subject from prono-supinating the wrist. Each volunteered subject, following a period of familiarisation with the protocol, completed 20 trials of each hand grasp task. Movements were auditory paced every 5s. Each hand movement collected in a different run. At least 5 min of rest was provided between each series, and it has been prolonged upon the subject's request.	40
3.4	The overall acquisition system used in this study. The wires and cables are not in the connected as this illustration is only for clarification	41
3.5	The LabQuest Mini interface contains five (5) input sensors with three analog ports (CH1–CH3), two digital ports (DIG1 and DIG 2), a mini-USB connection, and a power adapter port (no main electrical power will be used in this study)	42
3.6	The Logger Lite software graphical user interface (GUI). This GUI will guide the subject during the data collection and makes it easy to attain a certain amount of force needed to be exerted during the session.	43
3.7	The EMG sensor and cable that has been used in this study.	46

3.8	The hand dynamometer that has been used to measure force exertion from the subject. This sensor uses the analogue port as its input. Unique design for a separate task can be seen in the figure, as highlighted in the red circles. The small circle represents the force sensor location for the finger pinch and the bigger circle designed for hand grip force.	47
3.9	Example of electrodes placement for the forearm and upper arm muscles as recommended by SENIAM (Merletti (2000); Merletti and Hermens (2000)); (A, B, D and F) Electrode placement for the selected forearm and upper arm muscles involved in pronation and supination with curl exercises, and (C and E) electrode placement for the selected forearm muscles involved in finger(s) pinching and hand grasping. The 11 muscles involved in this study are: FDS, FCR, FCU, FPL, PT, PQ, ECRL, EDC, ECU, PT, and PQ.	50
3.10	Experimental setup for EMG data acquisition system developed by Vernier	51
3.11	Sketch for a human upper forearm muscles under consideration for the study proposed; A) Anterior compartment and B) Posterior compartment.	51
3.12	Finger pinches muscle contractions of forearm with four groups of movements: (A) index finger pinch, (B) middle finger pinch, (C) ring finger pinch and (D) little finger pinch.	53
3.13	: Hand gripping positions for hand dynamometer at various wrist angle positions: (A) at 120° (B) at 90° (C) at 60°, and D) curl exercises.	54
4.1	Examples of segmentation strategy for EMG data in the preprocessing condition. The blue arrow shows the disjointed and adjacent segmentation while red arrow for the overlapped segmentation. L = window length, τ = processing time and C = classification decision (Asghari Oskoei and Hu (2007); Englehart and Hudgins (2003))	60
4.2	The Fourier transform (FT) is the general practice in the measurement of time series signal. The fundamental practice of FT is changing domain of operation in the TD into the FD. (Adapted from Matlab software application)	70
4.3	Top:Fourier series of a signal in TD (sine wave); Bottom: signal in FD. . .	72
4.4	WT approaches are contrary to the STFT as it imposed a timely adjustable window (Daubechies (1990)). WT technique produce essential frequency localisation properties in both TD and FD.	74
4.5	The general approach of Wavelet transform process.	74
4.6	Principal component analysis for feature reduction problem strategy are illustrated. The steps shows how the new dataset projected from the PCA computation that will be used in the classification.	77
4.7	Uncorrelated linear discriminant analysis (ULDA) and their transformation steps for feature reduction problems. The transformation process has to follow the condition sets to assure the non singularity of Within-class (S_w) scatter matrices	78
4.8	The basic architure of ANN with the generations from different layers such as input layer, two hidden layers, and the output layer. Activation functions of the hidden layers and the output layer were chosen as tansig and purelin separately.	81

5.1	Block diagram illustrated the overall approaches in achieving the proposed assessment and subject muscle performance towards proper EMG site selection	89
5.2	Raw EMG signal of handgrip at 90 <i>deg</i> force with muscle fatigue occurrence after 80% MVC.	91
5.3	Comparison of handgrip EMG signal power frequency spectrum with (80% MVC) and without fatigue (20% MVC). The zoomed box (green) shows that the amplitudes is shrinked towards lower frequencies when fatigue occurred. The estimated power for muscle with fatigue are higher than the estimated signal without fatigue.	91
5.4	Variations of power frequency spectrum produced at different MVCs. These are also highlighted using zoomed version to give clear pictures on the muscles and their power performances.	92
5.5	The changes of the average value of frequency performance between three properties selected; median frequency has shown a characteristic of fatigue index, while peak and mean frequencies exposed the real features for the muscle performance selections. These indications give new insight in assessing the muscle performance and fatigue phenomenon.	93
5.6	Analysis comparison for the muscle selection strategy based on average peak power and their mean frequency. These characteristic will be the ultimate tools in this study for the muscle selection. Muscle will be chosen based on their peak power and their suitabilities according to SENIAM.	95
5.7	The illustration model of basic EMG signal propagations between two neighbourhood deep muscles, X and Y. The signals travelled all the way through the deep muscle layers regardless of their distances, through fat and skin before reaching the detection sites (E1 to E4). Each detection sites will have their own characteristics of EMG signal.	98
5.8	The average value of maximum voluntary contraction for all subjects. This show the variation of force produced between each hand movement at varying contraction level. Hand grip force dominated the average value as compared with finger pinches. Classification accuracy were most affected by these variations characteristic.	100
5.9	i) Example of disposable electrode placement on the paired forearm muscles, FDS and FCR: seven classes of hand movement studied in this experiment, three for handgrip force movement (a, b, c) and four for finger pinch movement (A, B, C, D)	101
5.10	EMG signal with its amplitudes and forces versus time. This signal was separated by at least 5s rest for each movement. EMG data were collected at sampling frequency of 2000 Hz.	102
5.11	Example of raw EMG signals for six types of muscles for FP1 movement. This signal was taken from one of the subjects at their best fresh muscle which is 20 %MVC for 5 consecutive seconds.	102
5.12	Examples of raw EMG signals at 20% MVC for finger pinches after pre-processed by eliminating the rest state between each force movements. There are four classes of hand movements involved with the fingers in this study.	104

5.13	Examples of frequency spectrum of EMG signals for finger pinches with respect to Figure 5.12. The frequency shows different characteristic within each finger pinches. This as shown in zoomed section of each frequency spectrum.	105
5.14	Examples of raw EMG signals at 20% MVC for hand grip after preprocessed by eliminating the rest state between each force movements. There are three classes of hand movements involved with the fingers in this study.	106
5.15	Examples of frequency spectrum of EMG signals for hand grip force with respect to Figure 5.14. The frequency shows different characteristic within each hand grip movement. This as shown in zoomed section of each frequency spectrum.	107
5.16	Graphical illustration showing TD features and their class of separabilities between two adjacent flexor muscles FCR and FDS concerning the PCA and ULDA. PCA not successful in separating the movement class. This creates new insight into how well PCA adapted to the variations of the feature for different class movements, especially as proposed in this study.	112
5.17	Graphical illustration showing TD features and their class of separabilities between two adjacent extensor muscles ECRL and EDC with respect to the PCA and ULDA. Although PCA seems to have good class separability, ULDA proves to be more efficient where all the class movements are compact and within their group boundary. This will results in better classification with ULDA.	113
5.18	Graphical results illustrate FD features and their class of separabilities between two adjacent flexor muscles FCR and FDS with respect to the PCA and ULDA. PCA was unable to separate the movement classes in a good way as all classes were undetermined within their group. This creates unstable classification and might be related to the disability of PCA to reduce the redundancy problems in the FD features.	114
5.19	Graphical illustration showing FD features and their class of separabilities between two adjacent extensor muscles ECRL and EDC with respect to the PCA and ULDA. ULDA with FD features performed very well as compared to PCA for both muscles (refer Figure 5.19b and 5.19d).	115
5.20	Example of classification sequence for FD features of ECRL muscle. The classification time plot is highly successful presenting the actual and estimated class of hand movement with 2.6114% error.	115
5.21	The average classification accuracies for all the studied muscles using both the proposed PCA and ULDA reduction techniques with various FN. The adjacent muscles performed similarly in their accuracy for both categories. However, ULDA outperformed the PCA by achieving smaller FN of reduction components, FN=7 to made an accuracy >95%.	116
5.22	Scatter plots of 9 TD features for FP1 at various percentages of MVC. The plots was statistically measured their Pearson's R linear correlation coefficient at $p < 0.05$ confident level.	119
5.23	Example of confusion matrix Pearson's R correlation coefficient of 9 TD features, at FP1 for various percentages of MVC. Results averaged from all subject involved in this study. The highest concentration red box shows the most positive linear correlation $r = 0.996$. The acceptable range was set at $r > 0.95$	120

6.1	The basic fusion strategy introduced for this study.	129
6.2	The eight (8) mother wavelets used in this topic.	136
6.3	(a)Examples of the FP1 raw signals, converted into wavelet scalogram with respect to the Gaussian wavelet; (b) correspondence table of scales and frequencies associated to the analyse wavelet.	137
6.4	The scalogram representation for the FP1 hand movement using Gaussian wavelet at level 4 (gaus4). These shows the variations of coefficient amplitudes at different time and scale for different muscles, even at the same movement.	138
6.5	The scalogram representation for the FP1 hand movement using Coiflet at level 4 (coif4). These shows the variations of coefficient amplitudes at different time and scale for different muscles, even at the same movement.	140
6.6	Figure (a) shown here to indicates the best correlation between two muscles signal (FDS and BB) for FP1, it is shown that correlation tends to develop over all scales, but it is not quite high until it reaches >500 scales; (b) shown that, these two muscles are sharing the same frequency component which is really good, and (c) is used to understand the phase lag between the max correlation coefficient of these two signals. From there, we could see that they were having a good correlation at scales from 565 to 700. This is a good indicator for us to see whether these signals are out of phase or can be shifted in phase relative to one another.	144
6.7	Another examples for FP1 task using the proposed wavelet cross correlation between two muscles, showing certain levels of association between the two muscles at different region of human upper arm. Warmer colouration shows the scales which correlation is manifested by each pair of muscles tested in this study.	146
6.8	Examples of two subjects data for the correlation coefficients between their respective paired muscles. This approach was done for all the subjects to identified all the correlation coefficients gathered for the study.The variation of maximum correlation coefficients at their own patterns are revealed.	147
6.9	The assessment strategy for the muscle chosen used in this study. The highlighted muscles are related to the muscles within the two regions of human upper forearm. This technique will generate a new insight of getting the useful muscles to be use in various application both for normal and amputated people.	150
6.10	The average maximum correlation for the hand movement task as described in (a) and (b).	151
6.11	The average classification rate for each subject involved in this study with respect to diffrent feature reduction (PCA and ULDA) for three different domains; (a) time domain, (b) frequency domain and (c) time frequency domain-FEFC.	153
6.12	Comparison of TD, FD, and TFD performances based on the bar plot with normal distribution measures.	154
A.1	Official approval letter from the Ethical Review Committee The University Of Sheffield.	173
A.2	Additional researcher added on the approval letter	174
A.3	Letter of Consent	175

A.4	Participant information sheet page 1-amended version in 2018 due to the ethical policy changes	176
A.5	Participant information sheet page 2-amended version in 2018 due to the ethical policy changes	177
A.6	Participant information sheet page 3-amended version in 2018 due to the ethical policy changes	178
A.7	Participant information sheet page 4-amended version in 2018 due to the ethical policy changes	179
A.8	Participant information sheet page 5-amended version in 2018 due to the ethical policy changes	180
A.9	Participant information sheet page 6-amended version in 2018 due to the ethical policy changes	181
B.1	Average power for each muscles.	182
B.2	(a)Bar, and (b) box plot; comparisons study for the muscle average power performances.	183

List of Tables

2.1	Upper arm muscles, attachments and main actions	24
2.2	Forearm muscles, attachments, and main actions	25
2.3	Previous study based on human upper arm isometric contraction	27
2.4	Previous study based on human upper arm using both isometric and isotonic contraction	28
2.5	Previous study based on human upper arm isotonic contraction	29
2.6	Previous study based on human upper forearm muscle contraction and analysis of study	31
2.7	The preview of analysis domain of EMG signals	33
3.1	Summary of the recommendations proposed by SENIAM for most of the study involving the EMG signal. This recommendations recognised as a standard for many researchers in their reporting or analysis.	39
3.2	Data acquisition system and accessories or tools used in this study.	41
3.3	The technical specifications for LabQuest mini data acquisition system used in this study.	43
3.4	The subject preferences for the study.	44
3.5	Subjects configurations and their specific average 100 %MVC profiles listed for references. Most of the subject shown high variations in the force produced when they were asked for full exertion of muscle contraction.	44
3.6	The example of a subject MVC's and proportional value in force exertion	45
3.7	EKG sensor and cable that has been used in this study.	46
3.8	Hand dynamometer specifications used in this study. The maximum force this device can handle is up to 850 N. Force exceeded the maximum value may break the sensor.	47
5.1	The properties of EMG power frequency spectrum; median, peak, and mean frequencies calculated for all subjects. The average values for each property with their respective muscles was shown to justify the muscles chosen. The statistical analysis demonstrated significant differences between all the three power frequency properties at different muscles, $p < 0.05$ was observed.	96
5.2	Six time domain (TD) features; root mean square (<i>RMS</i>), integrated absolute value (<i>IAV</i>), zero crossing (<i>ZC</i>), waveform length (<i>WL</i>), slope sign change (<i>SSC</i>), auto regression 6th order (<i>AR6</i>), and six (6) frequency domain (FD) features; root square zero order moment (m_0), root square second (m_2) and fourth order moments (m_4), sparseness (<i>S</i>), irregularity factor (<i>IF</i>), and lastly waveform length ratio (<i>WLR</i>). There are 12 features in total and each feature was determined to be used in this study. . .	110

5.3	Training and testing data classification accuracies using PCA and ULDA for both time and frequency domain features, FN=10. Training data has excellent performance for both domain and reduction technique. However, performances of testing data are slightly low. This might be due to the variations of the features among subjects.	116
5.4	The table shows an example correlation coefficient between each feature as proposed in this study. The correlation calculated using Pearson R statistical method. This proves the best linear relationship between each feature at $r > 0.95$. The number indicated in the table was set as a feature and denoted as follows: 1. Mean, 2. Standard deviation, 3. Variance, 4. Skewness, 5. Kurtosis, 6. Mean absolute deviation, 7. Minimum, 8. Medium, and 9. Maximum	118
5.5	Linear correlation coefficient using Pearson's R ($r > 0.95$) for finger pinches using TD features at different MVCs; Legend: * Linearly correlated within each paired ; * Linearly correlated within each paired; * Linearly correlated within each paired; * Not linearly correlated	118
5.6	Linear correlation coefficient using Pearson's R ($r > 0.95$) for finger pinches using FD features at different MVCs	120
5.7	Linear correlation coefficient using Pearson's R ($r > 0.95$) for hand grip forces using TD features at different MVCs; Legend: * Linearly correlated within each paired ; * Linearly correlated within each paired; * Linearly correlated within each paired; * Not linearly correlated	121
5.8	Linear correlation coefficient using Pearson's R ($r > 0.95$) for hand grip forces using FD features at different MVCs	121
6.1	Correlation score for mutual information definition.	133
6.2	Parameter setup for the mother wavelet analysis	137
6.3	Overall eight (8) wavelets performances for subject 1 on finger pinch 1 (FP1). This is just to show the variations may occurs on different wavelet at the different scale and frequency components.	139
6.4	Overall wavelets performance for the finger pinches	141
6.5	Overall wavelets performances for the hand grip movement	142
6.6	The five(5) muscles correlation coefficients revealed and tabulated. These includes the scale location for each paired muscles for the finger pinches movement.	148
6.7	The five(5) muscles correlation coefficients revealed and tabulated. These includes the scale location for each paired muscles for the hand grip force movement.	149
6.8	Processing time cost comparisons for the all methods used in this study.	155
B.1	An example of statistical values of 4 subjects for handgrip force	184
B.2	An example of statistical values of 4 subjects for finger pinch	185
B.3	Average wavelet scales and their true frequency based on mother wavelet	186
B.4	Average cross-correlation values and their respective locations.	187
B.5	Subjects compilation classification and processing time based on their average from 3 trials	188
B.6	Average statistical classification performance based on different domain and feature reductions.	189
B.7	One-way ANOVA analysis for classification performances	189

B.8	Two-way ANOVA analysis for classification performances	189
B.9	Average statistical processing time performance based on different domain and feature reductions.	190
B.10	One-way ANOVA analysis for processing time performances	190

Acronyms

Ag-AgCl	Silver Chloride
AMG	Acousticmyography
ANN	Artificial Neural Network
ANFIS	Adaptive Neuro Fuzzy Inference System
AR	Auto Regression
BB	Biceps Brachii
Br	Brachialis
BR	Brachioradialis
CB	Coracobrachialis
CNS	Central Nervous System
CWT	Continuous Wavelet Transform
ELM	Extreme Learning Machine
EMG	Electromyography
ECR	Extensor Carpi Radialis
ECU	Extensor Carpi Ulnaris
FCR	Flexor Carpi Radialis
FCU	Flexor Carpi Ulnaris
FD	Frequency Domain
FDP	Flexor Digitorum Profundus
FDS	Flexor Digitorum Superficialis
FIS	Fuzzy Inference System
FPL	Flexor Pollicis Longus
ICA	Independent Component Analysis

IED	Inter Electrode Distance
k-NN	k Nearest Neighbour
LDA	Linear Discriminant Analysis
MAV	Maximum Amplitude Value
MCA	Mutual Component Analysis
MDF	Median Frequency
MF	Muscle Fatigue
MLP	Multi Layer Perceptron
MMG	Mechanomyography
MPF	Mean Power Frequency
MUAPs	Motor Unit Action Potentials
MVC	Maximum Voluntary Contraction
PCA	Principal Component Analysis
PF	Peak Frequency
PL	Palmaris Longus
PQ	Pronator Quadratus
PT	Pronator Teres
RMS	Root Mean Square
SSC	Sign Slope Change
STFT	Short Time Fourier Transform
SVM	Support Vector Machine
TB	Triceps Brachii
TD	Time Domain
TFD	Time Frequency Domain
UFA	Upper Forearm
WL	Waveform Length
WVD	Wigner-Ville Distribution
ZC	Zero Crossing

Chapter 1

Introduction

Many people suffer from losing their forearm or upper arm due to diseases, accidents, or war. In England, there are 44 actively operating prosthetics service centres. Diabetes 42% and dysvasculature 72% are the most common reasons for the amputation (source from NASDAB,2009). There are more than 130 diabetes amputation cases reported every week, based on an analysis by Diabetes UK. The annual number of diabetes-related amputations has increased up to 7,000 in 2015. This is 4.83% of increment from the previous year, 2014. The human UFA amputation statistics in England has increased dramatically with 300 cases per year.

The statistics in Malaysia show that amputation cases have increased dramatically since 1990 due to accidents and chronic diseases such as diabetes. In 2010, it was estimated that more than three million Malaysians suffered from diabetes. This could lead to amputation if the disease gets worse. Performances currently achieved with prosthetic control are yet far from imitating the real function of the human hand. Most of the prosthetic devices available in the market today do not provide sensational feeling and are not a natural substitution for the missing limb.

The main focus of this study is on the forearm and upper arm of normally limbed subjects, with normal hand and fingers movement before and after fatigue. It is aimed to provide benchmark analysis and strategies of data collection for UFA regions, parameters of feature extraction, and classification accuracy. This could be the reference for amputation cases where the findings will help clinicians to understand the variations of normally limbed subjects compared to amputee subjects. Therefore the enhancements of the EMG

data collection strategies including force variations and fatigue for different hand or finger movements, and robust classification techniques are essential for the development of suitable prosthetic controls.

Since the 1980s, there have been numerous studies on the human normal limbed surface EMG signals for movement identification to be used as input for prosthetic arm control. These studies have used a non-invasive recording technique of surface EMG on the forearm ([Doerschuk et al. \(1983\)](#)) and upper arm ([Winters and Kleweno \(1993\)](#)). This shows the importance of such studies in order to help people with such a problem to have a better life.

In this chapter, a brief background of the EMG signal is given. The motivation of the study is also discussed. The motivation is also discussed, and the problem statement is outlined. Hypotheses and research questions are listed to support the study objectives. Finally, the objectives and scope of the study are pointed out at the end of this chapter.

1.1 Background of EMG

Electromyography (EMG) is one of the significant components in the nerve conduction studies. EMG is one of the techniques for detecting, recording and evaluating the action potential produced by the muscles of the body. It is also known as the diagnostic procedure for the muscle health assessment and the motor neurons control. The origin of EMG action potential or pulse comes from the central nervous system (CNS).

The brain sends the signals once the person wants to move their body parts. This will initiate the muscle fibres through the motor neuron and the muscle contracts. The brain signal is transferred along the nerves through the motor neurons carrying information in pulse repetition or known as frequency. The action potentials generated from this occasion is known as Motor Unit Action Potentials (MUAPs)([Stein and Milner-Brown \(1973\)](#)).

The EMG is the accumulations of the amplitudes produced or known as MUAPs. When the muscles contract, the individual motor unit firing rate and the number of motor unit activation rise linearly to the voluntary muscle contraction of the person. EMG gives easy

access to understand the physiological operation that manifests the generation of muscle force, movement, and functions. The generation of EMG signals allows us to do countless activities to interact with the world. The use of EMG and its properties has been discussed extensively in [De Luca \(1997\)](#).

1.2 Motivation of the study and its significance

Classification of information based on the human UFA movements is needed to improve the capabilities of disabled people, both physically and physiologically. A disabled person may have problems or weaknesses in the muscles contraction or is amputated, thus with difficulties to produce different kinds of hand, fingers, and wrist movements. Therefore, the EMG acquired from their UFA muscles can be used to help them to move as ordinary people. The signals relating to curl exercise, fingers pinch, handgrip force, wrist rotation from the UFA muscle help develop the control system of a prosthetic arm. The prosthetic arm control should be essential enough for the disabled person to perform like the normal one.

Fingers pinch, hand grip, curl exercise, and wrist movement identifications will lead to various applications of prosthetic arm based controllers. Many of the prosthetic limbs available in the current market give narrow applicability for the users. Some of them lack the precision of control, due to the limited access of the data acquisition, inaccuracies in signal processing, and with a small number of degree of freedom for the movements.

A direct approach of assessing all the muscles involved in the human UFA regions with various movements could be one of the solutions for improved functionality. The fatigue study during the task also would be an advantage as the current controllers are impractical because they cannot classify the low level of muscle contraction or muscle fatigue (MF). Therefore during this study, data acquisition of EMG in the human UFA region will be enhanced, with a suitable algorithm in processing the signals to be identified, overcoming the current shortcomings.

The significant component in achieving reasonable prosthetic arm control lean on the

suitability of features and classification algorithm. In the last 20 years, research on the development of pattern classification to distinguish various arm movements has intensively been carried out by many scholars. For example, pattern classification based on fuzzy mapping function was introduced in [Sang-Hui and Seok-Pil \(1998\)](#). This kind of study was extended by many, utilizing multiple classification algorithms as discussed in [Guersoy and Subasi \(2008\)](#); [Lalitharatne et al. \(2013\)](#); [Subasi and Kiymik \(2010\)](#). However, most of the studies focus only on a single region of the human UFA. For instance, they only focus on the forearm muscle or upper arm muscle. The current research focuses on paralysed persons or those amputated in the middle region between the forearm and upper arm, where the current single system approach will not be adequate.

1.3 Hypothesis

If the muscles activity is producing signals associated with the power magnitudes, their response within various kinds of events is excellent for study to magnify the individual skills and form the new way in the human-machine interaction. The hypotheses of the study are listed below:

- Since the forearm is considered an upper arm region, the hand's movement can be identified both from the forearm and upper arm muscles. It is possible to decode the hand movements using surface EMG both from the forearm and upper arm of the normally limbed subject.
- Normal EMG signals from muscle contraction are highly correlated with the force generation.
- Fatigued EMG signals are shown by a decline in the spectral moment parameters and an increase in those temporal moment parameters.

1.4 Research questions

The motivation and hypotheses of the study have created the following research questions:

1. What is the relation between the human UFA muscles (forearm and the upper arm) and the specific movements, force, MVC, and angles?
 - Is it reliable to decode finger and hand movements using both forearm and upper arm muscles? And if so, are there any significant differences in features from both muscles?
 - What is the relation between the two muscles region and the statistic of the EMG? Are muscles needed to cooperate to produce a robust control strategy?
2. Do the variations of the force, percentage of MVC (%MVC), and angle depend on each other?
 - What happens to the variations or changes of the parameters? How do these variations affect the classification performance of the system?
3. How well the current study devise methodology, features extraction and classification technique for the forearm and upper arm control?
 - What are the optimal features to be used for the study? How stable the features will be? What is the characteristic of the time, frequency and time-frequency domain characteristics?
 - The number of EMG channels needed for good classification accuracy?

The research questions listed will lead to the research objectives for the study. This will include the new data acquisition strategy for multi region of the human UFA and will improve the training and classification development of the algorithms. The signals from various muscle sources will reveal any between them.

1.5 Study objectives

The problem statement arise from the previous motivation, hypothesis, and research question for this study is based on the current achievement so far. Since there are so many disabled people or amputated people having difficulties in term of their muscles becoming weak, thus unable to produce certain hand movements. This also contributes from the current tech developed for this people are narrow in their applicabilities for the user. This is due to the limitation in data acquisition and the inaccuracy or discrepancy of the signal used in the application.

The objectives of the study is developed based on the problems stated earlier. Direct approach of assessing and establishing the inter relations of all the muscle involved in the human UFA regions with various hand movements could be one of the solutions. The fatigue study as well would be an advantages as it becomes major contributor for making the current controller become useless. Hence, it is hoped that from this motivations, the new types of protocols, features and classification development could be done as this would overcome the current shortcomings. Therefore, to tackle the issues discussed earlier, the following set of study objectives are devised:

1. To develop a suitable methodology for surface EMG acquisition, best muscle position and features extraction for the classification purpose.
2. To investigate development of a suitable approach for muscle selection and electrode placement of the human UFA via surface EMG acquisition based on different hand grip force, fingers pinch, %MVC, angle, and wrist movement.
3. To establish relationships between forearm and upper arm EMG signal parameters for prediction of hand grip force, fingers pinch with various forces as well as wrist movement.
4. To propose robust features extraction parameters, classification algorithm to coup with normal EMG and MF with high classification accuracy.
5. To validate the proposed features, method and classification accuracy in comparison

to previously reported method in the literature.

1.6 Scope of the study

The scope of the study is limited to the following:

- The human UFA region such as forearm muscle and upper arm muscle are considered in this study. This will include surface EMG procedures for data collection.
- The study includes fifteen (15) subjects; males and/or female aged 20-40 years, normally limbed without any neuromuscular problems.
- The experimental procedures for the study involve the forearm and upper arm muscles of the subject. The emphasis will be on activities of the human UFA movements related to: i) extraction of EMG signals both from the forearm and upper arm muscles and regions contributing to finger(s) pinching at various wrist movements, ii) extraction of EMG signals from both muscles and regions contributing to the hand grasping, wrist movements, and curl exercises, iii) extraction of EMG signals from both muscles and regions contributing to pronation and supination of hand with curl exercises, vi) extraction of EMG signals from both muscles and regions contributing to curl exercises alone.
- The experimental set up and analysis tools used in the project will include the data acquisition system (manufactured by Vernier), a unit of LabQuest mini, a unit of hand dynamometer, 2 channel EMG sensors, Logger Lite software package and a computer. The disposable (Ag-AgCl) diagnostic tab electrodes (Kendall 5400) will be used in the study.
- Matlab R2015b version 8.6 and OriginPro 2019 software for the analysis and plotting.

1.7 Contributions

The contributions to knowledge of the research comprise of the following:

- i. The nature of human upper forearm EMG signals on different muscles localisation are identified using a proposed practical procedure for detection, and analysis. This is in conjunction with the standards procedure from SENIAM (Merletti (2000); Merletti and Hermens (2000)).
- ii. Proposed new acquisition strategies and development, including EMG acquisition system to be used, subject preferences, sensors selection, and muscle selection protocol.
- iii. Established a new way of interpretation of EMG based analysis, such as classification systems and algorithms involving pre and post processing, feature extraction and projection, classification and performance analysis.
- iv. Investigated and evaluated the new approaches of data collection based on the developed protocols and assessing the human upper forearm muscles with force variations, contributing towards optimising the best classification performance.
- v. Minimised the number of EMG channels or muscles used in the data collection, this will optimise the cost, and reduce the complexity and computational time in data analysis.
- vi. Development of a new feature for the best classification scheme and achieving significant enhancement in term of classification accuracies.

The contributions arising from this study are published and presented in several educational events as given below:

- * **WMB Wan Daud**, N. A. and Tokhi, M. (2017). Assessment strategy of human upper forearm inter-relation and muscle fatigue. In CLAWAR2017: 20th International Conference on Climbing and Walking Robots and the Support Technologies for Mobile Machines. London South Bank University.

- * **Daud, W. M. B. W.**, Abas, N., and Tokhi, M. O. (2018). Effect of two adjacent muscles of flexor and extensor on finger pinch and hand grip force. In 2018 5th IEEE International Conference on Control, Decision and Information Technologies (CoDIT), pages 140–145.
- * Abas, N., **Daud, W. M. B. W.**, Abas, M. A., and Tokhi, M. O. (2018). Electromyography assessment of forearm muscles: Towards the control of exoskeleton hand. In 2018 5th IEEE International Conference on Control, Decision and Information Technologies (CoDIT), pages 822–828.
- * **Daud, W. M. B. W.**, Abas, N., and Tokhi, M. O. (2018). Classification performance based on feature reduction of number of adjacent forearm muscles using EMG signals. The Proceedings of the Institution of Mechanical Engineers, Part 1: Journal of Systems and Control Engineering - JSCE-18-0261- Under second review

1.8 Thesis structure

The thesis is divided into seven (7) chapters. The foundation of the work and the literature review are included in Chapter 1 and Chapter 2. Chapters 3 and 4 contain the methods, materials, and subject preferences employed in this research, and present the general knowledge on EMG signals, mathematical modelling of the features used in this study. Chapter 5 addresses several analyses of the study, found through the work and that are used for development in Chapter 6. Finally, Chapter 7 reviews the overall achievement of the study, conclusions, and states the limitations of the work as well as recommendations for future works related to the study. A summary of each chapter is provided in the paragraphs below.

Chapter 2 presents details of the literature reviewed on this study. This involves discussions on previous research study, the outcomes and the methodologies used. The human upper forearm based EMG signal model, characteristics, fatigue manifestation and muscles coordination are also discussed in detail to give an overview about the study.

Chapter 3 provides details of investigations for the development of enhanced approaches of detecting, analysing, and classifying the human upper forearm EMG signal. These

include discussion on the standard procedure in detecting the EMG signal using muscle coordination, positioning, and electrode placement published by SENIAM. Then, the newly developed acquisition strategies are proposed and implemented for this study. The proposed development includes EMG acquisition system to be used, subject preferences, sensors selection, and muscle selection protocol. The chapter also describes in detail the data collection strategies utilised in this study, which have been awarded ethical approval from the Ethical Committee of the University of Sheffield. Several protocols have been developed to consolidate in this study so that the data collected can be used to achieve the objectives of the study.

The state-of-the-art classification systems and algorithms are introduced and discussed in Chapter 4. Particularly, the entire processing series of the classification system is described in detail, such as pre and post-processing, features extraction, dimensional reduction and projection, classification, as well as performance analysis. These approaches are briefly explained and the justification of using them in this study is presented. This chapter forms the basis for the classification approaches that are employed in Chapters 5, and 6. The study employed two approaches of dimensional reduction, namely PCA and ULDA. These are explored and tested with LDA classifiers.

Chapter 5 explores and evaluates the new approaches of data collection and assessing the human upper forearm muscles with force variations, as well as muscle fatigue. The chapter provides proposition for the most appropriate use of muscle to establish the inter-relation between two regions of the human upper forearm with the statistical features extracted from the TD and FD domains. This study presents an insight into the overall objectives of the study, which ultimately proposes and developed of new features using TFD to distinguish the best classification accuracies for the specific hand movements. This is achieved by analysing the EMG signal from the particular muscles as denoted in the chapter. A new fuzzy mutual information based feature (FEFWC) is utilised and analysed using two feature reduction technique, PCA and ULDA. LDA has been chosen as the classifier to compare the classification performances between the new features and other features from TD and FD. The results produced shown distinctively significant, especially on the

proposed features developed. This is supported by the statistical analysis performed using ANOVA, which is presented in detail in Chapter 6.

Chapter 7 presents an overall discussion and conclusions of the work, with specified contributions of the study. The limitations of the study and analysis are listed in this chapter, and future works are suggested in relation to the study objectives.

Chapter 2

Literature review

2.1 Introduction

In this chapter, an overview of EMG signals origination and propagation, characteristics of EMG, muscle fatigue and the human UFA is presented. This will give a brief explanation of the EMG signals of the human UFA as well as the applications related to the EMG. The analysis approaches for time domain (TD), frequency domain (FD), and time-frequency domain (TFD) are discussed in terms of the strengths and limitations. Thus, the proposed improvement of the study is highlighted.

2.2 The model of EMG signal

In the 1660s, Francesco Redi became the first to explore muscle activities from electric ray fish. He discovered that the fish muscles generated electricity once they were in a specific condition (voluntary contraction). Then, Luigi Galvani was credited as the founder of neurophysiology for his finding using frogs. He established that electrical stimulation of muscular tissue produces contraction and force ([Raez et al. \(2006\)](#)).

EMG is a visual imitation of electrical activity from muscle's exercise. The EMG is an extracellular surface registration of the voltage potentials that happen during a muscle compression. Muscle cells are polarized at rest. This means the cells have insignificantly unbalanced concentrations of ions beyond their cell membranes. An abundance of positive sodium ions on the outside of the layer produces, resulting in an outer layer having more

positive charge compared to the inner membrane. The hidden cell potentials can roughly at 90 millivolts (mV) less than the outer membrane. The $90mV$ difference is known as the resting potential ([Vernier Software Technology \(2019a\)](#)).

The average cell membrane is approximately impermeable to the entry of sodium. But, stimulation of a muscle cell causes an increase in its permeability to sodium. Sodium ions travel into the cell through the opening of voltage-gated sodium paths. This forms a change (depolarization) in the electrical field throughout the cell. This difference in cell potential from negative to positive and back is a voltage pulse defined as the action potential. In muscle cells, action potential triggers muscle contractions.

EMG signals are derived from the time variation of muscle contraction. It is a technique of detecting and recording the excitation of the electrical potential of the activated muscles. The generation of the EMG originates from the flow of the ions through the muscle fibre. The brain command generates the ions and innervated by motor neurons through the motor unit. The surface EMG signal recorded by means of the electrode exposed the real activities of individual muscle (or group of muscles). This was the results of the properties of firing rates of motor units, as a function of time and force ([De Luca \(1985\)](#)).

This creates the MUAPs, known as the basic building block of the neuromuscular system. It is also referred to as a fundamental element of EMG signal propagation, and the MUAPs model is thoroughly discussed in [McGill \(2004\)](#). Most MUAPs amplitudes range from $100\mu V$ to $10mV$. Figure 2.1 shows the MUAPs development from the individual muscle fibres of activated motor units.

MUAPs is much depended on the size of muscle fibre, which is a larger amplitude in long fibre. The shape of MUAPs also influenced by many factors such as the innervation zone, and muscle fibre number ([Merletti and Parker \(2004\)](#)). The intended movement such as finger pinches or hand gripping will require more force; hence the central nervous system responds by increasing the motor units activation and firing rates of every single motor units.

The signals generated from these activities are presented from the signal characteristics

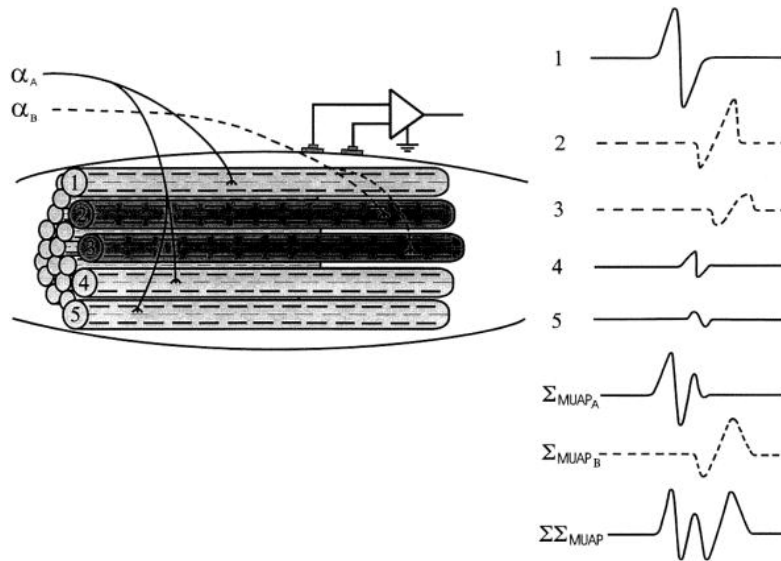


Figure 2.1: MUAPs developed from individual muscle fibre action potential composition [Kamen and Caldwell \(1996\)](#)

such as their intensity and the power spectrum. This can be referred to as RMS, MPF, MNF or rectified mean value of their frequency spectrum. All these characteristics are attributed to as the global sEMG variables because they represent the overall picture of the muscle condition. These variables allow EMG to be modelled and related to the underlying properties of the central and peripheral in the muscle ([De Luca \(1982,8\)](#); [Luca \(1979\)](#)).

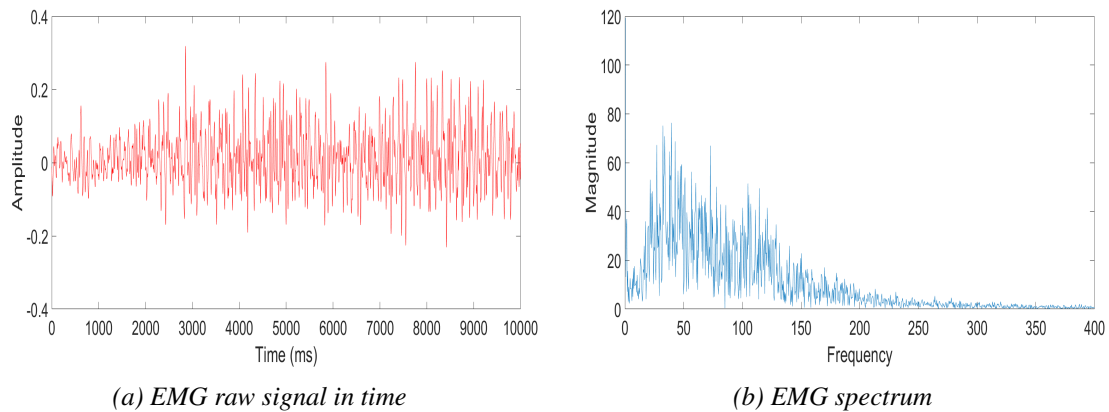


Figure 2.2: The raw EMG signals and its power spectrum for references. This details can be found in Appendix B

EMG is known by many as a bandpass random signals where the energy was realised in the specific bandwidth (1-400 Hz) ([Merletti \(1999\)](#)). This type of signals are special when initialising their spectrum, and they exhibit a series of localisation peaks whose their stochastic properties ([Zivanovic \(2014\)](#)) determines time and frequency. EMG is

considered stochastic in its process whose their amplitude is based on the muscle activation level, and the spectral properties are based on the conduction velocity (Bonato et al. (2001); McGill (2004)). The basic model of EMG signal for dynamic contractions has been used in this study can be represented as:

$$x(t) = a(t)f(t) + n(t), \quad (2.1)$$

where $f(t)$ is a unit-variance random process expressing the stochastic features of the signal, $a(t)$ is the modulating signal that shows the power or amplitude of the EMG signal, and $n(t)$ denotes instrumentation and biological noise which may occur in EMG signal. Sometimes the noise can be neglected if the proper preprocessing technique takes place before analysing the EMG signal.

Thus far, the mathematical model developed for EMG signal was based on the human muscle contraction, and most of the EMG model contributed in many studies are restricted to the current physiological knowledge (Zivanovic (2014)). Consider Figure 2.2 shows an EMG signal from one channel of muscle and their frequency spectrum using the Welch method. The mathematical representation for EMG signal $x(t)$ can be approximated as a K component of a time-varying model $\hat{x}(t)$:

$$\hat{x}(t) = \sum_{k=1}^K A_k(t) \cos(2\pi f_k(t)t + \theta_k), \quad (2.2)$$

where $A_k(t)$ and $f_k(t)$ are the instantaneous amplitude and frequency respectively. Mathematical equation in (2.2) can be rewritten in a simply and better way as follows:

$$\hat{x}(t) = \sum_{k=1}^K a_k(t) \sin(2\pi f_k(t)t + b_k(t) \cos(2\pi f_k(t)t), \quad (2.3)$$

$$a_k(t) = -A_k(t)\sin\theta_k, b_k(t) = A_k(t)\cos\theta_k, \quad (2.4)$$

In equation (2.3), the unknown parameters $a_k(t), b_k(t)$, and $f_k(t)$ need to be estimated. For N measurement points $t = t_1 \dots t_N$, the expression (2.3) becomes an N -dimensional linear system with $3NK$ unknowns. Such a system cannot be solved; however it can be assumed that in the analysis window the time variations of $a_k(t), b_k(t)$, and $f_k(t)$ are continuous, and therefore can be approximated by the following time polynomials for $k = 1 \dots K$:

$$a_k(t) = a_0^{(k)} + a_1^{(k)}t + a_2^{(k)}t^2 + \dots + a_M^{(k)}t^M = \sum_{m=0}^M a_m^{(k)}t^m, \quad (2.5)$$

$$b_k(t) = b_0^{(k)} + b_1^{(k)}t + b_2^{(k)}t^2 + \dots + b_M^{(k)}t^M = \sum_{m=0}^M b_m^{(k)}t^m, \quad (2.6)$$

$$f_k(t) = f_0^{(k)} + f_1^{(k)}t + f_2^{(k)}t^2 + \dots + f_M^{(k)}t^M = \sum_{m=0}^M f_m^{(k)}t^m, \quad (2.7)$$

By inserting equation [2.5 – 2.6] into [2.3]:

$$\hat{x}(t) = \sum_{k=1}^M \sum_{m=0}^M a_m^{(k)}t^m \sin(\lambda_k(t)) + \sum_{m=0}^M b_m^{(k)}t^m \cos(\lambda_k(t)), \quad (2.8)$$

$$\lambda_k(t) = 2\pi \left(f_0^{(k)}t + \sum_{m=1}^M f_m^{(k)}t^m + 1 \right), k = 1 \dots K \quad (2.9)$$

The argument $\lambda_k(t)$ is written as a sum of the linear and non-linear spectral distributions. It could be analytically distinguished by transforming the sine and cosine in equation (2.8). Therefore, for the k th component we have:

$$\sin(\lambda_k(t)) = \sin\left(2\pi f_0^{(k)}t\right) \cos\left(2\pi \sum_{m=1}^M f_m^{(k)}t^{m+1}\right) + \cos\left(2\pi f_0^{(k)}t\right) \sin\left(2\pi \sum_{m=1}^M f_m^{(k)}t^{m+1}\right) \quad (2.10)$$

$$x\cos(\lambda_k(t)) = \cos\left(2\pi f_0^{(k)}t\right) \cos\left(2\pi \sum_{m=1}^M f_m^{(k)}t^{m+1}\right) - \sin\left(2\pi f_0^{(k)}t\right) \sin\left(2\pi \sum_{m=1}^M f_m^{(k)}t^{m+1}\right) \quad (2.11)$$

Furthermore, it can be assumed that for a short-time analysis the non-stationary trigonometric terms in equations (2.10) and (2.11) can be approximated by a single term Taylor series:

$$\cos\left(2\pi \sum_{m=1}^M f_m^k t^{m+1}\right) \approx 0, \quad (2.12)$$

$$\sin\left(2\pi \sum_{m=1}^M f_m^k t^{m+1}\right) \approx 2\pi \sum_{m=1}^M f_m^k t^{m+1}, \quad (2.13)$$

Furthermore, equation (2.9) can be rewritten by combining equations (2.10) – (2.13) as follows:

$$\hat{x}(t) = \sum_{k=1}^K s_k(t) \sin\left(2\pi f_0^k t\right) + c_k(t) \cos\left(2\pi f_0^k t\right), \quad (2.14)$$

$$s_k(t) = \sum_{i=0}^{2M+1} \left[a_i^k - 2\pi \sum_{m=0}^{i-2} b_m^k f_{i-m-1} \right] t^i = \sum_{i=0}^{2M+1} s_i^k t^i, \quad (2.15)$$

$$c_k(t) = \sum_{i=0}^{2M+1} \left[b_i^k - 2\pi \sum_{m=0}^{i-2} a_m^k f_{i-m-1} \right] t^i = \sum_{i=0}^{2M+1} c_i^k t^i. \quad (2.16)$$

Equations (2.14) – (2.16) represent the EMG time varying multicomponent signal. The non stationarity property was acquired by the $2M + 1$ which is known as the order of polynomials $s_k(t)$ and $c_k(t)$. Basically, the actual model of the EMG signal is linear in its parameters, This can be seen in the polynomial coefficient of $s_i^{(k)}$ and $c_i^{(k)}$ using simple linear equation solutions. Equations (2.15) and [2.16] shows the correlation between two main components in the EMG signal which are the amplitude and the frequency. These coefficients permit the estimation for $a_k(t)$, $b_k(t)$, and $f_k(t)$ for every specific demand of application.

2.2.1 EMG characteristics

The characteristics of EMG signals greatly depend on the function of the EMG itself, muscle fibre activation, electrode characteristics, and the data acquisition system used in the recording. These extrinsic factors alter the shape of EMG signals during its way from the muscle membrane to the electrodes.

EMG signals are considered as non-stationary as their characteristics change over time (Phillips et al. (2003)), especially on the number and firing rate of motor units, force and joint angle (Cechetto et al. (2001)). However, EMG signals are also known as stationary in their characteristics for short periods. It is a one-dimensional (1D) time series signal of muscle activity upon a certain level of muscle excitation. As mentioned in the previous chapter, EMG signals are the addition of each single action potential or MUAP trains. It is assumed that the stochastic nature of the signal based on the surface electrode pick up the region and random nature of the MUAPs (Hudgins et al. (1993)). EMG signal is an

algebraic composite of the activated MUAPs influenced by several factors such as physiological and anatomical properties and characteristics of instrumentation. It is different from one person to another. Figure 2.1 demonstrates the motor units functionality and how each of the muscle fibres involvement furnishes to the action potential and frequency attributes of the EMG signals (Kamen and Caldwell (1996)).

The Kukulka and Clamann (1981) did the study on the identification of the recruitment and discharge characteristics of motor units in BB muscle during stationary contraction from 0 to 88% MVC. They tested the stationarity of the EMG signals with an occurrence of short interspike less than $20ms$ intervals. Therefore, to produce robust EMG features, the instantaneous value of a short segment of energy for the EMG signal is possible to be used.

2.2.2 Muscle fatigue manifestation

Research has been carried on the influence of MF on EMG single amplitudes and forces (Dideriksen et al. (2010)). They conclude that the amplitudes of EMG are not a viable solution towards estimating muscle activation and the force during fatigue. MF is a phenomenon that happens for every creature with muscles in their body, such as human and animal. Every daily activity performed is always involved with muscle activation development in the muscular system territories. In the human body movement, muscular systems played an important role followed by the structures in the body known as skeletal systems. There are many definitions derived for the MF phenomena, and it has been extensively discussed in studies considering the factors involved. One of the best descriptions has been given by Allen et al. (2008); muscles that are utilised intensively manifest a gradual decline of production and improvement after a period of rest.

MF is available from different parts of the muscle body, as it is divided into two components, namely muscle recruitment (central component) and the neuromuscular transmission (peripheral component) (González-Izal et al. (2012)). Earlier studies have described MF as the existence of an individual critical threshold with the involvement of the central and peripheral components (Yoon et al. (2008)). On the occasion of fatigue, various muscle

properties are transformed and these constitute a major factor in contributing to the decline of skeletal muscle working capacity. The properties can be in the firing rate and motor unit action potentials ([Adam and De Luca \(2005\)](#)), the neuromuscular system ([Benjamin and Roger \(2007\)](#)), intracellular metabolism ([Westerblad et al. \(1991\)](#)), and intra-extra cellular ionization. For instance, ([Bigland-Ritchie et al. \(1983\)](#)) found that there were changes in the motor unit firing rates during fatigue when the maximal voluntary contractions were sustained for 40s-120s, and it is shown by the progressive decline in both the range and mean rate of motor unit potentials. However, one cannot believe that these variations in the motor unit further effect to submaximal fatiguing isometric contractions since it is inadequately documented throughout this sort of practice and remain a matter of debate ([Gamet and Maton \(1989\)](#)).

The on-going research to date has described the fatigue phenomenon with many meanings, considering all the processes and the mechanisms, but these disparities in viewing the problems can be explained by the full range of exercise models, protocols, and methods applied in fatigue studies of human muscle ([Vøllestad \(1997\)](#)). [Rogers and MacIsaac \(2011\)](#) have summed up the MF as the recruitment and de-recruitment of active motor units in the neighbourhood electrodes, and the position of the electrode of the muscle activation area with changes of muscle shape. There is an assumption made based on gravity and muscle contraction dynamics; movements of a biological limb are considered as nonlinear ([Bhuiyan et al. \(2014\)](#)).

Researchers have studied MF by observing muscle activation trends and changes in its properties using different modalities and techniques. These have led to useful results in areas of myoelectric control and prosthetics ([Jahani Fariman et al. \(2015\)](#)), neuromuscular disease and rehabilitation ([Riley and Bilodeau \(2002\)](#)), human-machine interaction ([Song et al. \(2006\)](#)), sports performance and ergonomic analysis [Ma et al. \(2011\)](#), and electrical stimulation for functional study ([Thrasher et al. \(2005\)](#)). The obvious reason for the study is that MF may lead to injury problems if not seriously monitored. For instance, detection of MF during work in progress involving repetitive movement of muscle and load may help the employer to prevent their work from getting injured.

MF study and analysis depend on the conditions of the methodology and approaches used in the data collection. It can be in terms of isometric and isotonic strength tests (Adam and De Luca (2005); Arendt-Nielsen and Sinkjær (1991)), endurance test (Krogh-Lund and Jørgensen (1993)), neuromuscular biopsy and imaging as well as surface EMG (Cifrek et al. (2009)). Cechetto and his colleagues studied the effects of four time-varying factors on the mean frequency and result from the study indicate that the number and firing rates of active MUAPs and the muscle force contribute to relatively small changes in the MF (Cechetto et al. (2001)). They also suggested that muscle geometry needs to be taken into account as a fatigue index when dealing with dynamic contractions.

It is shown in Figure 2.3 that MF shifts the frequency contents of the EMG signal towards lower frequency (Petrofsky and Lind (1980)). Few studies have been carried out on determining parameter changes of surface EMG with inconclusive results (Anam et al. (2013); Krogh-Lund and Jørgensen (1991,9); Thongpanja et al. (2012a)). These have suggested that further studies are needed to identify those phenomena and hence contribute towards better development of surface EMG means. This will enable one to explore and distinguish variations in MF in relation to the conditions in external load both for continuous static and dynamic repetitive tasks.

This is also supported by finding that the amplitude variations shrink towards zero (Venugopal et al. (2014)) as the number of MUAPs firing rate increases to maintain the muscle force at increased amplitude (Enoka et al. (2011)). Santos et al. (2016) have suggested for research on upper forearm MF to focus on the improvement of the experimental protocols and instrumentation, as they are the most influential factors on the result of such studies.

2.2.3 Human upper forearm

The human upper forearm (UFA) comprises of the forearm and upper arm, as shown in Figure 2.4(A). The forearm is physiologically part of upper arm combinations between the elbow and the wrist. The forearm is specifically created to help human to perform daily activities or movements such as fingers flexion, hand grip, wrist movement, and curl

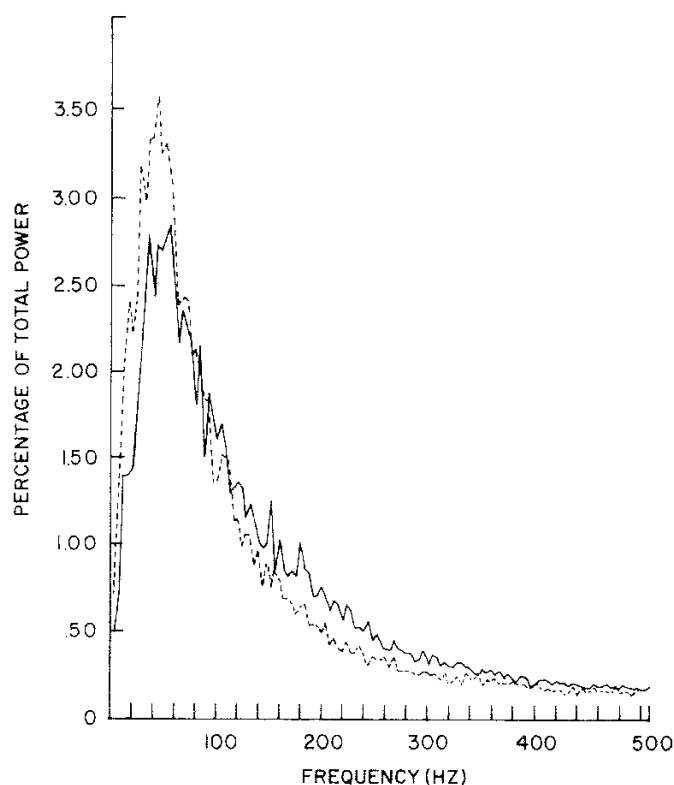


Figure 2.3: Example of power spectrum recorded from the fresh muscle (solid line) and fatigue (broken line) [Petrofsky and Lind \(1980\)](#)

exercise. The upper arm muscles are the main components for flexion and extension. There are three groups of muscles of the upper arm responsible for the flexion of the forearm – brachialis, biceps brachii (BB), and brachioradialis (BR). The anterior part is for the extensor- triceps brachii (TB). This is shown in Figure 2.4(B).

The forearm muscles are divided into four layers, from first to fourth layers, and two compartments (anterior and posterior). Figure 2.4(C) shows the muscles that lie within each segment. The anterior compartment is separated by the posterior compartment by two bones (ulna and radius), interosseous membrane, and lateral intermuscular septum ([Parson \(2009\)](#)). Figure 2.5 shows a cross-section of the forearm and the muscles of interest available in the forearm region. Muscles of the anterior compartment flex the forearm, and this is known as pronation. Supination is derived from the forearm extension of the posterior muscles. All the muscles of the anterior and posterior compartments play essential roles for the hand and fingers movement, respectively.

The importance of human UFA analysis for the healthy and normally limbed subjects

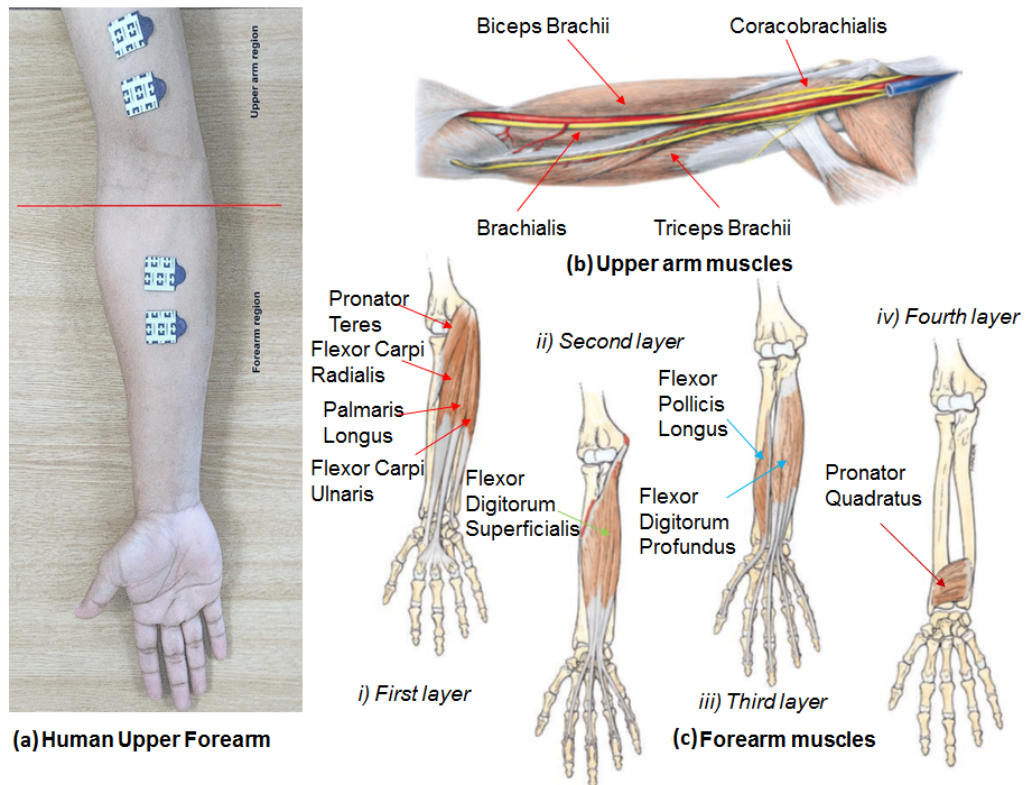


Figure 2.4: The human upper forearm regions and muscles; A) Upper arm and forearm, B) Upper arm muscles; Biceps Brachii (BB), Triceps Brachii (TB), Coracobrachialis (CB), and Brachialis (Br), C) Forearm muscles; Pronator Teres (PT), Flexor Carpi Radialis (FCR), Flexor carpi Ulnaris (FCU), Palmaris Longus (PL), Flexor Digitorum Superficialis (FDS), Flexor Pollicis Longus (FPL), Flexor Digitorum Profundus (FDP), and Pronator Quadratus (PQ).

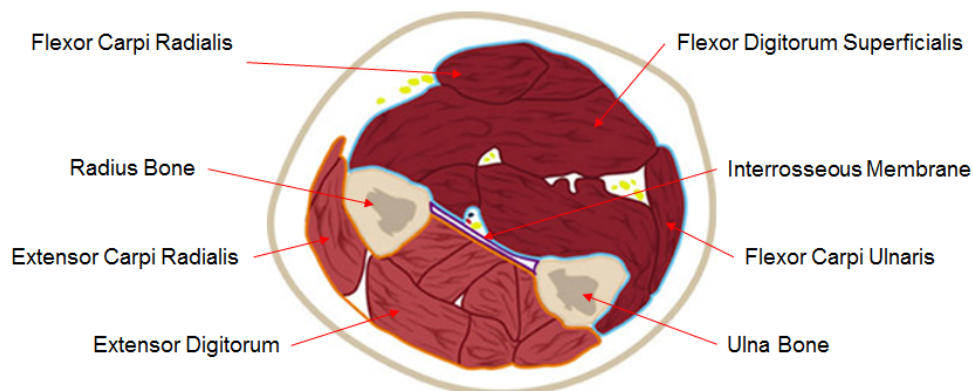


Figure 2.5: Cross section of forearm showing the muscles available for the study

is crucial as the benchmark strategy for indicating the standard mean of its use. It can be used as a reference for above elbow amputee study in the future. There is the need for normally limbed survey on the upper limb region to help genuine understanding of the

Table 2.1: Upper arm muscles, attachments and main actions

Muscle	Attachment/Location	Main Action
BB	Connected to the anterior compartment of the forearm. The muscle is developed from two heads: long head and short head, large and thick muscle.	Acts to flex and supinate the forearm. Major supinator of the forearm.
CB	Muscle that comes from structure of scapula.	Helps to flex and adduct arm.
Brachialis	In the middle brachial region, lies underneath the biceps brachii, located deep in the upper arm, supporting biceps brachii for arms flexion	Flexes forearm in all positions.
Anconeus	The muscle right of the elbow, helps the elbow extension, with small triangular shape, and can be found around the elbow region.	Assists triceps in extending forearm, stabilizes elbow joint and abduct ulna during pronation
TB	Located at the back of the arm, develops from 3 origins; long head, medial head, and lateral head.	Chief extensor of the forearm.

variation between the above elbow amputees with the ordinary person.

For instance, [Zardoshti-Kermani et al. \(1995\)](#) has studied on an above-elbow amputee, and they tried to put some noise to study the robustness of their proposed features and controls. However, this would be good if they can have a reference with the usual standard so that they can evaluate their robustness.

The upper arm muscles and its primary function are listed as in Table 2.1 and the locations of the muscles are shown in Figure 2.4(B). The BB muscle is responsible for further specific movements in conjunction with three different joints (tri-articulate). It is positioned at the anterior of the upper arm housing the humerus bone. The main functions of the BB are:

1) Supination using the proximal radius joint, the muscles attach to forearm diagonally and contribute to produces to the forearm twist, permitting to turn palms from upside down. For example, this forearm action should be used for turning the knob of a door or ignition of the car.

2) Elbow flexion; flexion together with the humerus joint (elbow). The bending along with the elbow joint, is generally accomplished throughout a BB curl. During contractions, the tendon is stretched towards the two heads, leading the elbow to bend.

3) Shoulder flexion. The BB performs various powerless functions inside the shoulder complex, for example, aiding the forward flexion from the shoulder blades (bringing the

arm forward and upwards) along with backing within the stabilization inside the shoulder joint.

Unlike other muscles discovered on the front of the body, the BB accounts for pulling movements not like pushing movements. The BB, the muscle will be the antagonist towards TB muscle and comprises around 33% of muscle tissues together with the upper arm. There are two (2) additional muscles which can be about the anterior with all the humerus that assist the BB. In addition, CB muscle also known as the brachialis muscle. Efficiency lies underneath and aside from the BB.

Table 2.2: Forearm muscles, attachments, and main actions

Muscle	Attachment/Location	Main Action
FCU	Originates from the medial epicondyle and the ulna.	Flexes and adducts hand (at the wrist)
PL	Medial epicondyle of humerus	Flexes hand at the wrist.
FCR	Originates from the medial epicondyle.	Flexes and abducts at the wrist.
PT	Two origins, medial epicondyle and coronoid process of the ulna.	Pronates of the forearm.
FDS	Two heads, medial epicondyle and the radius	Flexes the metacarpophalangeal joints and flexes at the wrist.
FDP	Originates from the ulna.	Only muscle that can flex joints of fingers and joints of wrist.
FPL	Originates from anterior surface of radius.	Flexes phalanges of first digit (thumb)
PQ	Originates from anterior surfaces of ulna	Pronates the forearm

The focus on the current research is on the relations of the forearm muscles and upper arm muscles. The linkages are strong, and it is envisaged to develop a suitable measurement strategy using both regions of the human UFA, to establish suitable means for achieving high classification for dexterous control of prostheses. The interest is to study and explore the new features in the presence of such phenomena as MF to help avoid the risk of getting impaired ([Monjo \(2015\)](#)) or probabilities of detecting neuromuscular disorder and disease.

[González-Izal et al. \(2012\)](#) have concluded in their studies that approaches associate with several sets of EMG features for measuring force variations yield better understanding about MF. They have also suggested that more research is demanded to expand procedures

that combine EMG variables for estimating changes concerning MF. The MF of human UFA muscles is studied here as a way of determining suitable solutions in such areas, as, to the author's knowledge, there is no such research considering both muscle regions. This involves maximum voluntary contraction, different loads, and maximum holding towards fatigue.

2.3 Review of surface EMG assessment of the forearm and upper arm

This section presents an overview of EMG assessment techniques in the context of human UFA. The review also includes limitations associated with previous studies. The relations between both muscle regions on human UFA also highlighted in this section.

There have been many studies on the surface EMG of human UFA, especially for classification and control. Most of the studies have generally focused on only the single region of the muscle of UFA and fatigue ([Ahamed et al. \(2014\)](#); [Miyoshi et al. \(2009\)](#); [Rojas-Martinez and Mananas \(2014\)](#); [Roman-Liu et al. \(2004\)](#); [Takahashi et al. \(2006\)](#); [Yao et al. \(2015\)](#); [Zhou et al. \(2011\)](#)).

For example, the studies on human UFA have been based on %MVC, considering various implementations such as isometric and isotonic movements, muscle endurance tests, multi-features classifications. A comparison of the reported studied is given as in Table 2.3, Table 2.4 and Table 2.5. Unfortunately, there are few studies published based on %MVC.

2.4 Relationship between surface EMG of forearm and upper arm muscles, force, %MVC and wrist angle

There are numerous studies on surface EMG of human UFA control region such as forearm and biceps brachii reported in the literature. However, fewer studies published on %MVC, where classifications are made using multi features and fatigue as a comparison. A con-

siderable amount of research has been done on EMG signals focusing on the BB muscle movement analysis with fatigue.

Table 2.3: Previous study based on human upper arm isometric contraction

Author(s)	Muscles	Methodology/ Movement	Features	Specialty	Findings
Krogh-Lund and Jørgensen (1991,9,9)	TB, BR and BB	25%MVC of maximal duration, 15%MVC with 135° elbow angle, 30%MVC with 135° elbow angle	Mean, MDF, RMS	Muscle fibre, conduction velocity (CV) and fatigue	CV influences the %MUAPs firing frequencies
Doud and Walsh (1995)	BB	50%MVC with elbow angle	Center frequency	Muscle length interaction and fatigue	fatigue significantly influences the EMG center frequency
Mamaghani et al. (2002,0)	Upper trapezius, anterior deltoid, BB, BR	(20, 40, 60%MVC) with 3 elbow angles (120°, 90°, 60°) and add on shoulder angles	Mean frequency, RMS	EMG, AMG, goniometer, and MMG	RMS of AMG has an excellent correlation with elbow angle, and RMS of MMG has a high association with force production
Ravier et al. (2005)	BB	70%MVC and short contraction (3s) at different strength	Power spectral with two linear segments	fatigue new frequency indicator	proposed indices able to differentiate between fatigue and non fatigue states
Dimitrova et al. (2009)	BB	(20, 40, 60, 80, 100 %MVC)	MPF, median frequency and new spectral indices Finsmk	new spectral fatigue indices Finsmk	The responsiveness of the signs to fatigue depended on the electrode placement and its longitudinal site in respect of the end-plate region and ends of the muscle fibres.

Table 2.4: Previous study based on human upper arm using both isometric and isotonic contraction

Author(s)	Muscles	Methodology/ Movement	Features	Specialty	Findings
Bai et al. (2012)	BB	(20,40,80 %MVC) and 90° elbow angle	Mean of time frequency of STFT and CWT	second order of polynomial and CWT	both techniques reveal a significant reduction in signal power comparison ratio and the fatigue levels increase as muscle fatigue develop.
Subasi (2012)	BB	Force levels with 30%MVC	AR,CWT	classifies the EMG signals into normal, neurogenic or myopathic.	The study shown that ANFIS modelling is better than the DFNN and MLPNN

However, most of the research has focused only on certain number of %MVC. For [Krogh-Lund and Jørgensen \(1991,9,9\)](#) used isometric contractions based on 25% MVC, isometric flexion with 15% and 30% of MVC and elbow angle 135°.

[Mamaghani et al. \(2001\)](#) have reported studies on mechanomyography (MMG) and EMG in isometric contractions from four different muscles at 20%, 40% and 60% MVC and with 60°, 90°, and 120° angles. They compared the differences between MMG and EMG signals from muscle length and found a significant difference in frequency content with respect to %MVC. Previously in their study, they reported that the mean power frequency (MPF) and the root mean square (RMS) value of the MMG and EMG signals changed according to the joint angle.

Differently, by using goniometer, [Ravier et al. \(2005\)](#) investigated the isometric movement of 100° elbow angle to analyse the fatigue fluctuations based on a median frequency (MDF) shift. Moreover, [Dimitrova et al. \(2009\)](#) proposed new indices based on spectral features for various force levels of analysis. They suggested that the proposed indices leaned on the electrode positioning and the location of the muscle fibres during contraction. Studies have shown that maximum angle for elbow would influence high RMS value for static contractions. It has been found that at an angle of 90°, muscle fibres in the BB are at optimal length for force production. [Soylu and Arpinar-Avsar \(2010\)](#) studied the variations of MVC and how it affects fatigue. [Subasi \(2012\)](#) used time-frequency features

Table 2.5: Previous study based on human upper arm isotonic contraction

Author(s)	Muscles	Methodology/ Movement	Features	Specialty	Findings
Soylu and Arpinar-Avsar (2010)	BB	subjects approached the highest force level in 2s by insignificantly expanding the force, and then contracted the BB muscle maximally	median frequency, integrated EMG	data used not influenced by the muscle fatigue	which is not influenced by the fatigue from the initial starts of EMG and its peak time
Jordanic and Magjarevic (2012)	BB	Curls exercise	Median frequency	fatigue estimation using the modified periodograms	fatigue indices defined as the slope of the linear regression model fitting the median frequencies of the electromyographic signal in the least square sense
Ahamed et al. (2013)	BB	muscle activity between the region of the endplate and distal tendon insertion with different genders and right or left arms, concentric and eccentric contraction	Not mentioned	activity between the region of the endplate and distal tendon insertion	there are no significant differences between male left and female right and male right and female left arm muscles
Venugopal et al. (2014)	BB	repetitive flexion and extension of the elbow with a 6 kg load and 30degree angle	Multiple time window features rectangular, hamming, trapezoidal and Slepian	Using mutiple windowing techniques and fatigue	k-nearest neighbour algorithm is found to be the most accurate in classifying the features, with a maximum accuracy of 93% with the features selected using information gain ranking
Al-Mulla et al. (2015)	BB	3 trials of dynamic, exercises with and 3 trials of 70% MDS and elbow angle	Higher-order statistics, Mean Frequency (MF), Median Frequency, Power Spectrum Density, RMS, Daubechies 4 (Db4), Mexican Hat (Mex H), Pseudo-wavelet (p-w)	Optimal elbow angles for separation with segmentation (Non-Fatigue and Fatigue)	optimal elbow angles can be used for fatigue classification, one of the features and on average of all eight features showing 87.90% highest correct classification for

and independent component analysis (ICA) for dimension reduction, and artificial neural network (ANN) for classification. However, latest studies shows that LDA was comparable or much better than ANN in the classification accuracy ([Resnik et al. \(2018\)](#)).

2.5 Surface EMG features extraction and classification

Surface EMG features extraction and classification are the main important criteria in prosthetic design and control. These was first studied in the 1970s and the research has been growing very fast. This has included signal acquisition protocol (data acquisition technique, electrodes placement, muscle selection), features extraction (segmentation or reduction) mainly for purposes of classification.

2.5.1 Features extraction

Feature extraction selection and strategy are essential for classification, especially in EMG neuromuscular study and fatigue. The purpose is to improve classification robustness and accuracy. The informative features can be represented as individual, group or derivation from both classes as multi-features. It has to be very selective and sensitive to the studied phenomena. This will help much in the offline and the real-time applications since it can reduce the computational load's problems.

It is generally agreed that multi features provide more complete information as compared to any single feature ([MacIsaac et al. \(2006\)](#)). Therefore, there is a need for feature reduction process after the features have been identified. This is believed as another factor that will affect the classification performance ([Yan and Liu \(2013\)](#)), and the stage of choosing the robust features is key to better classification performance, not the classifier.

EMG fatigue signals are acknowledged as a non-physical variable, where the assessment of the MF needs to be identified from EMG signals measurable physical variables as new definable indices. [Roman-Liu et al. \(2004\)](#) have argued that MF is noted by the EMG amplitude only if there is both a decline in the FD features and an increment in the TD features.

Table 2.6: Previous study based on human upper forearm muscle contraction and analysis of study

Author(s)	Muscles	Methodology/ Movement	Features	Findings
Petrofsky and Lind (1980)	FCR	Isometric strength and endurance of the handgrip muscles	Centre frequency and mean frequency	centre frequency might provide a useful index of fatigue for sustained submaximal isometric contractions.
Khushaba et al. (2009)	8 forearm muscles	datasets taken from UCI repository, 7 limb motions position	TD,CWT	the proposed DEFLDA technique proved to be successful in achieving better performance
Scheme et al. (2011)	around the forearm, 10 electrodes	nine motion classes consisted of wrist flexion-extension	MAV, ZC, SSC, and WL.	proposed control scheme (1 versus 1 classifier's ULDA-based) was the best
Thongpanja et al. (2012a)	4 forearm muscles, PL, supinator longus, ECR and pronator radii teres	normal subjects with different loads: (2, 4, 6 and 8 kg)	time dependence of the median and mean frequency	suggested new approach for determining MF and loads for the PL muscle, unfortunately, the performance is worse than for the BB muscle
Anam et al. (2013)	2 channel ECU and EDM, FDS and PL	finger movements	SSC, ZC, WL, Hjorth time domain parameters, Skewness , AR	proposed system which consists of the SRDA, the optimized ELM and the majority vote was able to recognize the individual and combined finger movements
Al Omari et al. (2014)	4 forearm muscles, extensor digitorum, ECR, PL, and FCU	eight hand movements	WL, Wilson amplitude, RMS combination	the highest classification rate achieved was 95 % by GRNN using energy of wavelet coefficients
Al-Angari et al. (2016)	Normal subject with 5 hands movements, Around forearm muscles	eight hand movements	MAV, SD, WL, Energy, ZC, SSC, AR, Wavelet decomposition, sample entropy	correlation-based method (CFSS) and a distance-based method (DFSS)
Resnik et al. (2018)	Amputated subjects shoulder and upper arm muscles	five upper arm movements	not stated	compare PR control based on LDA classifier
Bai et al. (2019)	Shoulder muscles (64 points)	eight shoulder movements	spatials and time frequency domains	optimisation technique reduced the number of points used

Noticeable studies have been reported on various techniques of analysis of MF with respect to the human UFA muscles separately. Several studies have reported fatigue analysis during static loading, multi fingers coordination in force (Danion et al. (2000)), forceful handgrip task (Alizadehkhayat et al. (2011)), arm wrestling (Ahamed et al. (2012)), dynamic contractions of biceps curls (Jordanic and Magjarevic (2012)), neck and shoulder muscles (Chowdhury et al. (2013)), gender comparison using dominant arm and contraction (Ahamed et al. (2013)), cricket bowlers during bowling (Ahamed et al. (2014)), and optimal elbow angles (Al-Mulla et al. (2015)).

Analysis Domains

In analysing the surface EMG, there several domains that could be employed individually or in combination. Features identification and domain analysis were known as the main criteria in fatigue study (Venugopal et al. (2014)). Time domain (TD) descriptive statistic features such as root mean square (RMS), waveform length (WL), maximum amplitude value (MAV), zero crossings (ZC), slope sign change (SSC), and TD frequency related feature autoregression (AR) is the most conventionally used. Mean frequency (MNF), peak frequency (PF), and median frequency (MDF) are frequency domain (FD) features considered. To overcome the time-varying characteristic of the EMG signals, various time-frequency domain (TFD) features are reported and used in many studies such as short-time Fourier transform (STFT), Wigner-Ville distribution (WVD), and continuous wavelet transforms (CWT). Each domain has its strength and weakness for analysis, and these are highlighted briefly in Table 2.7.

Hudgins et al. (1993) have proposed the most useful features used in the TD. However, those do not fit with the natural behaviour of the EMG signal, which is time varying. Several studies have subsequently been reported employing TD, FD as well as TFD techniques. The performances of these approaches with features extracted are assessed and compared. However, no study was performed for determining the best features contained both in the forearm and upper arm muscles.

Table 2.7: The preview of analysis domain of EMG signals

Domain	Advantage	Drawback	Notes
Time	Simple, low computational cost, and easy implementation	Unable to deal with non stationarity (time varying) property of EMG signal	“Most cases preferred TD features based for their low complexity, which is desirable for real time implementation.”
Frequency	Good frequency localization and suitable for EMG signals	some FD features have the same discrimination in TD	“EMG features based on FD are not good in EMG classification.” Thongpanja et al. (2012a)
Time-Frequency	Good time and frequency resolutions	Complex, expensive, require more processing time	“The performance of TFD features is similar to that of TD features.” Hargrove et al. (2007)

[Thongpanja et al. \(2012a\)](#) have suggested that EMG features based on FD were not good enough in EMG signal classification. They provided a detailed review and theoretical background of 37 features and pointed out the best features to be used in the EMG study to avoid redundancies in using those features. However, their study did not take MF into consideration. This probably may differ as the different strategy may propose a new finding in the analysis.

2.5.2 Classification

Classification of surface EMG from both forearm and upper arm offers more intuitive and reliable information for purposes of control. In general, it is agreed that various classification algorithms such as ANN, linear discriminant analysis (LDA), k nearest neighbour (k-NN), support vector machine (SVM), multi-layer perceptron (MLP), Extreme Learning Machine (ELM) and others give a similar performance in terms of accuracy. It remains whether there are other optimal and suboptimal feature sets for classification that are yet to study. This has been listed as in Table 2.6.

[Hargrove et al. \(2007\)](#) has classified ten classes of isometric contraction from surface EMG, and intramuscular EMG collected simultaneously. They concluded that there is no difference in classification accuracy from both types of EMG forearm muscles. They also suggested that to achieve optimal classification accuracy, the number of channels should be within three channels only. [Khezri and Jahed \(2009\)](#) designed a unique classification system for rehabilitation purposes using a combination of two classifiers ANN and fuzzy

inference system (FIS) yielding a new adaptive neuro-fuzzy inference system (ANFIS). The proposed classification algorithm successfully produced useful identification for six types of hand movements.

[Khushaba and Kodagoda \(2012\)](#) have investigated multi features classification performance based on the feature reduction algorithm mutual component analysis (MCA). The developed feature reduction yielded a satisfactory result. Several studies have been conducted similarly to this work but using different feature reduction technique ([Al-Angari et al. \(2016\)](#); [Anam et al. \(2013\)](#); [Geethanjali \(2015\)](#)). Despite recent development and research studies that have been discussed in [Bai et al. \(2019\)](#); [Resnik et al. \(2018\)](#), there is a significant gap found in the study methodology and the features proposed in these studies.

An intuitive approach to achieve better classification performance is thus needed. The new strategy adopted for this study consists of several aspects; signal acquisition protocol features extraction and classification. For this study, time and frequency domain (TD and FD) approaches are employed in the preliminary study. The study will then look into details in the time-frequency domain (TFD) using wavelet transform. Wavelets are the most applicable analysis technique for signals such as EMG. Wavelets necessitate the time and frequency components of a time-varying signal. It presents better time and frequency resolutions for the classification technique. These approaches will improve the gap of the previous study mentioned earlier.

2.6 Summary

This chapter presents details of the literature reviews on this study. This involved discussions on previous research study, the outcomes and the methodologies used or available for the reference. The human upper forearm based EMG signal model, characteristics, fatigue manifestation and muscles coordination also discussed in details to give an overview about the study interest. The research reviews based on EMG topics were discovered and tabulated in tables to provide better analysis of the methodologies, analysis and muscles chosen.

Chapter 3

Research methodology

3.1 Introduction

The research methodology has been developed based on the objectives of the study stated earlier. This will be executed to achieve the main goal of the study, human UFA analysis, classification, and validation. For the objectives as mentioned earlier, a research study is implemented to unlock a new set of dilemmas related to the multi-region of human UFA muscles and classification based control is adapted to establish the relationship between both regions. There is always the need to develop a scientific methodology, tools and equipment used in this study. The approach that have been developed in this methodology will be thoroughly described in this chapter. The proposed research methodology is executed in five stages, as shown in Figure 3.1. The stages are divided based on the objectives of the study, stated in Section 1.5. For the first stage, the development of the new data acquisition protocols, muscle selection, and data collection will be performed. The second stage includes signal conditioning and preprocessing technique for establishing the relationships among EMG upper forearm, force variation, %MVC and wrist angle. The development of suitable feature extraction, feature reduction and selection of suitable classifier are in stage 3. Analysis and evaluation of the overall classification performance and validation of classification performance through the modelled control system will be carried out in stages four and five, respectively.

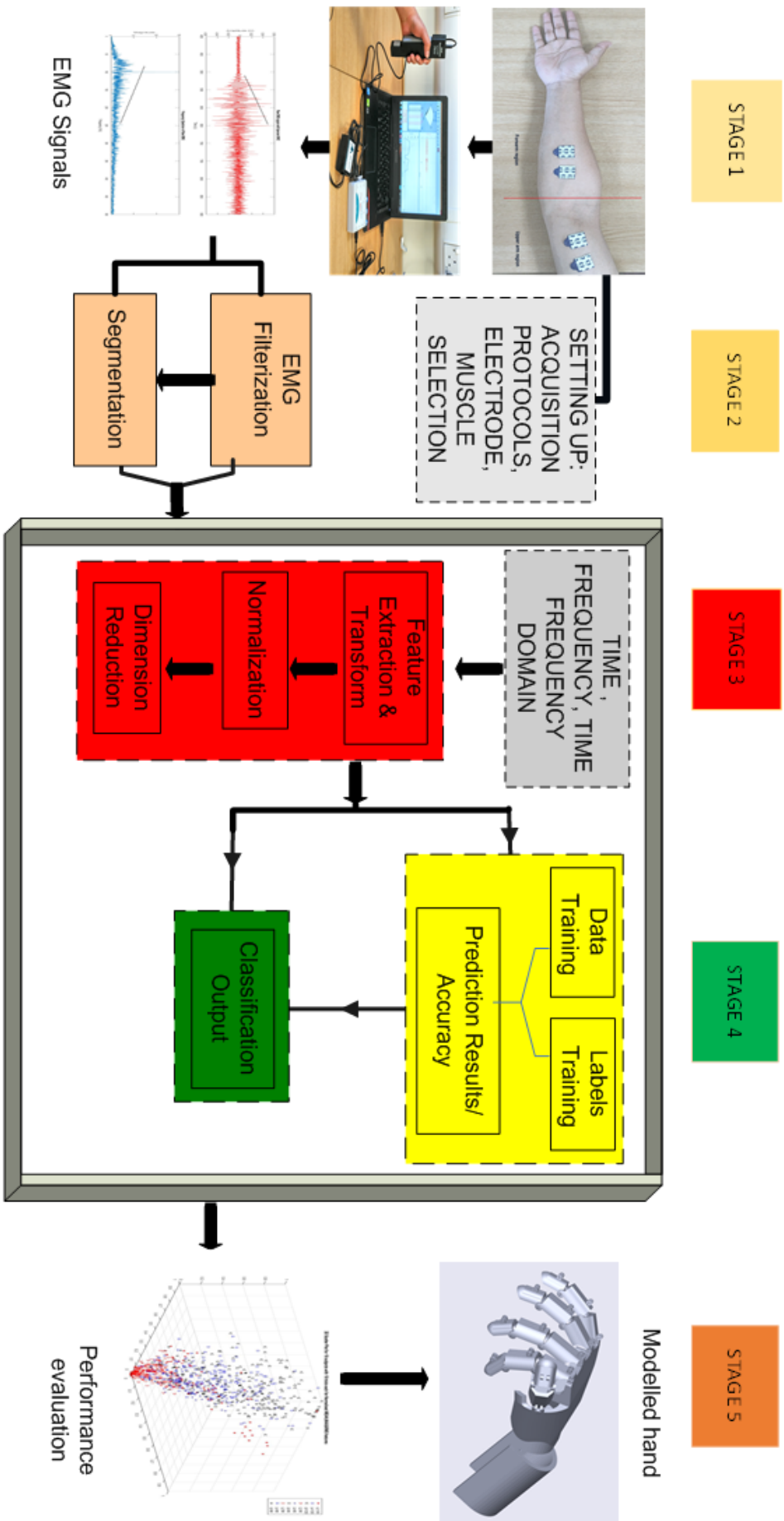


Figure 3.1: Block diagram of the research methodology proposed in this study

3.2 Surface EMG under European recommendations

The real issue in using a signal such as EMG in the analysis is their main source of origin. This has been debated for many years by researchers worldwide since 1900. The works of literature related to this kind of matter were so limited, until in 1996 a group of researchers proposing the SENIAM to publish a recommended standard for EMG detection. This project run from 1996-1999. The full report of this project was published in 2000, which was fully funded by the European Commission (BIOMED II-Program) (Merletti (2000)). Since then, recommendations of the report have been used as the main reference for any activities related to surface EMG.

There are two objectives created from this project, firstly as the knowledge transfer and exchange between a researchers from different countries. The common interest also can be shared from this kind of activity. Secondly, to develop recommendations on essential elements which include experimental results or clinical data. The important elements may include sensors, experimental procedures, signal processing as well as their modelling strategy.

The main issues discussed in report were suggestion on manufacturing electrode and their shape or size. The electrodes to be used in this topic has to well adhere to the skin surface so as to reduce the effect of noise. Meanwhile, they also recommended suitable inter-electrode distance and the electrode material. Additionally, factors such as patient comfort, sensor or electrode placement, including skin preparation have to be taken into consideration. This will guarantee good protocols for EMG detection and taking care of patient welfare. Their recommendations for surface EMG sensors are listed in Table 3.1.

The recommendations as suggested above are followed in the current study for data collection. The electrode used in this study was developed by using good materials, such as Ag/AgCl. It has pre-gelled surfaces, to help the electrode fixed at their position and maintain good contact with the skin. The electrodes used are to have low impedance and steady performance in their transition. The electrode size should be 10mm or less. The electrode used in this study is shown in Figure 6.5c. This electrode is commercially available in the market.

Another criterion followed is the gap between two differential EMG channels or known as the inter-electrode distance (IED). The IED is the distance of the centre to centre of two electrodes. It has to be at minimum of 20mm or a quarter from overall muscle length. This is shown in Figure 6.5d. Figure 6.5f shows an example of one EMG channel and its bipolar properties, the reference point for ground used in this study.

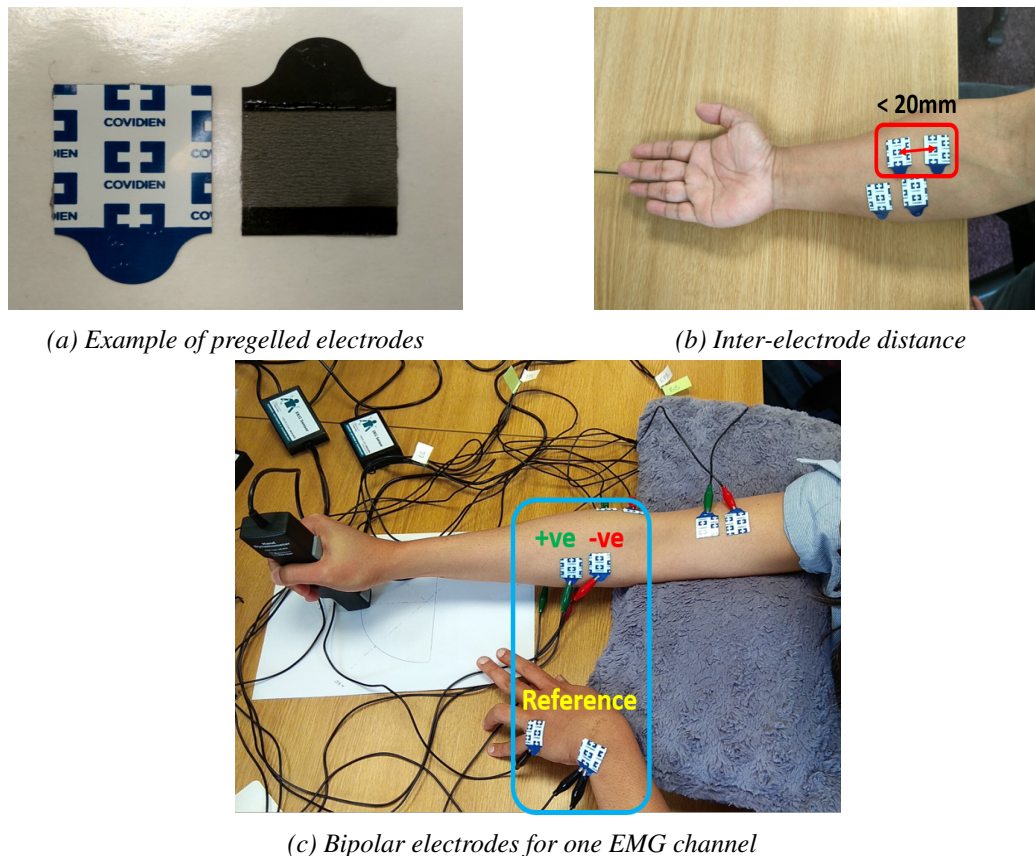


Figure 3.2: Illustrations of electrodes setup and its configurations as recommended by SENIAM used in this study. The details of these muscle selection can be found in Appendix A.

Before starting the procedure, SENIAM recommends for the subject skin preparation if they were needed, such as the hairy region. The skin also needs to be clean using alcohol to remove the dead tissues available on the skin surface. This step will help to obtain right EMG signals, at minimum power or noise interference. Hence, it will give the smaller common mode signals and better signal to noise ratio.

Furthermore, subject positioning plays an important role as it will reduce the motion artefacts during the EMG data collection. In this study, the subject were advised to attain their comfortable position as long as they never change the initial hand positioning during

Table 3.1: Summary of the recommendations proposed by SENIAM for most of the study involving the EMG signal. This recommendations recognised as a standard for many researchers in their reporting or analysis.

Parameter	SENIAM Recommendations
Electrodes	
1. Size	Diameter < 10mm
2. Electrode Distance	< 20mm or quarter the muscle length, whichever is smaller
3. Location	forearm and upper arm muscle regions
4. Reference	an electrically inactive region such as wrist or ankle
Amplifier	
1. Filter: High pass	threshold for frequency analysis < 10 Hz threshold for EMG movement analysis 10 Hz - 20 Hz
2. Filter: Low pass	threshold for basic applications 500 Hz (frequency sampling > 1000 samples per second) cut off for special wide band applications 1000 Hz (frequency sampling > 1000 samples per second)
3. Gain	Suitable to bring the signal into the input range of the A/D converter with desired input resolution
Sampler and A/D converter	
1. Frequency sampling	> 1000 samples per second for general applications > 2000 samples per second for wide band applications
2. Number of bits A/D	12 (requires amplifier with variable gain) 16 (fixed gain amplifiers may be used)

the task. This will give the subject more freedom as a different subjects have different types of excellent position for relaxing. The subject has to be in calm, relaxed and comfortable position before data collection begins. Examples of subject preferable position before the data collection are shown in Figure 3.3.

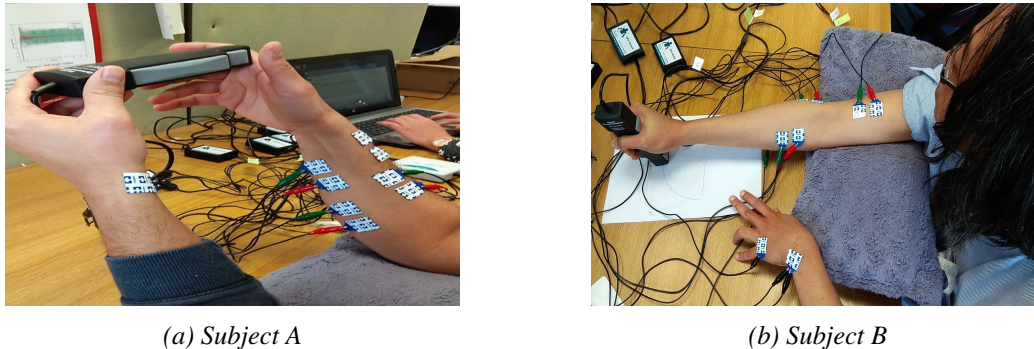


Figure 3.3: Subjects at their preferable positioning before EMG data collection begin. Experimental protocol revealing the wrist inserted by pillow aid that stopped the subject from pronating the wrist. Each volunteered subject, following a period of familiarisation with the protocol, completed 20 trials of each hand grasp task. Movements were auditory paced every 5s. Each hand movement collected in a different run. At least 5 min of rest was provided between each series, and it has been prolonged upon the subject's request.

3.3 Development of new EMG data acquisition protocol

This section presents the development of a new data acquisition protocol for this study. There are lots of acquisition protocols suggested for this kind of research. However, the acquisition protocol published by many; they only refer to single region on muscle detection. Since the focus is to establish the relationship between two regions of muscles at one time, the new data acquisition of EMG signals of the human UFA is crucially needed. Hence, new acquisition protocols using multichannel EMG acquisition system was formed for this study. The EMG acquisition and their protocols were explicitly developed for this study with reference to SENIAM recommendations (Section 3.2), while requirement and considerations are discussed in the next subsections.

EMG acquisition system

This subsection describes the overall data acquisition used in this study. The data acquisition system was chosen based on the criteria and specification needed in order to achieve the scientific investigation proposed. The data acquisition system consists of the parts listed in Table 3.2. The overall system is shown in Figure 3.4.

Table 3.2: Data acquisition system and accessories or tools used in this study.

Item	Accessories details
1	One unit LabQuest Mini data acquisition
2	Five units EMG sensors and cables
3	One unit Hand Dynamometer
4	One unit of computer with battery powered with Logger Lite software
5	Disposable Ag/AgCl electrodes (Kendall 5400)
6	MATLAB software R2015b by MathWorks (License number : 976008)
7	USB connector cables
8	One unit stop watch
9	One unit dumbbell with variable weight

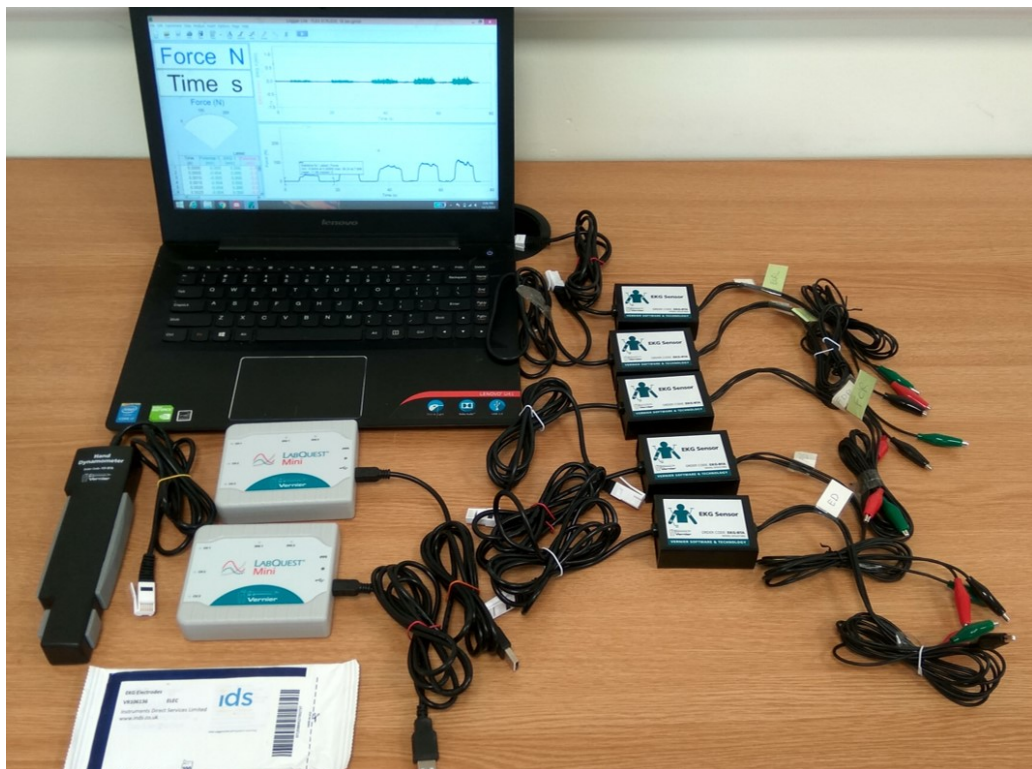


Figure 3.4: The overall acquisition system used in this study. The wires and cables are not in the connected as this illustration is only for clarification

Labquest mini

LabQuest mini is a powerful data acquisition system produced by Vernier Software and Technology, USA (Vernier Software Technology (2019c)). LabQuest Mini is a multi-channel, data collection interface that can be used to acquire data from Vernier sensors on multiple platforms, such as Windows and Mac computers and Chromebook. LabQuest Mini recommends a wired (USB) connection only.

This is an affordable, versatile data acquisition system and easy to use with sensor interface to collect EMG data while attached to a computer. It comes with 12-bit resolution and 5V input data acquisition. It also has three analogue inputs and two digital inputs. Figure 3.5 and Table 3.3 shows the LabQuest mini system and its specifications used in this study.

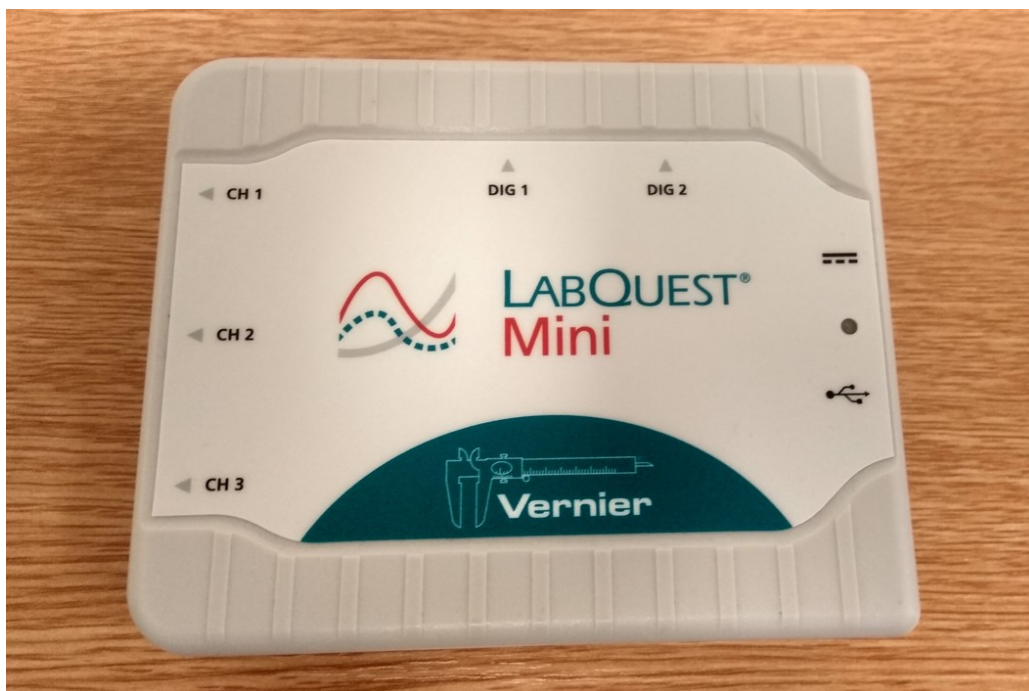


Figure 3.5: The LabQuest Mini interface contains five (5) input sensors with three analog ports (CH1–CH3), two digital ports (DIG1 and DIG 2), a mini-USB connection, and a power adapter port (no main electrical power will be used in this study)

In this study, only the analogue ports were used as input. Since EMG signals are required to be collected from several muscles (5 muscles) at one time, two Laquest mini had to be used in the data acquisition to acquire EMG signals from five channels sensor and one from the hand-dynamometer. The Labquest mini works with its own software

Table 3.3: The technical specifications for LabQuest mini data acquisition system used in this study.

Criteria	Specification
Inout voltage	5V
Resolution	12 bit
Connection	USB 2.0
Maximum sample rate (Computer)	100,000 samples per second (for one sensor) 10,000 samples per second (two or more sensors)
Maximum sample rate (Chromebooks)	10,000 samples per second
Minimum sample rate	0.00125 samples per second (800s/sample)
Size	8.6 cm × 10.5 cm × 2.7 cm
Weight	100g

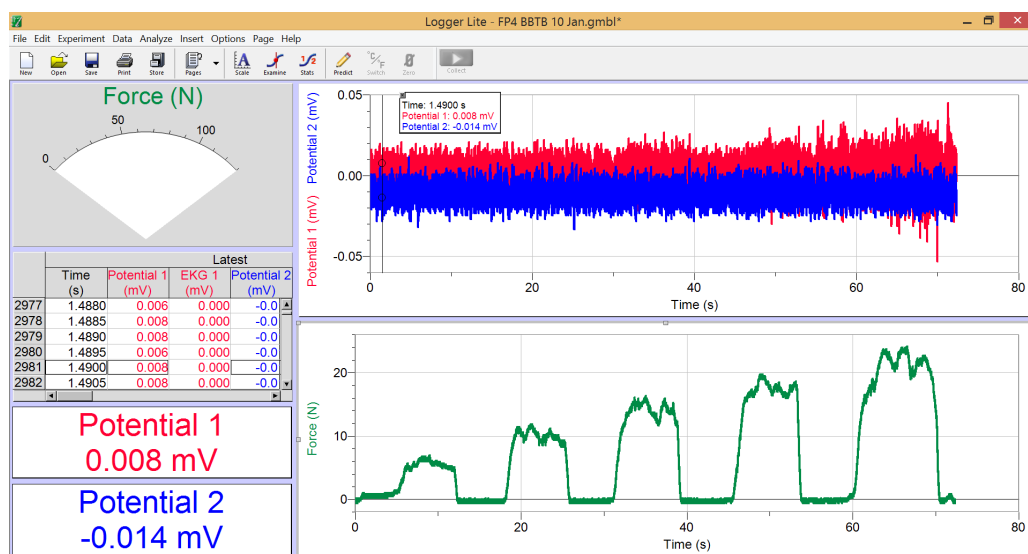


Figure 3.6: The Logger Lite software graphical user interface (GUI). This GUI will guide the subject during the data collection and makes it easy to attain a certain amount of force needed to be exerted during the session.

called Logger Lite. The graphical user interface (GUI) produced by this software is shown in Figure 3.6.

Subject preferences

The subjects are either males or females and aged between 20 – 40 years old. The subjects chosen must be normally limbed without any neuro-muscular problems. The subjects will be asked about their dominant hand, and will be briefly explained (orally or using visual aid, ie recorded video) and provided with informed consent prior to the study. The selection criteria of the subjects are shown in Table 3.4.

At the initial stage, the subject was asked to perform each pre-set hand movement

Table 3.4: The subject preferences for the study.

Criteria	Description
Gender	Male and Female
Age	20 to 40
Weight (kg)	60 to 90
Height (cm)	160 to 180
Health	Normal Limbed
Subject Hand	Dominant Hand or Arm

Table 3.5: Subjects configurations and their specific average 100 %MVC profiles listed for references. Most of the subject shown high variations in the force produced when they were asked for full exertion of muscle contraction.

Subject	Gender	Hand Movement at 100% MVC						
		FP1	FP2	FP3	FP4	HGN	HGF	HGE
1	F	55.8	56.5	34.89	25.78	128.4	75.37	62.65
2	M	75.3	45.63	42.88	30.15	121.7	119.6	101.6
3	M	69.5	38.2	32.6	25.4	125.5	96.5	83.7
4	M	112.2	65.18	59.65	34.21	269.5	234.8	217.4
5	F	68.81	63.92	35.32	18.57	152.5	112.7	103.3
6	M	139.2	126.2	53.96	45.7	267.2	175.3	168.4
7	F	62.41	41.85	24.9	22.71	243.2	146.3	139.3
8	M	114.2	74.74	68.59	45.28	240.7	195.6	210.8
9	M	51.85	41.67	25.14	23.66	190.4	119.8	99.07
10	F	46.3	43.56	34.58	21.64	93.21	80.33	61.85
11	F	17.40	15.40	12.73	8.70	28.3	25.50	22.22
12	F	9.52	8.89	6.63	5.45	12.78	9.23	7.55
13	M	112.3	69.22	55.87	34.36	336.5	187.3	148.8
14	M	48.55	36.45	28.32	25.12	209.5	151.8	126.6
15	M	52.52	38.55	30.65	27.22	212.7	159.45	129.3

* F= Female, M= Male

* Unit is in Newton (N)

with maximum force to determine their MVC force. This was done with the best of their capability, for three times with 5 minutes rest interval. The final average value was taken as their final 100 %MVC force. The average of full exerted MVC data for each subject has been tabulated as in Table 3.5. The subject consists of 15 subjects comprised of nine (9) males and six (6) females. Table 3.6 shows an example of one subject proportional MVC value in force exertion for the task.

Table 3.6: The example of a subject MVC's and proportional value in force exertion

Name		Subject 1					
MVC for FP1:		55.88					
MVC for FP2:		56.5					
MVC for FP3:		34.89					
MVC for FP4:		25.78					
MVC for HGN:		128.4					
MVC for HGF:		75.37					
MVC for HGE:		62.65					
MVC	FP1	FP2	FP3	FP4	HGN	HGF	HGE
20%	11.176	11.3	6.978	5.156	25.68	15.074	12.53
40%	22.352	22.6	13.956	10.312	51.36	30.148	25.06
60%	33.528	33.9	20.934	15.468	77.04	45.222	37.59
80%	44.704	45.2	27.912	20.624	102.72	60.296	50.12
100%	55.88	56.5	34.89	25.78	128.4	75.37	62.65

EMG sensor and cable

The Vernier EKG (Electrocardiogram or ECG) sensor acquires muscle potentials (voltages generated through the contraction of muscles) or heart ([Vernier Software Technology \(2019a\)](#)). The expression used as EKG is since the heart is one kind of muscle. It is just a notation to differentiate between the heart and the muscle. Figure 3.7 and Table 3.7 show the EKG sensor and its specifications.

The green and red heads are attached to a high-gain differential amplifier in the sensor that has been optimised for measuring bioelectric signals. The high-gain amplifier circuit that contains bioelectric signals is electrically isolated from an output circuit that sends data to the software. This gives the device safe and without any electrical shock for human use. The list of activities and experiments that can be performed using this sensor are listed as:

- i. Compare and measure subject surface biosignals or waveforms such as EMG and EKG.
- ii. Study contractions of muscles (EMG) in the arm, leg, or jaw.
- iii. Correlate measurements of grip strength and electrical activity with muscle fatigue.



Figure 3.7: The EMG sensor and cable that has been used in this study.

Table 3.7: EKG sensor and cable that has been used in this study.

Criteria	Specification
Offset	$\sim 1.00 \text{ V } (\pm 0.3 \text{ V})$
Gain	$1 \text{ mV body potential} / 1 \text{ V sensor output}$

Hand dynamometer

The hand dynamometer is a device or sensor which measures the force or strength exerted by the hand grip or finger pinches. The operation of hand dynamometer is quite simple and it also can be referred to as force sensor (Vernier Software Technology (2019b)). The subject needs to squeeze the sensors designed for hand grip and finger pinch separately.

Figure 3.8 shows the hand dynamometer sensor with specially designed buttons for separate tasks of hand grip and finger pinch (red circle). The corresponding specifications are given in Table 3.8.



Figure 3.8: The hand dynamometer that has been used to measure force exertion from the subject. This sensor uses the analogue port as its input. Unique design for a separate task can be seen in the figure, as highlighted in the red circles. The small circle represents the force sensor location for the finger pinch and the bigger circle designed for hand grip force.

Table 3.8: Hand dynamometer specifications used in this study. The maximum force this device can handle is up to 850 N. Force exceeded the maximum value may break the sensor.

Criteria	Specification
Accuracy	$\pm 0.6 N$
Power	$7 mA @ 5V DC$
Typical resolution	$0.2141 N$
Safety range	0 to 850 N
Operational range	0 to 600 N

Muscle selection

To have the best muscle selection for achieving the objective of the study, care has to be exercised to consider all the muscles available in the human UFA region. This will involve assessment strategies reported in the literature as well as those devised in this study.

It is believed that for multi-movement, the relationship between both regions of muscle is not as simple as a single movement where muscle amplitude is directly proportional to the force produced. For multi-movement, the simple relationship does not occur, as the movement does not depend solely on the specific muscle region, but also on another neighbourhood muscle. This is also believed to have happened in human arm joint variations.

It is aimed to have the minimum number of muscles selected for the study. The muscles selected will be tested by comparing each other. This will be implemented for all the subjects in future data collection. The initial research was performed for muscle selection, as discussed in Chapter 5. The ethical approval from The University of Sheffield Ethical Committee has been granted successfully.

The development of the new data acquisition protocol, muscle selection, and trial data collection performed and has shown satisfactory outcome.

3.4 Introduction to data collection

This data collection relates to several PhD projects together under Prof. M. Osman Tokhi's supervision in the Department of Automatic Control and Systems Engineering (ACSE), The University of Sheffield. The research students are Wan Mohd Bukhari Bin Wan Daud and Norafizah Abas. The purpose of this data collection is to investigate the interrelation between the forearm and upper arm EMG signals handgrip force, finger pinches, wrist angles, and curl exercises. This will be used for signal processing and analysis, and fed into the design of assistive exoskeleton hand control. The EMG signals are extracted from human upper forearm muscles using a non-invasive technique. A series of experiments are designed to collect the EMG signals for various hand grip force and wrist angle movement, from fifteen subjects. The subjects are either males or females and aged between 20 – 40 years old. The subjects chosen must be normally limbed without any neuro-muscular problems. All subjects will be briefed (orally or using a visual aid, i.e. recorded video) and provided with informed consent before the study. There are four experiments incorporated in this data collection: i) extraction of EMG signals from forearm muscles contributing

to the finger(s) pinching at various wrist movements, ii) extraction of EMG signals from the forearm and upper arm muscles providing to the hand grasping, wrist movements, and curl exercises, iii) extraction of EMG signals from the forearm and upper arm muscles contributing to pronation and supination of hand with curl exercises, vi) extraction of EMG signals from upper arm muscles contributing to curl exercises alone.

3.4.1 Pre-task protocols

1. Subject's weight, height, and hand length are measured and recorded for reference.
2. Subjects are seated in an armchair, with their forearm supported and secured at one position to withdraw the influence of varying limb positions on the generated EMG signals.
3. The areas of the skin where the electrode patches are placed are scrubbed with a paper towel to remove skin oil and moisture. (Detailed skin preparation procedures will only be carried out if necessary) The electrode patches (Kendall 5400 Diagnostic Tab Electrodes) used for the data collection are specifically designed for the most diagnostic application. No extensive skin preparation procedure is needed since the electrodes comprised of:
 - a. Conductive adhesive hydrogel to provide firm adhesion, reposition ability and low impedance for clear, reliable tracing as well as minimising adhesive residue to facilitate subject clean up.
 - b. Different adhesive levels to accommodate different skin types, application and monitoring situations
 - c. Laminated Carbon Vinyl to provide conformability to the skin, torsion relief and radiolucency
 - d. Silver/Silver Chloride (Ag/AgCl) sensing element to assist in making the electrode defibrillation recoverable.

4. Electrode patches are placed on the selected forearm and upper arm muscles (Figure 3.9 on subject's dominant hand and connected to the LabQuest mini data acquisition through the interfacing wire (3channels; red, green and black wire with alligator clip as shown in Figure 3.10). The red (or positive) alligator clip is connected to the electrode patch that measures the muscle activation while the green (or negative) alligator clip is connected to the other electrode patch on the same muscle within 24mm in distance between each electrode. The black (or reference) alligator clip is connected to electrode patch that is placed at the reference point (near to bone).
5. Hand dynamometer is connected to the LabQuest mini data acquisition and it is connected to a computer (battery powered).
6. Logger Lite software is launched and the hand dynamometer is calibrated. The raw EMG signals are recorded via Logger Lite software for further analysis.

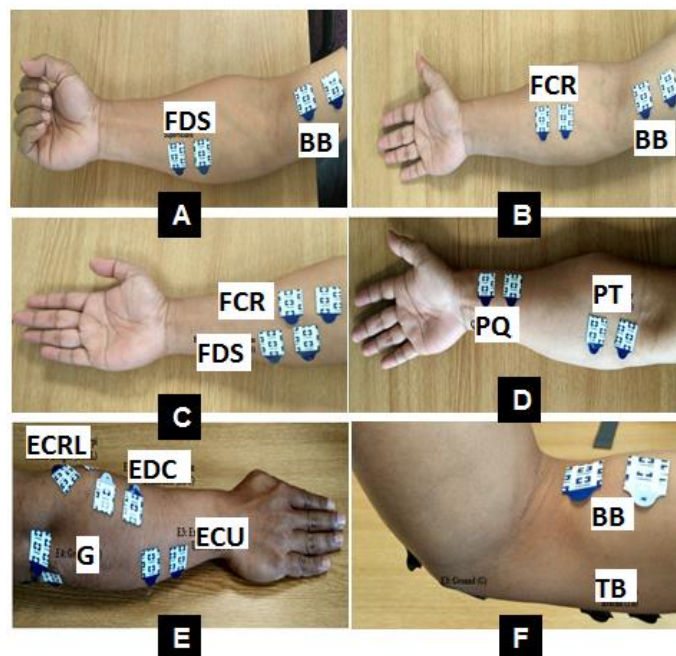


Figure 3.9: Example of electrodes placement for the forearm and upper arm muscles as recommended by SENIAM (Merletti (2000); Merletti and Hermens (2000)); (A, B, D and F) Electrode placement for the selected forearm and upper arm muscles involved in pronation and supination with curl exercises, and (C and E) electrode placement for the selected forearm muscles involved in finger(s) pinching and hand grasping. The 11 muscles involved in this study are: FDS, FCR, FCU, FPL, PT, PQ, ECRL, EDC, ECU, PT, and PQ.

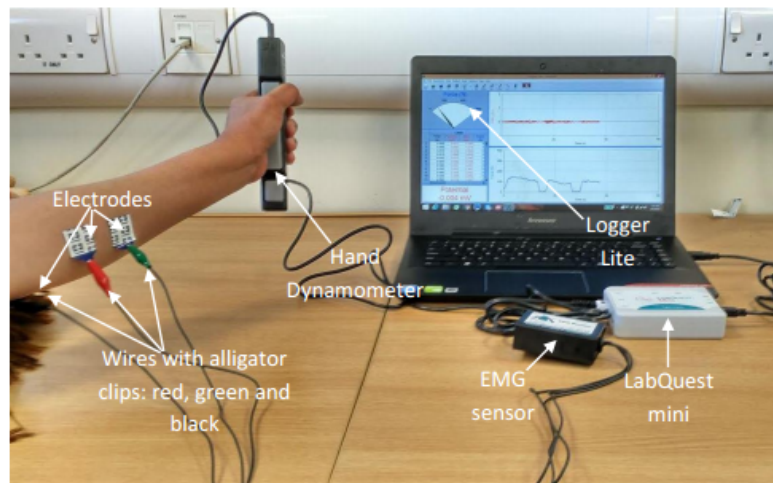


Figure 3.10: Experimental setup for EMG data acquisition system developed by Vernier

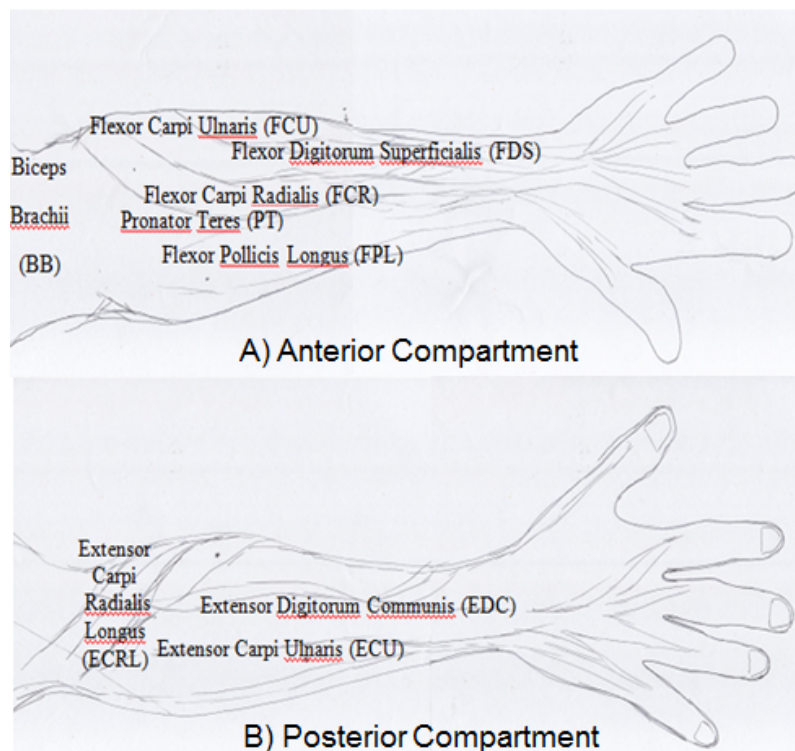


Figure 3.11: Sketch for a human upper forearm muscles under consideration for the study proposed; A) Anterior compartment and B) Posterior compartment.

3.4.2 Muscle Selection Protocol

The muscle selection completed by using practical assessment and analysis described below. The muscles are illustrated in Figure 3.11. Below are the protocol developed for the muscle selection:

- i. Electrodes are placed at the identified areas for each respective forearm muscles on subject's dominant hand as shown in Figure 3.11.
- ii. Subjects are instructed to grasp the hand dynamometer at maximum strength. The maximum hand grip force is recorded and considered as subject's maximum voluntary contraction (MVC).
- iii. Then, the subject is instructed to grasp (for 10 seconds) the hand dynamometer at various hand grip strengths (20, 40, 60, 80, and 100% of MVC) and also at various wrist positions (60°, 90°, and 120°). Rest sessions (for 5 seconds) are incorporated within the experiments to prevent muscle fatigue.
- iv. The raw EMG signals extracted are recorded in Logger Lite software for further analysis.

3.5 Experiment 1: Extraction of EMG signals on human upper forearm muscles contributing to the finger(s) pinching at various wrist movements

There are four (4) groups of finger pinches (Figure 3.12) involved in this study: index finger pinch, middle finger pinch, ring finger pinch and little finger pinch, at various wrist angles. Fifteen (15) classes of datasets are collected at different finger pinch strengths (20, 40, 60, 80, and 100% of MVC) and also at various wrist positions (60°, 90°, and 120°) until fatigue occurs. The data is collected for five datasets at each session to get a high number of input data for classification input.

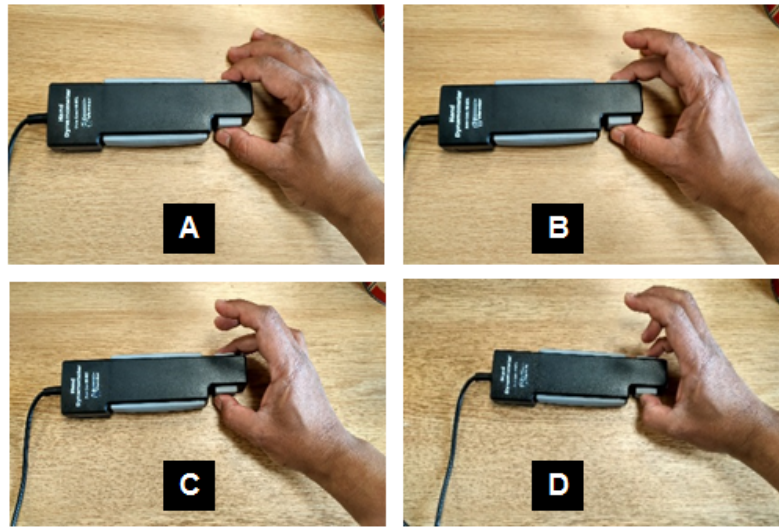


Figure 3.12: Finger pinches muscle contractions of forearm with four groups of movements: (A) index finger pinch, (B) middle finger pinch, (C) ring finger pinch and (D) little finger pinch.

3.5.1 Experimental protocols

- i. Subjects are instructed to pinch (for 5 seconds) the hand dynamometer using different finger groups (index finger pinch, middle finger pinch, ring finger pinch and little finger pinch) with maximum pinch strength. Rest sessions (for 5 seconds) are incorporated within each pinch to prevent muscle fatigue. The maximum finger pinch strengths for each finger group are recorded and considered as the subject's maximum voluntary contraction (MVC).
- ii. Electrode patches are placed on the selected forearm muscles (Figure 3.11A and Figure 3.11B). Then, the subjects are instructed to pinch (for 5 seconds) the hand dynamometer using different finger groups with various pinch strengths (20, 40, 60, 80, and 100% of MVC) at 90° of wrist angle (Figure 3.12A to Figure 3.12D). Rest sessions (for 2 seconds) are incorporated within each pinching to prevent muscle fatigue.
- iii. The raw EMG signals extracted are recorded in Logger Lite software for further analysis.
- iv. Steps 2 and 3 are repeated for different wrist angle positions (at 60° and 120°).
- v. Next, the steps 1 to 4 are repeated for different pinching strength (for approximately

10-15 second or until fatigue) with rest intervals (for 5 seconds).

3.6 Experiment 2: Extraction of EMG signals on human upper forearm muscles contributing to the hand grasping, wrist movements and curl exercise

There are six (6) groups of movement involved in this study: hand grasping at different wrist positions (at 60° , 90° , and 120°) (Figure 3.13A to Figure 3.13C), and hand grasping at different curl exercise positions (at 60° , 90° , and 180°) (Figure 3.13D). 30 classes of datasets are collected at different hand grip strengths (20, 40, 60, 80, and 100% of MVC) at various wrist positions and curl exercises until fatigue occurs. The data is collected for five datasets at each session to get a high number of input data for classification input.

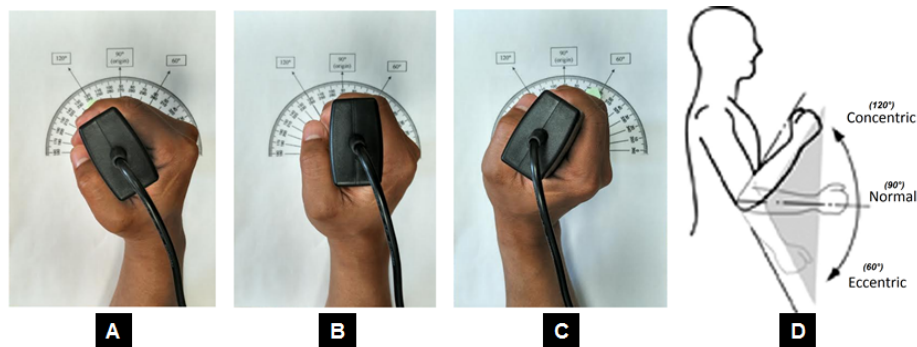


Figure 3.13: : Hand gripping positions for hand dynamometer at various wrist angle positions: (A) at 120° (B) at 90° (C) at 60° , and (D) curl exercises.

3.6.1 Experimental protocols

- i. Subjects are instructed to grasp (for 5 seconds) the hand dynamometer with maximum hand grip strength. Rest sessions (for 5 seconds) are incorporated within each grasp to prevent muscle fatigue. The maximum handgrip strengths are recorded and considered as the subject's maximum voluntary contraction (MVC).
- ii. Electrode patches are placed on the selected forearm muscles (Figure 3.11A and Figure 3.11B). Then, the subjects are instructed to grasp (for 5 seconds) the hand

dynamometer using different hand grip strengths (20, 40, 60, 80, and 100% of MVC) at 90° of wrist angle (Figure 3.13A to Figure 3.13D). Rest sessions (for 2 seconds) are incorporated within each grasping to prevent muscle fatigue.

- iii. The raw EMG signals extracted are recorded in Logger Lite software for further analysis.
- iv. Steps 2 and 3 are repeated for different wrist positions (at 60° and 120°).
- v. Next, the steps 2 to 4 are repeated for different curl exercise positions (at 60°, 90°, and 180°).
- vi. Finally, the steps (step 1 to 5) are repeated for different grasping time (for approximately 10-15 second or until fatigue) with rest intervals (for 5 seconds).

3.7 Experiment 3: Extraction of EMG signals on human upper forearm muscles contributing to pronation and supination of hand with curl exercise

There are six (6) groups of movement involved in this study: pronation and supination at different curl exercise positions (at 60°, 90°, and 180°). 30 classes of datasets are collected at different hand grip strengths (20, 40, 60, 80, and 100% of MVC) at various wrist positions and curl exercises until fatigue occurs. The data is collected for 5 datasets of each session in order to get a high number of input data for classification input.

3.7.1 Experimental protocols

- i. Subjects are instructed to grasp (for 5 seconds) the hand dynamometer with maximum hand grip strength. Rest sessions (for 5 seconds) are incorporated within each grasp to prevent muscle fatigue. The maximum hand grip strengths are recorded and considered as subject's maximum voluntary contraction (MVC).

- ii. Electrode patches are placed on the selected forearm and upper arm muscles. Then, the subject is instructed to grasp (for 5 seconds) the hand dynamometer using different hand grip strengths (20, 40, 60, 80, and 100% of MVC) with supination at 90° of curl angle. Rest sessions (for 2 seconds) are incorporated within each grasping to prevent muscle fatigue.
- iii. The raw EMG signals extracted are recorded in Logger Lite software for further analysis.
- iv. Steps 2 and 3 are repeated for different wrist positions (at 60° and 120°).
- v. Next, the steps 2 to 4 are repeated for different curl exercise positions (at 60° and 180°).
- vi. Finally, the steps 1 to 5 are repeated for different grasping time (for approximately 10-15 second or until fatigue) with rest intervals (for 5 seconds).

3.8 Experiment 4: Extraction of EMG signals on human upper forearm muscles contributing to curl exercise

There are three (3) groups of movement involved in this study: hand grasping at different curl exercise positions (at 60°, 90°, and 180°). 15 classes of datasets are collected at different hand grip strengths (20, 40, 60, 80, and 100% of MVC) for various curl exercises until fatigue occurs. The data is collected for 5 datasets of each session in order to get a high number of input data for classification input.

3.8.1 Experimental protocols

- i. Subjects are instructed to grasp (for 5 seconds) the hand dynamometer with maximum hand grip strength. Rest sessions (for 5 seconds) are incorporated within each grasp to prevent muscle fatigue. The maximum hand grip strengths are recorded and considered as subject's maximum voluntary contraction (MVC).

- ii. The subjects are instructed to grasp (for 5 seconds) the hand dynamometer using different hand grip strengths (20, 40, 60, 80, and 100% of MVC) at 90° of curl angle. Rest sessions (for 5 seconds) are incorporated within each grasping to prevent muscle fatigue.
- iii. The raw EMG signals extracted are recorded in Logger Lite software for further analysis.
- iv. Steps step 2 and 3 are repeated for different curl exercises positions (at 60° and 180°).
- v. Next, the steps 1 to 5 are repeated for different grasping time (for approximately 10-15 second or until fatigue) with rest intervals (for 5 seconds).

3.9 Summary

This chapter presents in details with regards on investigating the development of enhanced approaches for detecting, analysing, and classifying of the human upper forearm EMG signal. These include discussion on the standards procedure in detecting the EMG signal using muscles coordination, positioning, and electrode placement published by SENIAM. Then, the newly developed acquisition strategies have been proposed and implemented for this study. The proposed development includes EMG acquisition system to be used, subject preferences, sensors selection, and muscle selection protocol. The chapter also described in details on the data collection strategies utilised in this study, which has been awarded ethical approval from the Ethical Committee of the University of Sheffield. Several protocols have been developed to consolidate in this study so that the data collected can be used to achieve the objectives of the study. All experiments and data executed in this chapter not necessarily be used in this study.

Chapter 4

Pre-processing, feature and classification based methods

4.1 Introduction

As stated earlier, the proposed new framework of human UFA pattern classification system will offer an intuitive classification and control that will be more robust than the current single region of the human UFA classification. Furthermore, it is believed that this new technique of estimating the correlation between the forearm and upper arm muscles will overcome significant drawbacks such as the trade-off between adjacent muscles and crosstalk. The future steps are to perform and complete the EMG data acquisition from several subjects, carry out the features extraction and pattern classification as well as establish the relationship between human UFA with various hand grip force, MVC and angle. These technique was used by many in the previous studies, and been refered as many as been discussed in Chapter 3. Some methods has been used in this study for further investigation.

4.2 EMG pre-processing

The original source of the EMG signal and their model representation were discussed in Chapter 2. The initiation of MUAPs for EMG signal, manifest the neuromuscular activation by specific muscle contraction and allowed realisation of EMG model. The importance issue in analysing the EMG is based on the approach for interpreting the information

contained within the EMG signal.

This chapter presents the state-of-the-art of the study objectives based on EMG pattern classification. This forms the foundation of the work in this study. An overall block diagram of the study was presented in Chapter 3. The initialisation of the pattern classification for the study starts in stage 2. The signal is conditioned with a proper preprocessing technique such as filtering and signal segmentation. Then in stage 3, the feature extraction will take place as the EMG information content is best to be represented by features. This will include the normalisation and feature reduction if necessary. Then, pattern classification is performed to form the result in stage 4. In the final stage, the classification analysis is assessed to estimate the pattern classification efficiency of the method.

4.2.1 EMG signal conditioning

Various analytical approaches are implemented for the data or signal involved in this study. These include the filtering process, such as eliminating the direct current noise from the signal. The segmentation will be performed as the lengths of segments are the foremost important features that require to be concluded (Asghari Oskoei and Hu (2007)).

Generally, EMG investigations will include two types of segmentation scheme: 1) the disjointed scheme, where adjacent sections of a selected range will be used for the feature extraction and 2) the overlapped scheme, a section which overlapped the current with additional time and must be smaller than selected range.

Figure 4.1 shows an illustration of both the segmentation techniques that may be used in processing the EMG signal. The disjointed and adjacent segments are labelled using the blue arrow with the **L** marker representing the segment length of EMG for the feature extraction. The τ represents the time needed for the process to extract features and the classification. The classification decision, **D** is then decided seconds later. Furthermore, the overlapped segmentation scheme is represented by the red arrow.

The overlapped segment was used in this study for the EMG signal segmentation. The segment length chosen in this scheme is applicable for establishing multi-region characterisation, and the computational problems will be minimised. Studies have revealed that

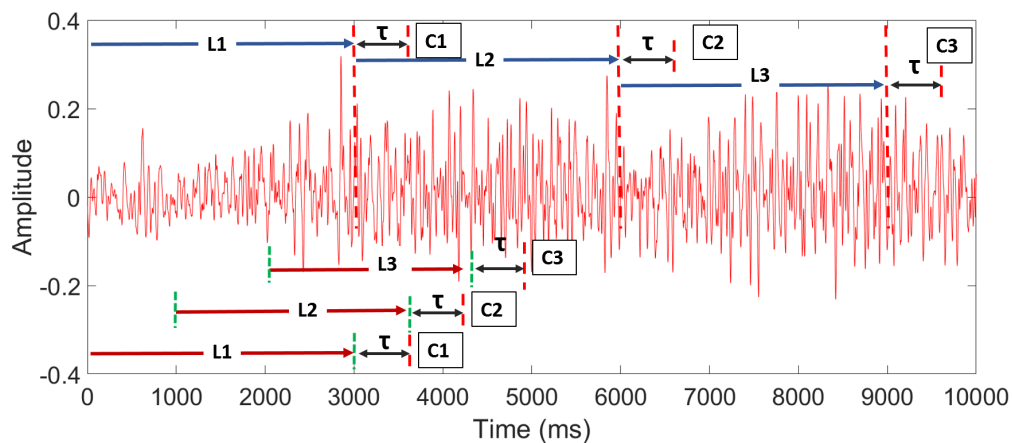


Figure 4.1: Examples of segmentation strategy for EMG data in the preprocessing condition. The blue arrow shows the disjointed and adjacent segmentation while red arrow for the overlapped segmentation. L = window length, τ = processing time and C = classification decision (Asghari Oskoei and Hu (2007); Englehart and Hudgins (2003))

there is a trade-off between the range of the segment used and processing time for classification (Englehart and Hudgins (2003); Farina et al. (2001)). They have concluded that configurable parameters will affect the classification performance, such as window length and time delay. However, the preprocessing of the EMG signal improves the accuracy, but sacrifices response time.

EMG signal were preprocessed digitally before the feature extraction procedure. A technique was employed to minimise the complexity of the processing by using 5s epoch window for each movement. The 5s signal was selected for each hand movement, and all the movements were combined in specific order so that they were correctly labeled. This is illustrated in Figure 4.1. This kind of preprocessing scheme is employed as continuous control of prosthesis requires the feature extraction to be done in a sliding window manner. The 5s epoch of disjointed window was used to ensure that no data was neglected since the acquisition protocols used require the subject to perform hand movement task in 5s time frame. 100ms overlapped window increment was used for the whole signal in the feature extraction process.

4.3 Feature extraction

Feature extraction is considered as the main part of the signal analysis. It gives the most compact and informative set of indicators, especially when dealing with condensed signals such as EMG. Feature extraction is needed in various signal analyses, as the process will produce a new reduced but highly informative set of data to represent the basic raw signal. The EMG signal features are selected to represent details of each segment of EMG data. This will allow the system to be reliable, and its robustness will not be argued.

The feature extraction process in regards of each time window at specific EMG channels will then be combined in global vector to yield the complete sets of the feature that will represent as the EMG pattern for a particular movement or task. [Hargrove et al. \(2007\)](#) stated that the feature extraction stage is crucial as it is the process of extracting the excellent and useful information that lies upon the EMG signal. Therefore, it will produce better separability between each class. Some researchers believe that the perfect choice of EMG features is much better than a good classifier. Various techniques of feature extraction have been utilised by many as previously discussed in Chapter 2.

4.3.1 Time domain features

The time domain (TD) features are known as the most advantageous features and commonly used in many classification studies. The primary benefit is the low complexity associated with extraction procedure, yet producing an outstanding performance as compared to other methods such as FD and TFD. Many studies have proved the usefulness of the TD, especially on their quick and easy implementations, and also without any transformation needed ([Asghari Oskoei and Hu \(2007\)](#); [Hudgins et al. \(1993\)](#); [Thongpanja et al. \(2012b\)](#); [Tkach et al. \(2010\)](#)). The major drawback associated with the TD is that the features are generated from stationary properties of the signal. Hence, the features are likely to have very high variations when dealing with non-stationary signal such as the EMG captured mostly in dynamic movements.

Since the TD features are solely calculated based on the EMG amplitudes, they are

very susceptible to noise acquired during the data collection. The temporal and spectral information is highly essential for differentiating class movements. Moreover, this will be the main criteria for distinguishing the TD and FD performance in the classification. Many researchers have utilised most of these features and it is deserving to note that not all of these features are employed together. The feature are selected for the classification study. Six TD features have been proposed to be used in this study and these are described in detail in the following subsections.

Root mean square

Root mean square (RMS) is modelled as Gaussian process which is akin to the normal muscle contraction procedure (Phinyomark et al. (2009)). It also resembles the standard deviation (SD) method (Phinyomark et al. (2012b)) the mathematical model for RMS is defined as follow:

$$RMS = \sqrt{\frac{1}{N} \sum_{i=1}^N x_i^2} \quad (4.1)$$

where x_i is the EMG signal, while N denotes the sample number of the signal. RMS is one of the most popular features used with EMG analysis (Boostani and Moradi (2003)).

Integrated absolute value

Integrated absolute value (IAV) feature is one of the most well known and commonly used by researchers in EMG signal study. Also known as integrated EMG (IEMG) value and computed using the moving average of the rectified EMG. This feature is also known by many other names such as average rectified value (ARV), mean absolute value (MAV), average absolute value (AAV), and the first order of v -order ($V1$) (Phinyomark et al.

(2012b); Tkach et al. (2010)). IAV is mathematically given as:

$$IAV = \frac{1}{N} \sum_{i=1}^N |x_i| \quad (4.2)$$

where x_i is the EMG signal, while N denotes the sample number of the signal.

Zero crossing

Zero crossing (ZC) is a frequency related in time domain analysis. It is a measure of the spectral component where the number of EMG magnitudes passes the zero amplitude level (Hudgins et al. (1993); Phinyomark et al. (2012b)). To avoid low-voltage fluctuation or background noise, threshold condition is applied and the mathematical definition is:

$$ZC = \sum_{i=1}^{N-1} \left[sgn(x_i \times x_{i+1}) \cap |x_i - x_{i+1}| \geq threshold \right] \quad (4.3)$$

$$sgn(x) = \begin{cases} 1, & \text{if } x \geq threshold \\ 0, & \text{otherwise} \end{cases}$$

Meanwhile, there is one feature that measures the ratio of upward ZC divided by the number of peaks (NP) (Al-Timemy et al. (2015)). This feature can only be measured using their spectral moments (SM); described later in Section 4.3.2 . The corresponding feature can be represented as:

$$IF = \frac{ZC}{NP} = \frac{SM_2}{\sqrt{SM_0 \times SM_4}} \quad (4.4)$$

Waveform length

Waveform length (WL) is a measure of the EMG complexity which is defined as the overall cumulative sum of the differences over each time segment of a signal. Some may define this feature as wavelength (WAVE), and also known as the total value of the absolute derivative signals. The formula for WL is given by,

$$WL = \sum_{i=1}^{N-1} |x_{i+1} - x_i| \quad (4.5)$$

where x_i is the EMG signal, while N denotes the sample number of the signal. Another feature that may be useful in this study and quite close to the WL, is given as waveform length ratio (WLR). WLR is the ratio of WL feature of the first derivative to the waveform length of the second derivative. The WLR definition is defined as:

$$WLR = \log \left(\frac{\sum_{i=0}^{N-1} |\Delta x|}{\sum_{i=0}^{N-1} |\Delta^2 x|} \right) \quad (4.6)$$

Slope sign change

Slope sign change (SSC) has common character as ZC feature. It represents the signal frequency information by calculating the changes of the slope sign (Hudgins et al. (1993)). The positive and negative slopes changes are counted within three sequential within their threshold function. This will avoid noises in the EMG background. The mathematical expression for this feature is:

$$SSC = \sum_{i=2}^{N-1} \left[f[(x_i - x_{i-1}) \times (x_i - x_{i+1})] \right] \quad (4.7)$$

$$f(x) = \begin{cases} 1, & \text{if } x \geq \text{threshold} \\ 0, & \text{otherwise} \end{cases}$$

The suggested value for the threshold parameter of this feature to be chosen is within $50 \mu V$ to $100 mV$ (Boostani and Moradi (2003); Phinyomark et al. (2009)). However, it may differ if the setting for the gain value of the instrument and background noise are not level.

Auto-regressive coefficient

Auto-regressive (AR) feature is based on the statistical approach on the spectral information of the EMG signal, when the peak location is known. It is a prediction models that describes EMG signal as a linear combination of the previous samples x_{i-p} and a white noise w_i (Boostani and Moradi (2003); Phinyomark et al. (2012b)). In many classification model, the AR coefficient is employed as feature vector. The general AR model is defined as below:

$$x_i = \sum_{p=1}^P a_p x_{i-p} + w_i \quad (4.8)$$

where P stands for the AR order at specific autoregressive coefficient a_p . There has been research studies suggested for the best AR order to be used in EMG analysis between fourth order (AR_4) (Boostani and Moradi (2003); Phinyomark et al. (2012b); Zardoshti-Kermani et al. (1995)) to sixth order (AR_6) (Asghari Oskoei and Hu (2007); Hargrove et al. (2007)). In this study, the author selected the AR_6 to be used as one of TD features. AR_6 was best tested with hand movement and finger flexion.

All the six TD features chosen in this study have been widely used by researchers as cited above. The combination of TD features with the AR has been proposed and used in the previous study such as (Khushaba et al. (2010)). They have shown that the feature is

achievable and works better in the classification of the EMG signal.

These features also prove to gain very high accuracy in classification as compared to any FD and TFD in hand movement detection algorithm ([Hargrove et al. \(2007\)](#)). This has been the motivation for this study to choose TD features as described earlier, for application into the EMG signal collected within this framework of research.

4.3.2 Frequency domain features

Frequency domain (FD) is another method that can be used to analyse EMG signal. Frequency or spectral components of a signal represent a transformation of time function to the sum or integral function of sine waves with different frequency bands. This analysis is familiar and well known in many studies, especially with regards to the EMG signal. Different to TD which shows the signal change over time, FD reveals how much signal lies in the frequency band or range.

The spectrum or power spectral density (PSD) of signal is the result of FD transformation, and is mostly used to study MUAPs recruitment ([Arendt-Nielsen and Mills \(1988\)](#); [Beck et al. \(2005\)](#); [Cechetto et al. \(2001\)](#)) or fatigue analysis ([Dalton and Stokes \(1993\)](#); [Doud and Walsh \(1995\)](#)) for EMG signal. PSD is the most useful tool in studying the frequency component of a signal. Different approaches to statistical properties have been applied to the PSD, which is defined as a Fourier Transform. It can be estimated using either periodogram or any other parametric methods.

There are two FD features or PSD variables that have been widely utilised in many research studies, these include mean frequency (MNF), and median frequency (MDF). Other suitable FD variables that can be used are peak frequency (PF), mean power frequency (MPF), total power (TP), frequency ratio, central frequency and spectral moments.

Therefore, six FD features are chosen for investigation in this study. These FD features are described below:

Peak frequency

Peak frequency (PF) is the frequency which attains the maximum power in the spectrum.

It is given as:

$$PF = \max(P_j), j = 1, \dots, M \quad (4.9)$$

where P_j is the power spectrum at frequency bin j .

Mean frequency

Mean frequency (MNF) is defined as the average value of frequency calculated from the sum of spectrum power from the EMG signal and the frequency divided by the total of spectrum intensity (Asghari Oskoei and Hu (2007); Phinyomark et al. (2012b); Sijiang and Vuskovic (2004)). The MNF is also known as central frequency and spectral center of gravity. The MNF is expressed as:

$$MNF = \frac{\sum_{j=1}^M f_j P_j}{\sum_{j=1}^M P_j} \quad (4.10)$$

where f_j is the spectrum frequency at frequency bin j , P_j is the power spectrum at frequency bin j , and M is the frequency bin length.

Median frequency

The division of two equal amplitude of frequency spectra is known as median frequency (MDF). This type of frequency can also be measured as half of total power.

$$\sum_{j=1}^{MDF} P_j = \sum_{j=MDF}^M P_j = \frac{1}{2} \sum_{j=1}^M P_j \quad (4.11)$$

Mean power frequency

Mean power frequency (MPF) is an average power of the EMG spectrum. The model of MPF equation is given as:

$$MNP = \sum_{j=1}^M P_j / M \quad (4.12)$$

Total power frequency

Total power frequency (TPF) is defined as an aggregate of the EMG power spectrum. This is mathematically described as:

$$TPF = \sum_{j=1}^M P_j = SM_0 \quad (4.13)$$

The TPF is also known as zero order spectral moment (SM_0) or can be referred to as the energy (Sijiang and Vuskovic (2004)). If $n = 0$ is applied in the equation above, it will be related to the Parseval's theorem. Therefore, SM_0 is a symbol of the total power in the frequency spectrum (Khushaba et al. (2014)).

Spectral moment

The spectral moment (SM) is another way of extracting the power spectrum from the EMG signal. It is a kind of statistical analysis approach that will produce a new feature based on the power spectrum. The definition for general order of SM_n is given as follows:

$$SM_n = \sum_{j=1}^M P_j f_j^n, n = 1, \dots, n \quad (4.14)$$

where n is the order number of the SM .

The features selected for use in this study are those that enable EMG based control,

attain maximum class separability, show robustness in a noisy environment, and are associated with computationally low complexity. This is crucially needed as the features will have to work in a real-time environment, to yield better pattern classification performance in EMG.

Since the EMG signal is well known for non-stationarity or transitory characteristics, using time or frequency domain alone is not enough for feature extraction. Fourier series gives only the whole time series analysis in one off.

4.4 Statistical analysis

In many research studies, the goal of scientific research must be able to clarify the purpose value of objective endpoint. This endpoint will conclude the level of research values that may indicate the works that have made. Descriptive statistics is one of the best methods for achieving that goal. Such statistical purposes should be used as a model to become habitual for researchers to determine which model they will adopt. In some way, the descriptive statistics are methods to organise, compile and present data in an enlightening way. If this is not taken into account in the research process involving large-scale data, its impact will result in abnormalities in the results of the study.

4.4.1 Descriptive statistic

Descriptive statistics are necessary for many studies involving the biometric analysis and is known as a prior requirement in making inferences or hypothetical evaluations ([Spriestersbach et al. \(2009\)](#)). Descriptive statistics is a process to produce well-presented data for the researchers to get more understanding of their subject of study. This strategy will surely need them to have excellent and accepted practice in their particular field of study.

4.4.2 Correlation coefficients

A linear relationship between two variables is a particular case of a monotonic relationship. Most often, the term “correlation” is used in the context of such a linear relationship

between two continuous variables.

In the biometric analysis, there are two types of the most commonly used to find the correlation coefficients. These are known as Pearson's product moment correlation coefficient and Spearman's rank correlation coefficient. The correct usage of correlation coefficient type depends on the type of variables being studied (Schober et al. (2018)).

Correlation is defined as a way of identifying the reciprocity, relationship, or association between two or more variables. Mathematically, correlation is a statistical approach to measure any possibility of two variable's association, whether it is linear or nonlinear (Mukaka (2012)). Correlation coefficient points the intensity of linear computation and association between the studied variables. Statistically, it calculates the closeness of the two variables co-vary, it merely represents as -1 for the perfect negative correlation, $+1$ as an excellent positive relationship. While through 0 , it means no correlation at all.

4.5 Time-frequency domain

4.5.1 Fourier transform

Wavelets found when Joseph Fourier introduced his theory in spectral study. He elaborated Fourier synthesis which is a method to switch TD, as denoted in TD ($x(t)$) to FD ($X(f)$) as presented in Figure 4.2.



Figure 4.2: The Fourier transform (FT) is the general practice in the measurement of time series signal. The fundamental practice of FT is changing domain of operation in the TD into the FD. (Adapted from Matlab software application)

For any periodic waveform (2π), the Fourier series generally can be referred as:

$$x(t) = a_0 + \sum_{k=1}^{\infty} (a_k \cos kt + b_k \sin kt) \quad (4.15)$$

while the Fourier coefficients for a_0 , a_k , and b_k are denoted as follows:

$$a_0 = \frac{1}{2\pi} \int_0^{2\pi} x(t) dt \quad (4.16)$$

$$a_k = \frac{1}{\pi} \int_0^{2\pi} x(t) \cos kt dt \quad (4.17)$$

and

$$b_k = \frac{1}{\pi} \int_0^{2\pi} x(t) \sin kt dt \quad (4.18)$$

$$X(f) = \int_{-\infty}^{\infty} x(t) e^{-j2\pi ft} dt; j = \sqrt{-1} \quad (4.19)$$

In general signal analysis, Fourier is excellent and valuable since its main result exposes the invisible spectral components of a signal. Due to the nature of FT, which discovered the entire signal at once, is known as its significant drawbacks. The consequence of this drawback is that the frequencies exhibited are inadequate and not localised in time. This can be seen as in Figure 4.3. So, it is challenging to determine where and when a particular situation develops, means that the application of the real-time based system not easily realised.

The narrower the window, the localisation details in the FD is compromised, while the

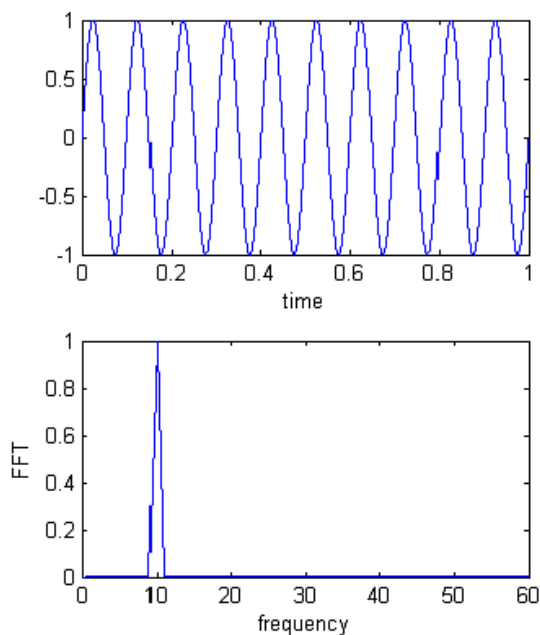


Figure 4.3: Top: Fourier series of a signal in TD (sine wave); Bottom: signal in FD.

wider the window, the localisation details in TD gets compromised. These known as the effect of the uncertainty principle. The equation of STFT can be referred as below:

$$X_{STFT}(\omega, \beta) = \int_{-\infty}^{\infty} x(t)h(t - \beta)e^{-j\omega t} dt \quad (4.20)$$

where β is the central point of windowed time, the STFT provides regional frequency content, the time and frequency resolution are depended on the windowed size. Shorter windowed time, up to a limited extent, similarly as quasi-stationary for a specific time. This means that window size is essential to measures the precision; denoted as a drawback of this technique. The STFT reveals the ineffective way of time-frequency localisation due to scale or “response interval” employed in its operation.

4.5.2 Wavelet transform

Wavelet transform (WT) described as another version of the improvement of FT. The connections between the FT, STFT, and the WT in term of properties, and another aspects are explained in this section. Observations of algorithm are described to gain a precise look of

wavelets characteristic.

The scale determines the first strategy in investigating the wavelets, one type of TFD analysis. Besides, wavelets are recognised as methods that perform many numerical designations and practised in interpreting the signal. WT algorithms run dataset of a signal at several occasion of translation and dilation. Vast detail information can be seen if viewing the signal from a large window. However, smaller details are visible if viewing with a shrunken window. The WT shows the estimation result of analysis in the composition of both the forest and the trees.

Current section unveils the method of WT investigation, covers the various opinions and debate of WT approaches, and decorate the analysis of the WT in the previous reports as described by (Bruce et al. (1996); Englehart et al. (2001)). WT has caught new enthusiasm among researchers in signal analysis and data processing.

WT are the best when implemented in various directions such as transient study, signal and communication as well as signal processing for multiple applications. WT gives a satisfying outcome to the dilemmas of the FT and STFT (refer Figure 4.4). The STFT produces fixed time and frequency resolution for the entire signal due to its fixed window size. But, in WT, different window size providing multiple resolutions of time and frequency resolution (Daubechies (1990)). The fundamental approach of WT property has exhibited a process of “dissociations” of a signal. It represents a signal power decomposition with specified detail coefficients. WT computed and provides details coefficients for each window made. Though, the width of the wavelet function varies with each spectral component.

WT described as a series of the regular FT which is working on a single scale either time or frequency, WT works on a multi-scale basis both for time and frequency. The mother wavelet decomposed raw signal into a scaled and translated component known as coefficients. This process overwrites the flaw in STFT which use fixed window size. The overall process of WT illustrated as in Figure 4.5.

The mother wavelet or known as wavelet function $\psi(t)$, is a zero mean function and

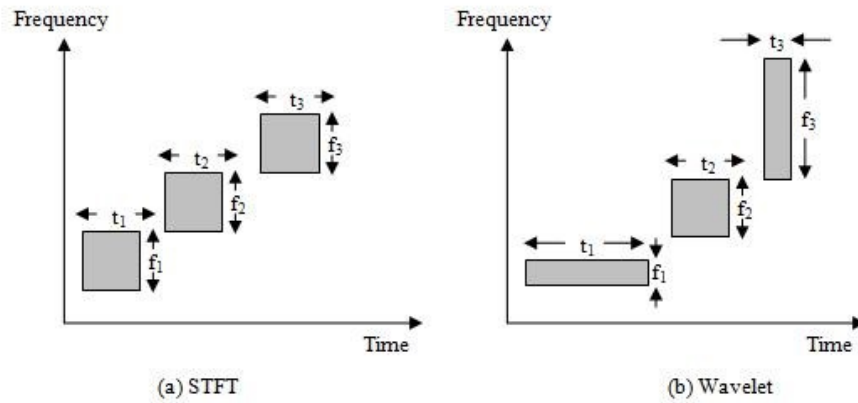


Figure 4.4: WT approaches are contrary to the STFT as it imposed a timely adjustable window (Daubechies (1990)). WT technique produce essential frequency localisation properties in both TD and FD.



Figure 4.5: The general approach of Wavelet transform process.

satisfies the admissibility condition:

$$C_\psi = \int_{-\infty}^{\infty} \frac{|\Psi(\omega)|^2}{|\omega|} d\omega < \infty \quad (4.21)$$

Where C_ψ and $\Psi(\omega)$ are the admissibility constant and the fourier transform of the wavelet function respectively.

The process should be averagely zero and centred in both time and frequency space, to be “admissible”, which expose the application of mother wavelet. This will satisfied the admissibility condition in WT. The window function of WT can be defined as, $\psi_{ab}(t)$:

$$\psi_{a\tau}(t) = \frac{1}{\sqrt{a}} \psi\left(\frac{t-\tau}{a}\right) \quad (4.22)$$

where a is identified as scaling factor and must be positive, τ is translation parameter (time shift), while $a, \tau \in \Re$ and $a \neq 0$. The mother wavelet denoted as the scale, $a = 1$ and position, $\tau = 0$. These will be utilised to produce other wavelets at various scales and translation.

4.6 Feature dimensionality reduction

Feature extraction method is a crucial method to elicit valuable information and to eliminate undesired component and interferences, embedded in the EMG signal. Successful classification greatly depends on the adoption of a feature vector. However, various investigations of the EMG signal classification have utilised a feature set that has carried some redundant features. Then, there is the need for employing the feature reduction strategy in the EMG analysis.

The features extracted could be showing a high degree of commonality in their attributes or dimensionality. Therefore, there is a need for a reduction technique able to minimise the feature dimensionality. Candidate techniques include principal component analysis (PCA), independent component analysis (ICA), and linear discriminant analysis (LDA) ([Chen et al. \(2013\)](#)). In this study, PCA and a variant of LDA have used to assess the performance of the features. These reduction techniques have been chosen for their ability to reduce the redundancy of the features.

Feature reduction comprises methods that can offer low-dimensional feature representation with improved discriminatory capability that are of predominant interest. Many approaches have been investigated for dimensionality reduction and feature extraction, such as PCA, ICA, and LDA. For LDA, is designed to especially fit for resolving classification dilemmas. It intends to maximise the proportion of the determinant of between-class sets of the calculated units to the determinant of within-class sets of the computed units.

Feature reduction has been utilised to withdraw problems correlated among huge dimension feature vector, and has been acknowledged as ‘curse of the dimensionality’ ([Hargrove et al. \(2007\)](#)) — this problem results with the implementation of high muscle chan-

nels. Feature projection helps decrease the feature dimensionality problems, and also to produce a feature set that enhances the classification performance as well as reduces the computational cost.

Two types of feature reduction techniques are explored in this study: PCA and uncorrelated linear discriminant analysis (ULDA) (Yang et al. (2008)). These will serve to lessen the dimension of the feature, also to provide a feature set that enhances the classification result and minimises computational cost. These two feature projection procedures are presented in the following subsections.

4.6.1 Principal component analysis

Principal component analysis (PCA) is known as a conversion method that has been applied due to its simplicity in signal pre-processing and analysis (Gokgoz and Subasi (2014)), feature reduction (Geethanjali (2015)) and controller design for assistive devices (Khushaba et al. (2016)) and rehabilitation systems (Brown et al. (2016)). PCA is an established method and is commonly adopted in many research works involving bio-signals (Güler and Koçer (2005)), and is introduced as a standard approach (Chan and Green (2007)) in classification studies. Various modifications in PCA have been developed to diminish the dimensional problems of data and for proper data visualisation recently.

The class label details are excluded in this process as it is depended on the data for the feature projection. PCA reconstructs the data matrix statistically through diagonalizing process by the covariance matrix. The method acquires the correlation among variables in the data. If the calculated and evaluated variables are associated, the first few substances manifest the correlation within the variables.

The steps of PCA computation are illustrated as in Figure 4.6. Consider an X dataset with n samples \times m measurements. The dimensional mean vector (μ) and covariance matrix of X are computed for the full data set by using subtraction. PCA will calculate the eigen decomposition of the covariance matrix of ($\Sigma X = X^T X$), producing the eigenvectors (W) as the principal components, and eigenvalues (λ) as the weights, which will be sorted with the highest magnitude as first. Eigenvalues are important for future analysis as

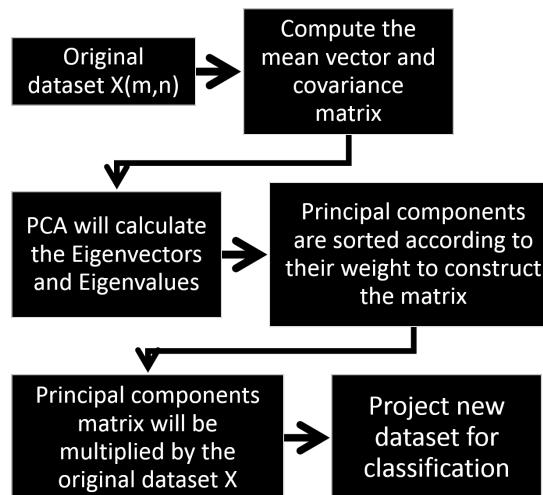


Figure 4.6: Principal component analysis for feature reduction problem strategy are illustrated. The steps shows how the new dataset projected from the PCA computation that will be used in the classification.

they will help in deciding the number of orthogonal components, while eigenvectors will establish the connection between the new components and the original variables. These are used to construct the principal components matrix, and then multiplied by the original dataset. This will produce the new dataset for the classification.

4.6.2 Uncorrelated linear discriminant analysis

LDA is a recognised technique for feature extraction and dimensional problem reduction. In recent years, it has been utilised in numerous studies such as sensors analysis (Akbar et al. (2016)), fingerprint recognition (Noor et al. (2018)), and text classification (Anwar et al. (2019)). LDA accepts as its input a set of greater dimension of features assorted into groups by determining a best projection that outlines the new features toward a reduced dimension space while maintaining the group composition. It decreases the within-class gap and concurrently maximises the between-class gap, consequently reaching the highest separation.

Another type of dimensional reduction technique employed in this study is a variant of LDA known as uncorrelated linear discriminant analysis (ULDA). LDA as widely discussed in Guersoy and Subasi (2008); Subasi and Gursoy (2010). It is a linear combination of variables that best separate classes or targets. ULDA was proposed by Jin et al. (2001),

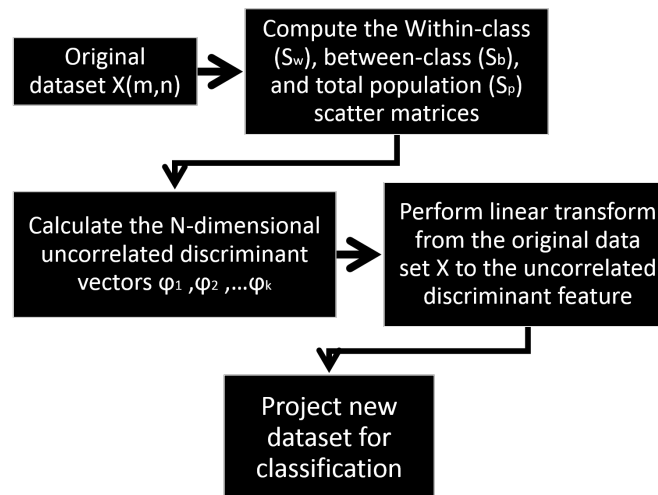


Figure 4.7: Uncorrelated linear discriminant analysis (ULDA) and their transformation steps for feature reduction problems. The transformation process has to follow the condition sets to assure the non singularity of Within-class (S_w) scatter matrices

due to limitation problems in classical LDA which require the scatter matrices to be non-singular, and due to lack of supervision of the dataset decorrelation. This will give poor results when dealing with high sets of redundant information in datasets.

The new approach of dimensional reduction, namely ULDA, which employs the Generalised Singular Value decomposition technique to deal with undersampled data by producing uncorrelated features in the transformed space introduced by [Jieping et al. \(2004\)](#). They have provided details on the ULDA which has thus been applied in many research studies as feature projection technique ([Khushaba et al. \(2008\)](#); [Phinyomark et al. \(2012a\)](#); [Yang et al. \(2008\)](#)).

Figure 4.7 shows the transformation steps for the ULDA feature reduction technique. ULDA is a supervised technique for feature extraction, using Fisher criterion based on discriminant analysis. While PCA explores for objectives of highest diversity in the data, ULDA attempts linearly joined variables described as uncorrelated discriminant vectors. The vectors maximise the classes separability regarding the Fisher criterion. The main difference between ULDA and LDA is that the vectors in the transformation matrix obtained by ULDA have to satisfy the constraint of so-called “S-orthogonality” ([Yuan et al. \(2008\)](#)).

4.7 Pattern classification strategy

Classification of hand movements employing an EMG pattern recognition have not gained the corresponding level of attention given to less dexterous arm movements, such as gross hand movements, grasping, and movement at the elbow, nor similar classification accuracy results give the same level of performance. Classification based EMG control attempts to analyse input data within a particular representation of pre-defined groups for the hand movements. It involves various approaches for the feature extraction, dimensional reduction and classification. This also includes data collection strategy applied in the current study. Feature sets and classifier types have been utilised by researchers to attain high accuracy such as artificial neural network ([Jahani Fariman et al. \(2015\)](#); [Khushaba et al. \(2014\)](#); [Subasi and Kiymik \(2010\)](#)), linear discriminant analysis ([Noor et al. \(2018\)](#); [Phinyomark et al. \(2012a\)](#)), and support vector machines ([Chen et al. \(2018\)](#); [Liu et al. \(2007\)](#); [Parsaei and Stashuk \(2012\)](#)).

In the last decades, standardised classification structure has been employed to analyse the collected EMG signals using pre-stated movement sets ([Englehart and Hudgins \(2003\)](#)). Thus, numerous types of feature and classification techniques have been used in many research studies exhibiting the usefulness of surface EMG control ([Asghari Oskoei and Hu \(2007\)](#)). [Tenore et al. \(2009\)](#) continued the notion of control strategy using EMG based on finger movements for flexion and extension of individual fingers using 32 channels EMG. They managed to achieve excellent classification, but it costed them a fortune in the processing time due to a large number of electrodes. However, a modification in the number of EMG channels, without discrediting the classification efficiency, would significantly elucidate the obligations for establishing state of the art prostheses.

[Hargrove et al. \(2007\)](#) analysed the classification accuracy of five pattern classification methods (multilayer perceptron, linear perceptron, LDA, Gaussian mixture model, hidden Markov model). They resolved that there was no significant difference in the performance of these classifiers. Furthermore, they suggested that superior accuracy can be achieved by using optimally three channels of EMG signal for the classification, provided the channels are chosen carefully and added that the selection of the feature sets and dimensionality

reduction is significant than the selection of the classification method. These works were then continued by [Scheme et al. \(2011\)](#), where they rated comparable achievement for ten classifiers tested.

Further investigation on LDA was done by [Khushaba et al. \(2012\)](#). They reported an average classification accuracy of $\approx 90\%$ in discriminating between individual and combined fingers movements. They used two channel EMG from eight participants for finger movements consisting of 10 classes of individual and combined fingers movements. In contrast, another set of studies in hand movements classification was done using both normal and amputee subjects. The variations of classification accuracies can be seen in this study as they used six EMG channels, resulting in 15 classes of fingers movements ([Al-Timemy et al. \(2013\)](#)).

Neither [Khushaba et al. \(2012\)](#) nor [Al-Timemy et al. \(2013\)](#) can confirm whether or not the classification accuracy was affected by the number of EMG channels involved in the study. However, the outcomes given by both studies are probably confined by the characteristics of the movement classes and the use of data for training or testing. Both of these circumstances influence the generalisation of the classification performances, and therefore there is a need for this new study to take measures in these contexts (EMG channel), the correlation between EMG muscles, their features and draw a conclusion based on the findings appropriately. Since this kind of study is dealing with large numbers of datasets, it is worth to notes that the classification windows for the datasets (CW) are calculated as follows:

$$CW = \frac{x_L - L}{L_{inc}} \quad (4.23)$$

where x_L is the size of the full dataset, L is the window length and L_{inc} is the window size increment. The orientation of the windowing techniques can be found in Section 4.2.1.

4.7.1 Artificial neural network

The multilayer perceptron (MLP) neural network is usually employed for use in EMG signal classification and has produced competitive achievement for steady-state movement classification and has been reported in various research studies with promising performances (Baspinar et al. (2013); Gandolla et al. (2017); Karlik et al. (2003); Mobasser and Hashtrudi-Zaad (2012)).

Artificial neural networks (ANNs) are biologically inspired algorithms where the knowledge about the problem is distributed in neurons and their connection weights. ANNs are non-linear mapping formations based on the function of human brain. They are important means for modelling, primarily at the underlying information association is unexplained. Figure 4.8 shows basic architecture and configuration of ANN consisting of three layers: input layer, hidden layer and output layer. Moreover, each layer has a weight matrix, a bias vector and an output vector.

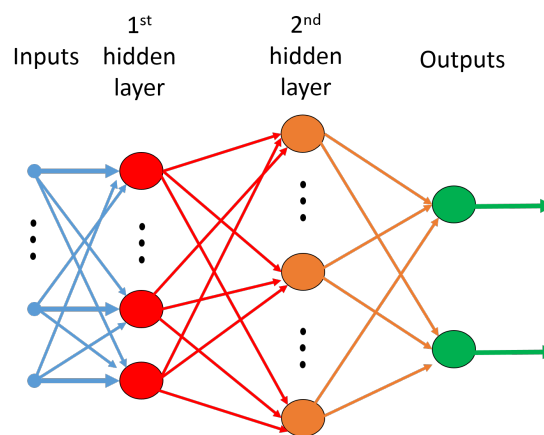


Figure 4.8: The basic architecture of ANN with the generations from different layers such as input layer, two hidden layers, and the output layer. Activation functions of the hidden layers and the output layer were chosen as *tansig* and *purelin* separately.

Back-propagation neural network

This type of back-propagation neural network (BPNN) classifier algorithm is known for effective training and better understanding of the system behaviour (Ahsan et al. (2011); Baspinar et al. (2013); Ibrahimy et al. (2013); Wang and Buchanan (2002)). The uses of BPNN abide by a group of standard processing systems which interact by transmitting

signals to each other over a large number of weighted connections.

The algorithm uses a hyperbolic tangent sigmoid function and linear functions are applied for the hidden layer and the output layer. This is done separately for each respective layer. The training process will adjust the connection weights and biases to map the desired output. The generalisation of ANN and their processes are achieved by updating weight and bias values corresponding to the Levenberg-Marquardt optimisation algorithm and gradient descent is applied as the learning function (Hagan and Menhaj (1994)).

The basic BPNN algorithm can be set by first initializing the values of weights and threshold levels of the network to small uniformly distributed random numbers, details for BPNN computation can be found in Karlik et al. (2003). The activation functions for the BPNN is known as $s_c : \mathbb{R} \rightarrow (0, 1)$ and defined by the expression (Rojas (1996)):

$$s_c(x) = \frac{1}{1 + e^{-cx}} \quad (4.24)$$

where c is a constant and must be positive. The shapes of the activation functions changes with respect to the value of c .

4.7.2 Linear discriminant analysis

Linear discriminant analysis (LDA) has been broadly utilised to classify human hand movements based on EMG data (Al-Timemy et al. (2013); Chen et al. (2013); Noor et al. (2018); Phinyomark et al. (2012a)). The purpose of LDA is to obtain a hyperplane that can classify the data points describing distinct hand movement classes. The hyperplane is acquired by examining for a prediction which shows the maximum gap among the average of the classes and reduces the diversity within the class as the data are assumed normally distributed.

Balakrishnama and Ganapathiraju (1998) give details of multi-class classification using LDA algorithm, and summarise the process as follows:

- i. Formulate the features dataset for training and testing, which will be classified in the

original space.

$$x_1 = \begin{pmatrix} a_{11} & a_{12} \\ a_{21} & a_{22} \\ \dots & \dots \\ a_{m1} & a_{m2} \end{pmatrix}, \dots, x_2 = \begin{pmatrix} b_{11} & b_{12} \\ b_{21} & b_{22} \\ \dots & \dots \\ b_{m1} & b_{m2} \end{pmatrix}, x_i = \begin{pmatrix} i_{11} & i_{12} \\ i_{21} & i_{22} \\ \dots & \dots \\ i_{m1} & i_{m2} \end{pmatrix}.$$

- ii. Compute the mean of each set of features (U_1, U_2, \dots, U_i) in class (i), and also the average mean of the entire input data (x_i)
- iii. Compute the mean global vector (U) for the whole data set, say for a simple two class problem;

$$U = p_1 \times U_1 + p_2 \times U_2 \quad (4.25)$$

where p_1 and p_2 are the apriori probabilities of the classes.

- iv. Subtract the mean from each data point to get the corrected mean data

$$x_i^o = x_i - U \quad (4.26)$$

- v. Determine the covariance matrix (cov_i) of the group (i) provided by

$$cov_i = \frac{(x_i^o)^T x_i^o}{n_i} \quad (4.27)$$

where n_i is the number of sample class (i)

- vi. Compute the combined within-group covariance matrix provided by

$$Pcov = \frac{1}{n_{total}} \sum_{i=1}^g n_i cov_i \quad (4.28)$$

where covariance matrix is represented by cov_i , number of class (i) samples n_i , and

the total samples number for all classes n_{total} , while g is the number of classes.

- vii. Compute the inverse of combined within-group P_{cov}^{-1} matrix
- viii. Employ the discriminant function rule for a k unit provided by

$$f_i = U_i cov^{-1} x_k^T - \frac{1}{2} U_i cov^{-1} U_i^T + \ln(P_i) \quad (4.29)$$

where x_k^T is the input sample data, and P_i is known as the prior probability vector;

$$P_i = \frac{n_i}{n_{total}} \quad (4.30)$$

The input sample numbers k that have maximum f_i are assigned to the class (i). The idea of LDA is to classify those features according to their movement class in which the apriori probabilities can be maximised. LDA performed similarly as ANN with better computational time. This has been discussed in detail by [Tkach et al. \(2010\)](#).

4.8 Classification performance evaluation

The ultimate measure of the classification scheme is to analyse the performance of the algorithms studied. A non-functional evaluation is utilised to assess the achievement of the classification strategy. In this technique, the evaluation should not involve the prosthetic arm to estimate the achievement of the classification method in the study. Therefore, accurate classification based on the user movement class can be used as a standard for the classification performance.

4.8.1 Classification accuracy

Accuracy is one metric for assessing a classification system. The percentage of correct classification of the system and its computational information are used to justify the per-

formance of the classification system, The percentage of correct prediction has been used in many studies and can be defined as:

$$\text{Classification Accuracy} = \frac{\text{Number of correct predictions}}{\text{Total number of predictions}} \times 100\% \quad (4.31)$$

As for binary classification, accuracy might be determined based on positives and negatives as below:

$$\text{Accuracy} = \frac{TP + TN}{TP + TN + FP + FN} \quad (4.32)$$

Where TP = True Positives, TN = True Negatives, FP = False Positives, and FN = False Negatives. Meanwhile, the percentage of error for a classification system can be found as :

$$\text{Error} = 100\% - \text{Classification Accuracy} \quad (4.33)$$

4.8.2 Classification plot

The classification plot can be used to show the results of classification utilising a trained classifier based on time series. A proper technique for the analysis of a classifier output is the classification plot, and this has been discussed in [Chan and Green \(2007\)](#). In this graphical plot, the correct class is drawn alongside the target class on the y-axis against a time scale in the x-axis. This type of plot gives an advantage of exhibiting the error distributions and the time location of these errors. The classification plot example can be found in Chapter 5, Figure 5.20.

4.9 Summary

The state-of-the-art classification systems and algorithms have been introduced and discussed. Particularly, the entire processing series of the classification system has been described in detail, such as pre and post-processing, features extraction, dimensional reduction and projection, classification, as well as performance analysis. These approaches have been briefly explained and the justification of using them in this study has been presented. This chapter forms the basis for the classification approaches that will be employed in the following Chapters 5, and 6. This study employed two types of dimensional reduction techniques, which are namely as PCA and ULDA. These two will be explored and tested with LDA classifiers. All the data collected with many trials are combined into the whole new dataset, which is then divided into two sets. The first 55% dataset will be used for the classifier training, and the rest 45% will be set as testing data and individual performance extracted using specified classifier. The scheme initiated for this classification will be used in this study unless pre-stated otherwise in the introduction topic.

Chapter 5

Assessment strategy of human upper forearm

5.1 Introduction

As stated earlier in the previous chapter, the development of this study was based on the investigation of the selected muscles involved in the human upper forearm movement. This has been taken as an initial investigation to understand the real way of signal propagation within the human upper forearm muscle. Despite many studies done in this context, this pilot study, however, tends to create a new approach which is using two region of muscles in the human UFA area as a benchmark strategy. Therefore, there is a need for a new protocol to be implemented as it will help to realise the real implementation of control with better performance through each individual muscle analysis.

The study hypothesis is that the EMG signal acquisition is the approximation of the weighted sum of all muscles sources. There are more than 10 muscles involved in controlling hand movements. The muscles locations and their types were discussed in Chapter 2 section 2.2.3. The flow from the hand is affected by the mean of the peripheral and central nervous system of human. These include the anatomical and physiological characteristic of human muscle. Besides, the instrumentation performance in data acquisition also affects the signal properties.

In this chapter a new novel approach of analysis for optimising the use of muscles and their proper channels is proposed. The data of nine subjects with the normal condition is used in this study. This study will allow to understand the importance of the muscle use-

fulness, muscle region and their variations and their distinctive characteristic concerning the designated movement procedures for the study. In general, the outcome from this study is expected to establish the information of muscles characteristics and their corresponding feature in the regional aspect. These will lead to the generalisation of the muscle to be used in the next chapter for real applicability in the use of selected muscles.

5.2 The assessment strategy for subject muscles and EMG site selection

To the author's knowledge, there are no studies reported investigating the relations of surface EMG signals of upper arm and forearm muscles region. The precision of EMG signal features and parameters proportionally vary with various MVC, index of hand movements as well as muscle fatigue (MF). The major challenge for the study is to identify suitable muscles to cooperate better with various hand movements as well as acknowledging the fatigue manifestation in the EMG signal. This particular study requires thorough investigation and better analysis so that the control performance is improved.

This involves maximum voluntary contraction, different loads, and maximum holding towards fatigue. Hence, the fundamental study is performed by investigating the signals acquired from the human upper forearm (UFA) to determine muscle characteristics and to establish the inter-relationship between both muscles of the forearm and upper arm. The relationships developed from these muscles will be useful for classification. The present study aims to investigate the applicability of human UFA muscles and MF indices at various force levels of MVC.

The improvement of data collection practicality will allow features extraction and classification. Hence, a fundamental study is performed by investigating the signals acquired from the human UFA to determine muscle characteristics and to establish the inter-relationship between both muscles of the forearm and upper arm. The present study aims to investigate the applicability of human UFA muscles and MF indices at various force levels of MVC.

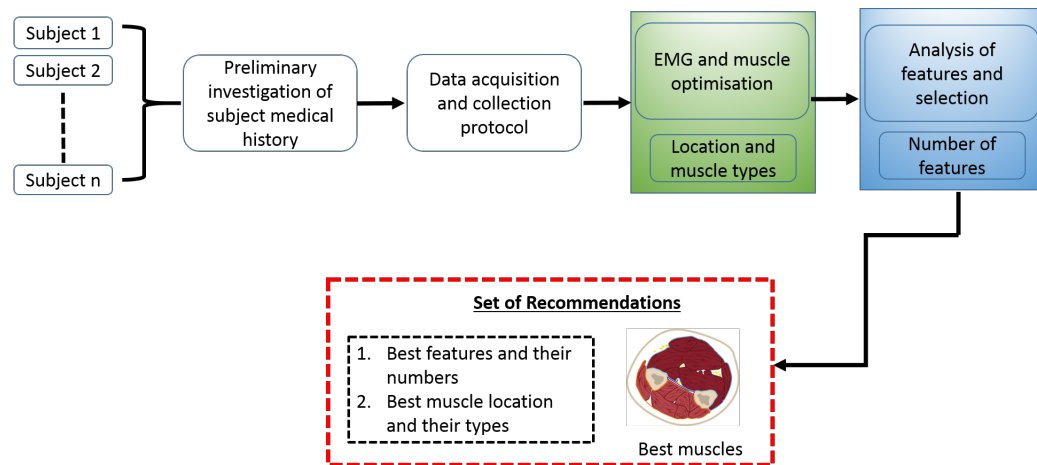


Figure 5.1: Block diagram illustrated the overall approaches in achieving the proposed assessment and subject muscle performance towards proper EMG site selection

5.2.1 Data acquisition system and protocol

To achieve a proper definitive solution for the EMG muscles and channel selection, nine (9) subjects were chosen for this particular section of the study. The subject preferences and acquisition systems were described in Chapter 3. In this assessment strategy, only hand grip force movements at the standard positions, i.e. 90° is used. Hand grip force involves both human upper forearm main movements such as fingers and palm grip. That is why it is suitable to be used as a pilot movement for the study. As the movement is generated by the muscle, the signal propagates from one muscle to another with respect to their functionality.

The schematic diagram of the proposed of the proposed assessment and subject muscle investigation of EMG site selection is shown in Figure 5.1. The design protocol involves several stages, where every detail for each step is explained in their own specific subsection. The general scheme of the assessment strategy utilised in this study and the analytical strategy has been proposed. The results from this study will be used in future analytical technique such as EMG conditioning and segmentation, feature extraction, dimensionality reduction and classification will also be considered.

5.2.2 Electrode placement and muscle channels

The subject muscles chosen for this assessment strategy are based on the previous study collection in Chapter 3 and Chapter 4. The muscles were also pre-examined by the medical experts before it has been decided to be used in this study. Therefore, there are nine muscles chosen and these are shown as in Figure 3.9. The electrode placement is the pre-examined best muscle location suggested for this study. In Figure 3.9, various approaches of data collection are investigated by variably pairing or combining the muscles as by variably paired or combined the muscles as shown in A, B, C, D, E, and G. The ground (G) electrode was located at the most bones known as medial epicondyle.

5.2.3 Assessing muscle fatigue

The MF phenomenon was investigated based on the EMG signal recorded from the subject. However, to achieve fatigue condition, the subject was asked to apply maximum hand grip force for a certain amount of time at each level of %MVC. As noted in Figure 5.2, the %MVC was stable at 80% before fatigue started to happen at around 70s. The fatigue has become obvious as the subject reached 100 %MVC, where the moment reduced as the force increased. As the subject tried to push harder and harder, the force still kept going down.

This can be compared with the fresh EMG signals at 20 and 40 %MVCs. The envelope of EMG activity, each spike represents the brain activity telling the muscles to be active. More spikes mean more muscle activity. As can be seen at 100 %MVC, the envelope of EMG increased even though the strength was actually decreasing as a function of time. This means that the brain is driving the muscle harder, but something happening peripherally in the muscle makes it weaker than required by the brain. This is called MF and the force variations degrade the EMG signal performance and cause fatigue.

The result of the present study demonstrates that the MF affects the frequency contents of the EMG signal. It is shown that the characteristic of the frequency shifts to the lower frequency when the muscle experiences fatigue (Figure 5.3).

The impact of power frequency at different %MVC on EMG signals recorded from

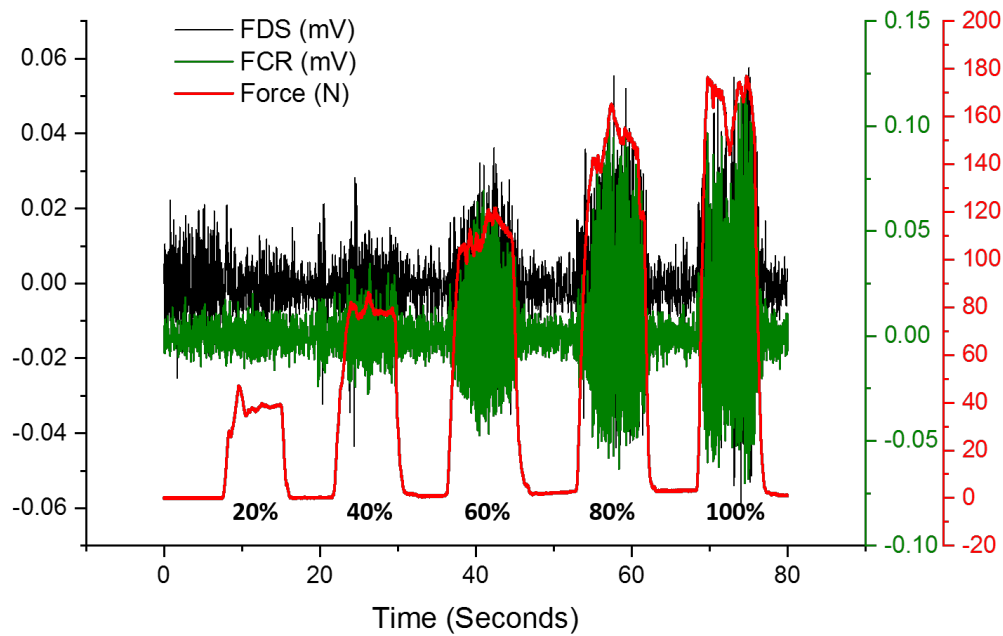


Figure 5.2: Raw EMG signal of handgrip at 90 deg force with muscle fatigue occurrence after 80% MVC.

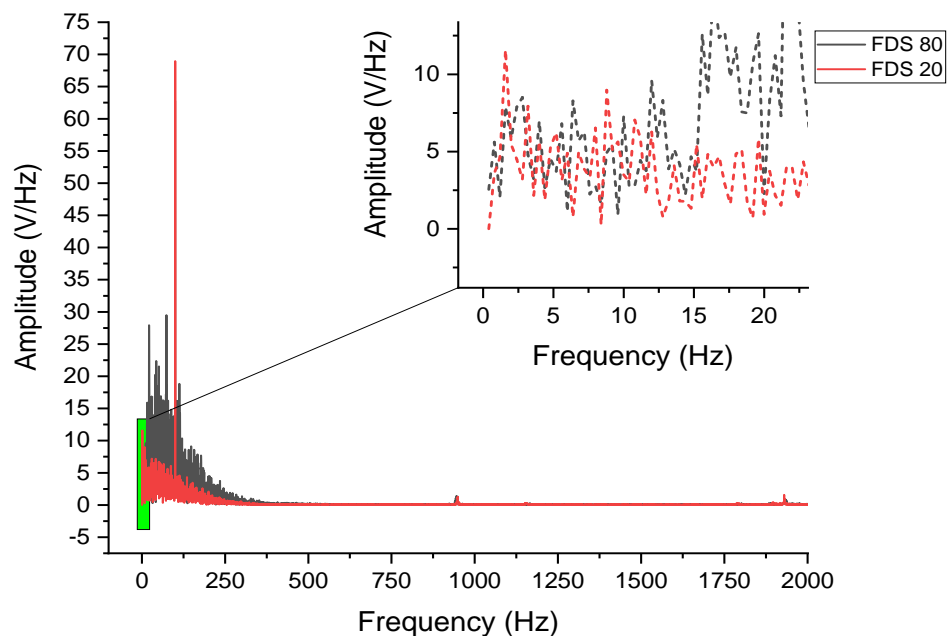


Figure 5.3: Comparison of handgrip EMG signal power frequency spectrum with (80% MVC) and without fatigue (20% MVC). The zoomed box (green) shows that the amplitudes is shrunk towards lower frequencies when fatigue occurred. The estimated power for muscle with fatigue are higher than the estimated signal without fatigue.

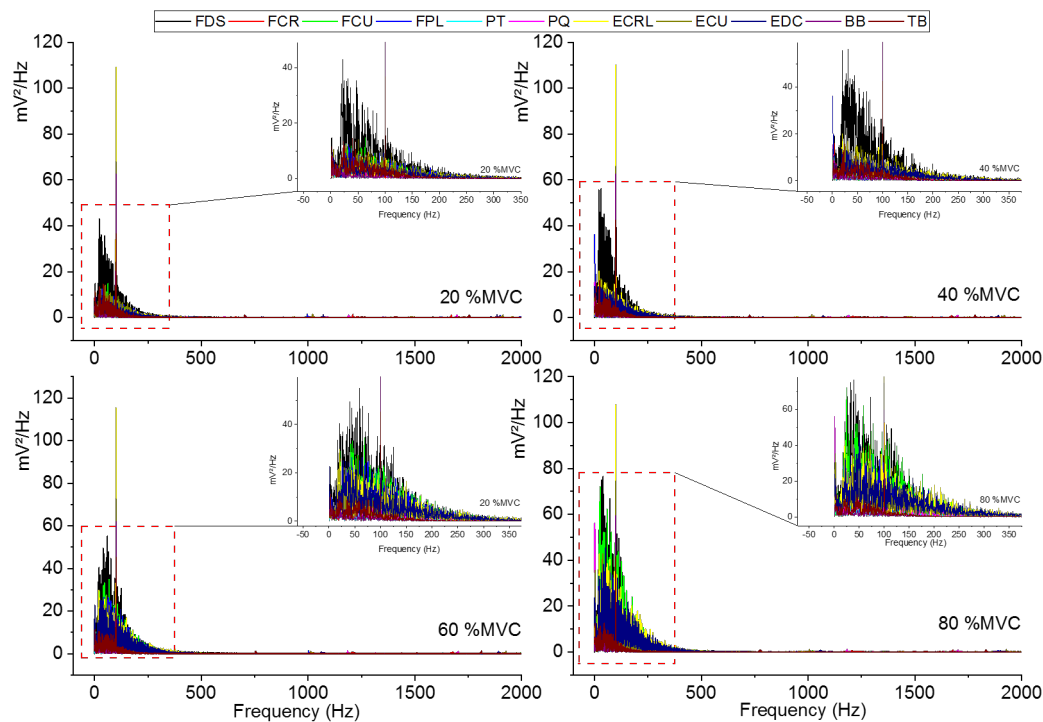


Figure 5.4: Variations of power frequency spectrum produced at different MVCs. These are also highlighted using zoomed version to give clear pictures on the muscles and their power performances.

the 11 muscles used in this study are shown in Figure 5.4. Significantly, each muscle was involved in such movement. As noted there were variations in the power output for each muscle concerning their MVCs. Figure 5.4 highlights the power frequency produced using the red dashed box. This characteristic will be compared and analysed for muscle selection shown Figure B.1 and Figure B.2 (Appendix B).

There are three properties from the extracted power frequency spectrum used, that is median frequency, peak frequency and mean frequency. All these properties are calculated for each muscle and subject involved in this study. Table 5.1 shows the average value for all subjects. With reference to Table 5.1, the effect of power frequency on 11 muscles was investigated at four levels of voluntary contractions. The main objective is to determine if signal power frequency information provides another strategic dimension, hence to identify the most suitable muscles to be chosen for regular use in the future study and the effect of muscle fatigue.

In Table 5.1, median power frequencies collected for each muscle consistently indicates that the frequency content from 40 %MVC to 80 %MVC shifted from higher frequency

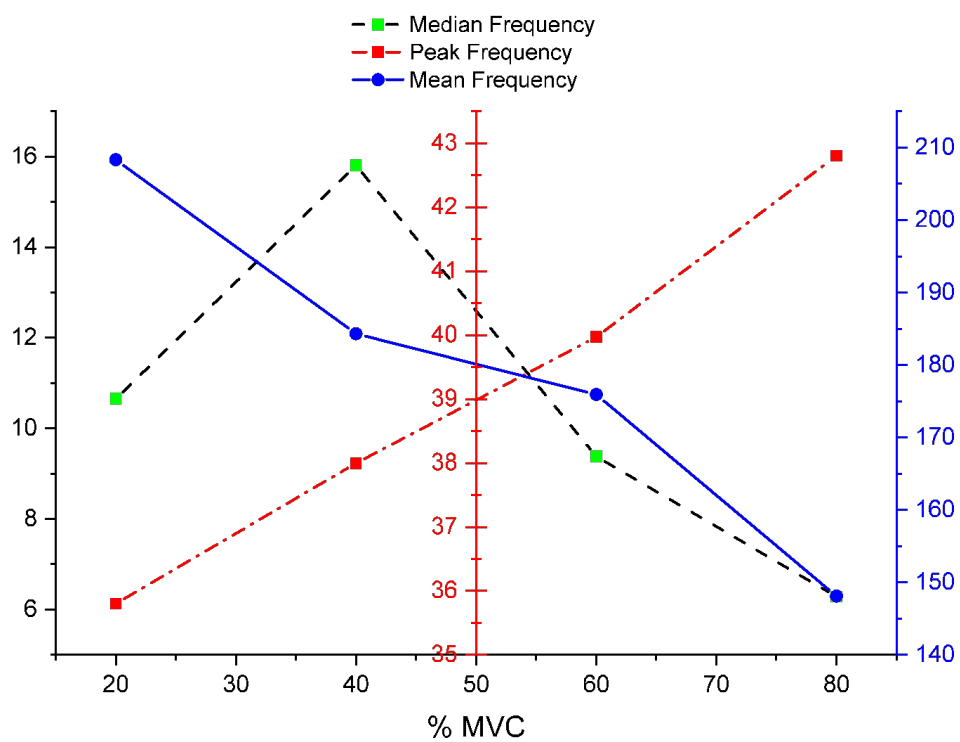


Figure 5.5: The changes of the average value of frequency performance between three properties selected; median frequency has shown a characteristic of fatigue index, while peak and mean frequencies exposed the real features for the muscle performance selections. These indications give new insight in assessing the muscle performance and fatigue phenomenon.

to the lower frequency. This demonstrates that the subjects appeared to endure fatigue when they reached 60 %MVC or higher, specifically in this study. The changes in median frequency, as a function of level contraction, are summarised for the whole muscles as in Table 5.1. A consistent significant slope degradation of the median power frequency between 60 %MVC to 80 %MVC for all muscles indicated that fatigue corresponded with no exclusion. This is supported the findings as discussed by [Sparto et al. \(2000\)](#). Median power frequency is known for its linear characteristic with the MUAPs. Therefore, median frequency is best to deal with fatigue and could be used as a fatigue index for the future study.

The selection of muscle is generalised in this study using only one component of hand movement, that is the hand grip force at normal position. In real life application, the hand grip covers all types of movement (grip and pinches) for the human hand. During hand grip force exertion, the muscles in the human UFA initiates EMG spikes to produce the fingers and grip strength. This was achieved by controlling the movements of the index, middle, ring and little fingers and the wrist. [Scheme et al. \(2011\)](#) suggested that the best %MVC to use are 20 and 80, where these data highly possible in reducing the force effect between two levels of contraction.

5.2.4 Muscle selection

Figure 5.5 presents and concludes the findings for investigation of muscle selection and muscle fatigue. The change in these properties was spotted when plotted as a function of the level of force contraction (%MVC). The results presented for fatigue indicators are based on their median frequency with the time-varying muscle strength used in the current study.

In assessing the muscles performance, two power frequency properties were used in this study. The peak frequency shows a steady linear increment while the mean frequency demonstrates a significant reduction for the preset MVC as shown in Table 5.5. These properties correlate well with the muscle performance and will be used in the muscle selection strategy. As indicated the proportion of power among different muscles play a

significant role in hand movement. Whenever muscles are imposed upon diverse force, the power ratio become the most important feature to be considered.

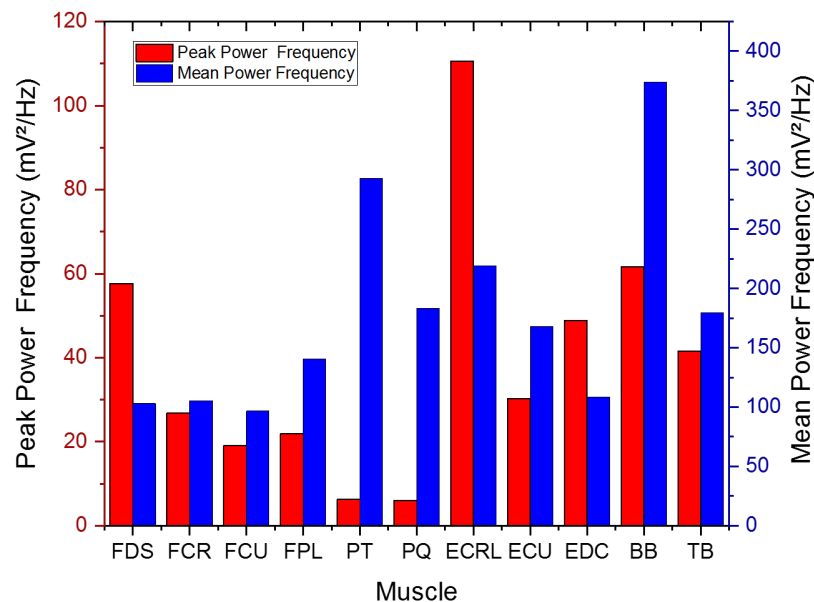


Figure 5.6: Analysis comparison for the muscle selection strategy based on average peak power and their mean frequency. These characteristic will be the ultimate tools in this study for the muscle selection. Muscle will be chosen based on their peak power and their suitabilities according to SENIAM.

From Figure 5.6, the peak power amplitude versus muscle suggest a tendency of few muscles to respond very well with the task performed. This will be a good reference point as these are needed to have suitable muscle selection to reach a plateau in the data consistency and accuracy of the human UFA classification. It was found that there were several muscles from both regions of interest giving good response to the movement. Some of the muscles produce relatively lower than other muscles performance such as FCU, FPL, PT, PQ, and ECU.

However, minimising the number of channels is the main focus of the study, two human UFA muscles will be selected for each region (forearm and upper arm). Therefore, two flexor muscles (FDS and FCR), two extensor muscles (ECRL and EDC) and two upper arm muscles (BB and TB) are chosen for the further study. Thus a total of six muscles to consider. The BB and TB muscles have shown different and attractive characteristic between each other; however, it is well known for BB muscle gives more valuable infor-

Table 5.1: The properties of EMG power frequency spectrum; median, peak, and mean frequencies calculated for all subjects. The average values for each property with their respective muscles was shown to justify the muscles chosen. The statistical analysis demonstrated significant differences between all the three power frequency properties at different muscles, $p < 0.05$ was observed.

% MVC	Median Power Frequency											
	FDS	FCR	FCU	FCL	PT	PQ	ECRL	ECU	EDC	BB	TB	
20	2.2282	2.75295	1.6944	3.62184	22.6139	16.7593	26.9897	3.9468	1.67575	31.8506	3.05619	
40	2.13445	2.88714	7.04599	4.78055	27.3056	24.4474	58.1443	2.61713	1.37812	39.2034	3.94451	
60	1.72997	1.57215	1.38811	1.57166	23.1316	10.9755	20.1901	1.87638	1.39637	36.0676	3.29967	
80	1.74078	1.49449	1.57658	1.49366	10.4657	6.35602	10.3081	1.71916	1.2643	29.6933	3.04586	
Average	1.9584	2.1767	2.9263	2.8669	20.879	14.635	28.9081	2.5399	1.4286	34.204	3.3366	
% MVC	Peak Power Frequency											
	FDS	FCR	FCU	FCL	PT	PQ	ECRL	ECU	EDC	BB	TB	
20	42.9613	18.6826	28.8541	17.3717	6.19638	5.54793	109.059	27.8617	37.9973	62.5782	36.6967	
40	56.2427	25.9806	10.5074	26.2005	4.1416	9.48907	110.101	26.0562	44.1017	62.5772	42.5779	
60	55.098	28.2788	14.697	18.9569	6.40506	2.95249	115.396	32.6077	58.1134	61.9558	45.2087	
80	76.43	34.192	22.0546	24.9365	8.41837	6.2005	107.754	34.5306	55.2611	59.4884	41.6056	
Average	57.683	26.784	19.028	21.866	6.2903	6.0475	110.577	30.264	48.868	61.65	41.522	
% MVC	Mean Power Frequency											
	FDS	FCR	FCU	FCL	PT	PQ	ECRL	ECU	EDC	BB	TB	
20	116.881	122.488	119.206	201.889	305.147	223.309	334.181	207.918	116.736	376.165	167.648	
40	106.53	116.534	70.9875	115.062	343.471	212.16	222.827	169.035	103.528	373.148	193.961	
60	88.3021	90.9125	94.1333	122.171	318.489	164.784	197.181	169.053	108.773	391.895	189.43	
80	100.155	91.4531	102.185	122.819	204.306	133.612	121.906	125.517	105.332	354.968	166.77	
Average	102.97	105.35	96.628	140.49	292.85	183.47	219.024	167.88	108.59	374.04	179.45	

mation in the analysis as the BB muscle is more prominent than TB. Therefore, it was concluded to choose only BB muscle for the upper arm area. This would be beneficial for developing new features involving two regions of muscles for classification, the FDS and BB muscles are chosen for this study.

5.3 Feature performance analysis

This study attempts to enhance the performance of EMG classification techniques. Therefore a new considerable research effort in the current use of features needs to be addressed. This study focused on finding the feasibility features of several types of hand movement with respective muscle contraction and muscle fatigue. Features are considered as the central part of this study, as it was the vital component behind the classification accuracy performance. Functional feature component addressed the sets of information localisation that represent the EMG signal accurately. Secure information relies on EMG signal are the most challenging problem to solve. Therefore, investigation on features in terms of the robustness, level of separability, computation complexity are important in this study.

The current study on EMG feature development focuses on various time (temporal) and frequency (spectral) indices, for achieving better classification and control technique. It is known that each domain used in the study came up with its pros and cons. This has been discussed by many researchers ([Asghari Oskoei and Hu \(2007\)](#); [Hudgins et al. \(1993\)](#); [Thongpanja et al. \(2012b\)](#); [Tkach et al. \(2010\)](#)). The study will use the indices extracted based on EMG time-dependent and power frequency analysis.

However, the determination of the signal quality and stability depends on the detection site that has been proposed. The detection site can be anywhere, as long as it is within the range and distance of the muscle signal. Therefore, the model of site detection is introduced, which affects the performance of the EMG detection according to the SENIAM protocol.

Figure 5.7 depicts the model of EMG signal propagation between two muscles X and Y, at four different detection sites. Each site detects the signals; however the signal quality

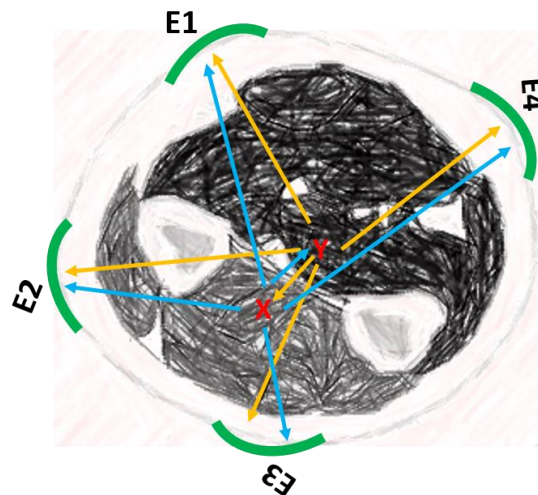


Figure 5.7: The illustration model of basic EMG signal propagations between two neighbourhood deep muscles, X and Y. The signals travelled all the way through the deep muscle layers regardless of their distances, through fat and skin before reaching the detection sites (E1 to E4). Each detection sites will have their own characteristics of EMG signal.

is based on the distance between the deep muscle and the sites. Distance is shown by the length of the propagation arrow for X muscle (blue) and Y muscle (yellow). As can be seen, there is also the crosstalk between the muscles as they are located side by side. These phenomena affect the performance of the amplitude and frequency of the signal. These non-stationary characteristics have opened so much argument within the researchers, where the feature extracted from the muscle in time and frequency domain are useful but not adequate for better recognition. The feature exploration and the detection technique are widely open for new findings.

Therefore, better accuracy only could be realised by extending the possibilities of exploration of the new features or the combination of the detection technique and the feature. In general, most of the muscles performing the hand movements, originate from all three layers in the human upper forearm. Another concern that has to be taken into consideration is the following:

- The signal amplitude is inversely proportional to the distance travelled ([Adam and De Luca \(2005\)](#)). This means, the deeper muscles located in the forearm, the lower amplitude will be detected. This could verify why the signals from the finger pinches are smaller than the hand grip force.

- The EMG signals acquired on the thick muscle tissue, fat and also the skin will produce narrow frequency bandwidth information.
- The fatigue gives a new set of muscle amplitudes and frequency characteristics as fatigue degrades the real muscle performance. This is the main problem faced by many researchers as fatigue has its own characteristics for each subject. This is also the reason why in this study, the muscle performance based on their MVC was designed, to gather information on the fatigue index and their variabilities between subjects.

In this study, the time and frequency domain features are used on deciding the robust EMG feature sets for the hand movement, while their performances will be compared with the new features extracted in the time-frequency domain. Even though many previous studies have focused on the same features, the combination of muscles used in this study rarely analysed or evaluated in other studies, since the current major drawback from these feature parameters was the nonlinear relationship between different types of muscle or contraction level. Hence, the investigation here focuses analysing the TD and FD features in terms of their best linear relationship within these two components. They will also be inspected in terms of their quality inseparability, robustness and low in computational criteria.

The previous works have proposed some of the features chosen in this study, but many research works have only focused on a few muscles rather than trying to investigate the whole tissue in a go. Thus, these measures have been catered in this study. Moreover, the approach in this study is much better as it concatenates within each subchapter where the evaluation is carried out in consecutive order and covered almost the whole muscle in the human upper extremities.

5.3.1 Data collection

EMG signals were recorded from fifteen (15) normally limbed subjects. Data collection protocols described for the volunteers, and they sat on a chair facing the battery-powered

computer with the LabQuest mini interface software (see Chapter 3). This could help them to visualize the real-time EMG signal for each channel while performing the task given. The forearm was fixed in one position, and it was resting on a comfortable base. Thus, it will give the subject a relaxation and calm in their position.

At the initial stage, the subject was asked to perform each pre-set hand movement with maximum force to determine their MVC force. This was done with the best of their own capability, for three times with 5 minutes rest intervals. The final average value was taken as their final 100 %MVC force. The subjects consisted of nine (9) males and six (6) females.

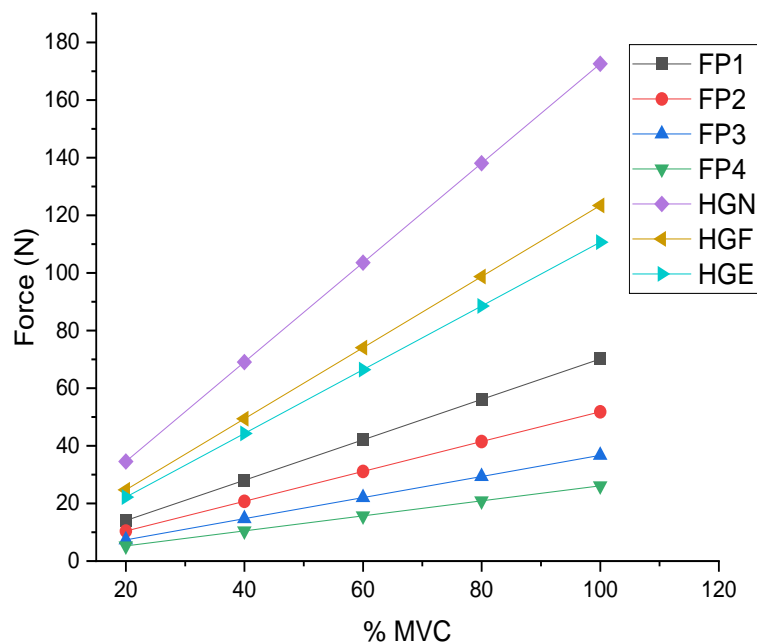


Figure 5.8: The average value of maximum voluntary contraction for all subjects. This show the variation of force produced between each hand movement at varying contraction level. Hand grip force dominated the average value as compared with finger pinches. Classification accuracy were most affected by these variations characteristic.

The electrodes were placed in the pair muscles (2 channels) for each session of data acquisition. This is to get a better signal without having noise such as crosstalk, minimise the number of detection sites and to understand the specific muscles in their corresponding functionality. There were three consecutive days of data collection for each subject to complete. However, this depended on subject availability during the data collection. Figure

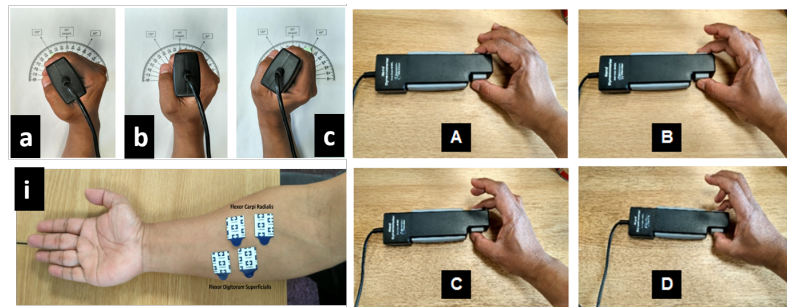


Figure 5.9: i) Example of disposable electrode placement on the paired forearm muscles, FDS and FCR: seven classes of hand movement studied in this experiment, three for handgrip force movement (a, b, c) and four for finger pinch movement (A, B, C, D)

5.10 shows the raw EMG signal collected from a subject. The signal duration for one set of data collection will be around 80s. This is because in every consecutive MVC, the subject will have to rest for 5s before they start the next hand movement.

5.3.2 Pre-processing

The study investigates the EMG activity between several muscles for each specific movement. Then, there will be an investigation of its relation in terms of the signal properties. This can be by means of time domain descriptive statistic analysis, frequency analysis, or the time-frequency analysis. It is believed that the propagation of the EMG signals originates from the brain, towards the muscle fibre from the upper arm and then the forearm back and forth. When the signals propagate from the same source, the interconnection between them will allow their identification. The relationships must be unique since it is in the same neighbourhood or region of interest.

The raw data from the source, as in Figure 5.10 will be pre-processed by selecting the first 5s of movement states in each particular MVC. This will make each movement separated from other MVCs. Therefore, the new data will be used in future analysis. The example of the new data after rest state removal are shown as in Figure 5.11. The shortening segment length of the raw EMG signal offers various benefits to the study, which is likely to enable fast response time in the classification process. The features extracted from EMG signals cannot be directly from individual raw samples as the detailed structure of the raw signal is considered lost (Hudgins et al. (1993)). Generally, the signal

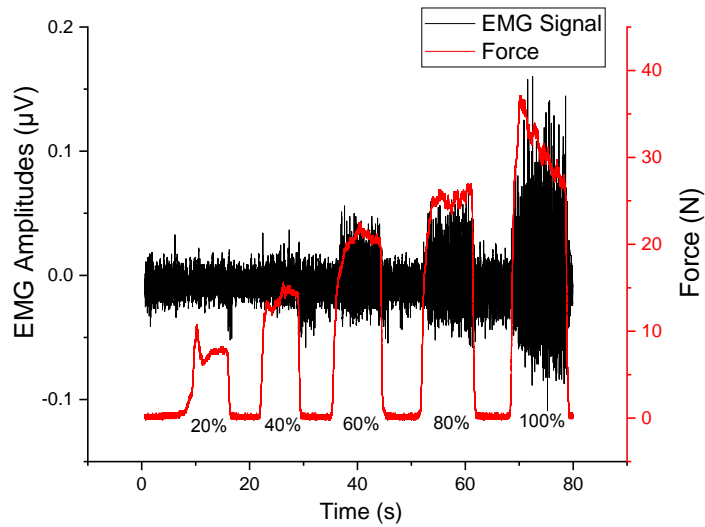


Figure 5.10: EMG signal with its amplitudes and forces versus time. This signal was separated by at least 5s rest for each movement. EMG data were collected at sampling frequency of 2000 Hz.

from each channel is differentiable as in Figure 5.11. However, there is also the noise, and it can be seen that for each paired channels such as FDS and FCR, the variations of amplitudes and frequencies are apparent.

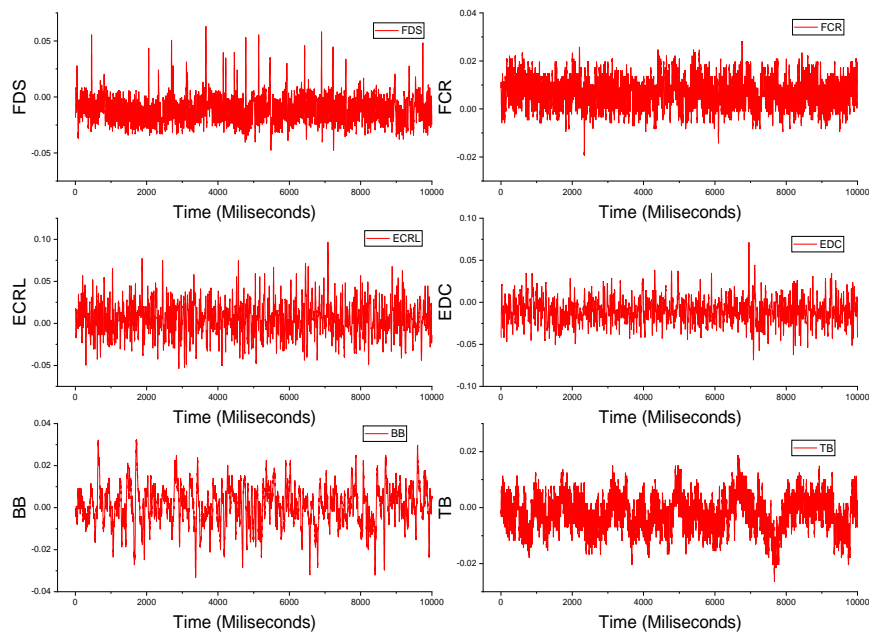


Figure 5.11: Example of raw EMG signals for six types of muscles for FPI movement. This signal was taken from one of the subjects at their best fresh muscle which is 20 %MVC for 5 consecutive seconds.

This can also be seen for other types of movement. It is noticeable that some of the background noise appears in parts of the channels. This can be caused by crosstalk, movement artefacts, power noise as well as high skin impedance between the electrode and skin. Therefore, there is a need to propose proper analysis, such as digital filtering to eliminate this activity.

The other signal property which is noticeable from Figure 5.11 is the distinction of the signal amplitudes between the muscles or channels. This amplitude variation information is very important in this analysis as it becomes the primary component that is considered for classification performance. In Figure 5.12, the four classes of hand movements specified for fingers are shown. This is only an example for the 20% MVC, which is assumed as the fresh muscle state. As can be seen, the variation of the amplitude in the respective muscles is shows very distinctive properties. For examples, the magnitudes of FDS, ECRL, and EDC are the highest, that is between 0.05 mV to 0.1 mV .

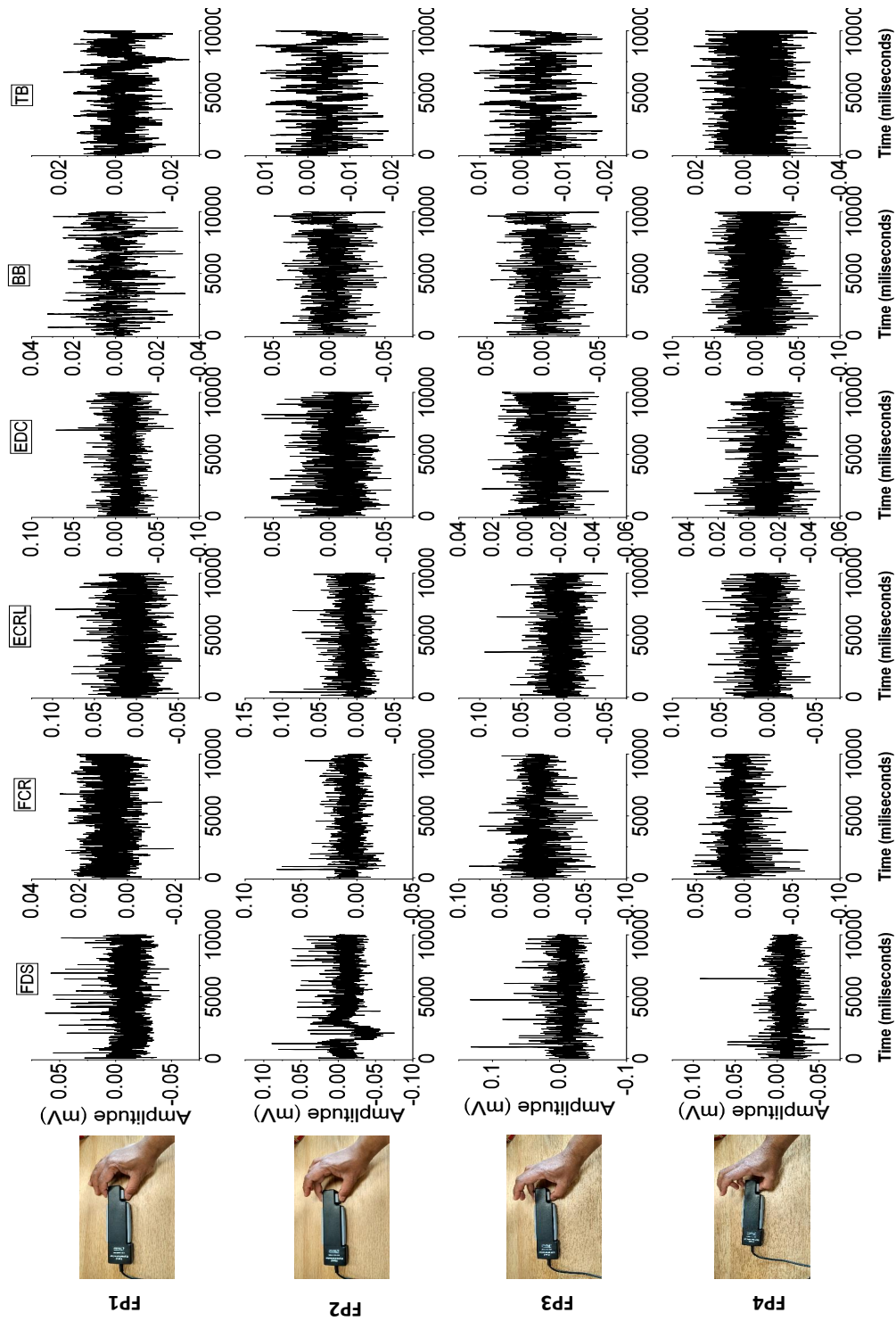


Figure 5.12: Examples of raw EMG signals at 20% MVC for finger pinches after preprocessed by eliminating the rest state between each force movements. There are four classes of hand movements involved with the fingers in this study.

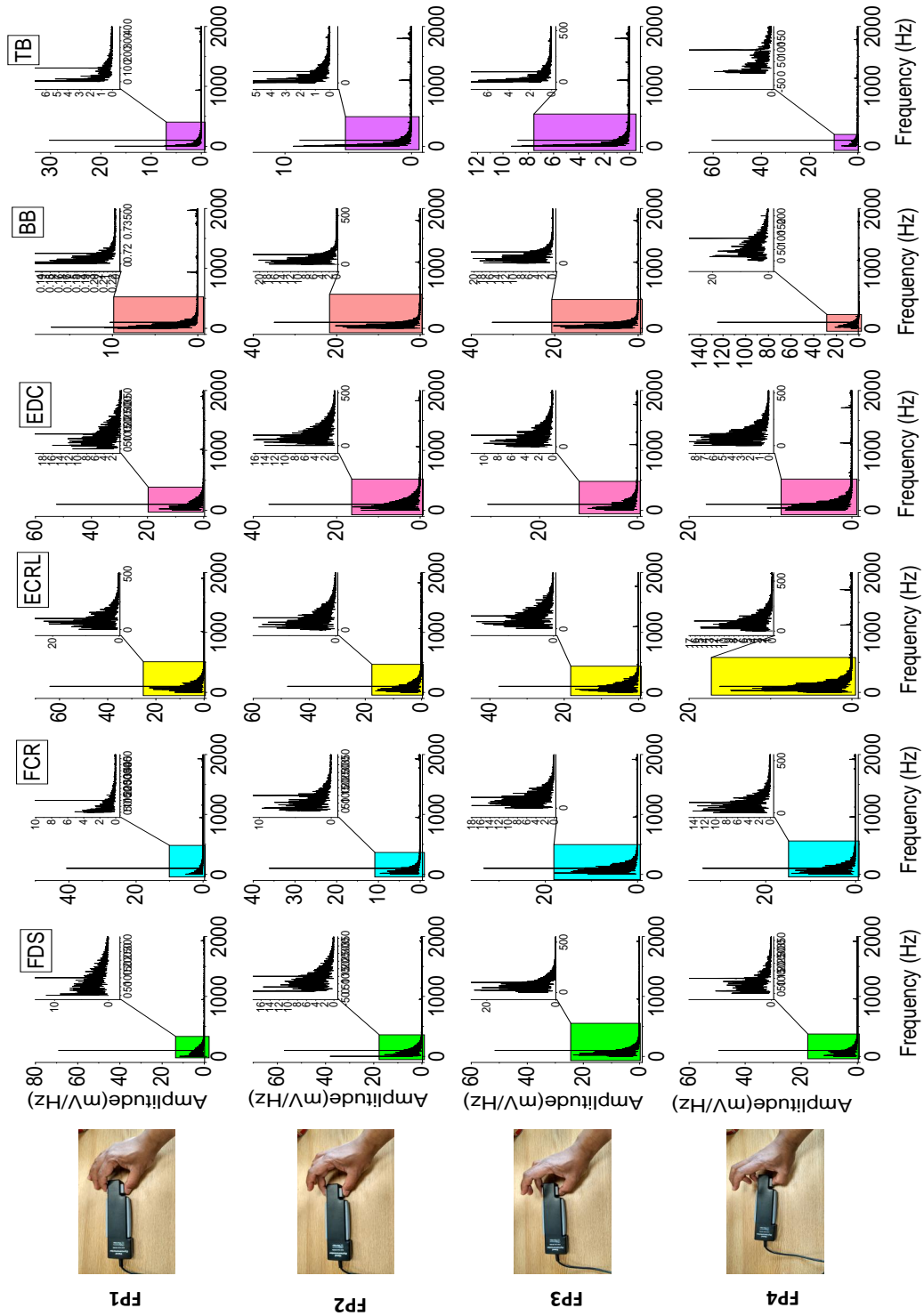


Figure 5.13: Examples of frequency spectrum of EMG signals for finger pinches with respect to Figure 5.12. The frequency shows different characteristic within each finger pinches. This as shown in zoomed section of each frequency spectrum.

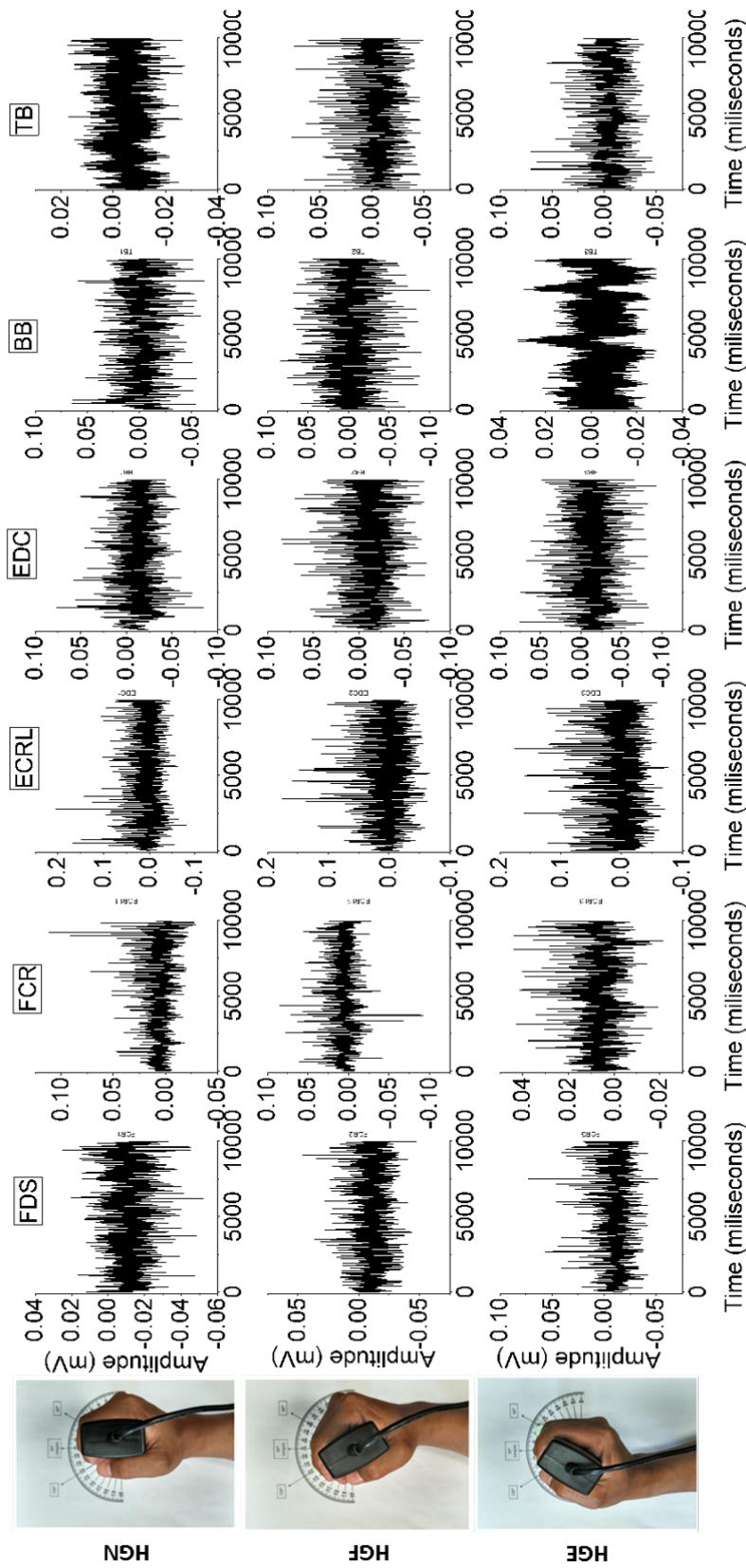


Figure 5.14: Examples of raw EMG signals at 20% MVC for hand grip after preprocessed by eliminating the rest state between each force movements. There are three classes of hand movements involved with the fingers in this study.

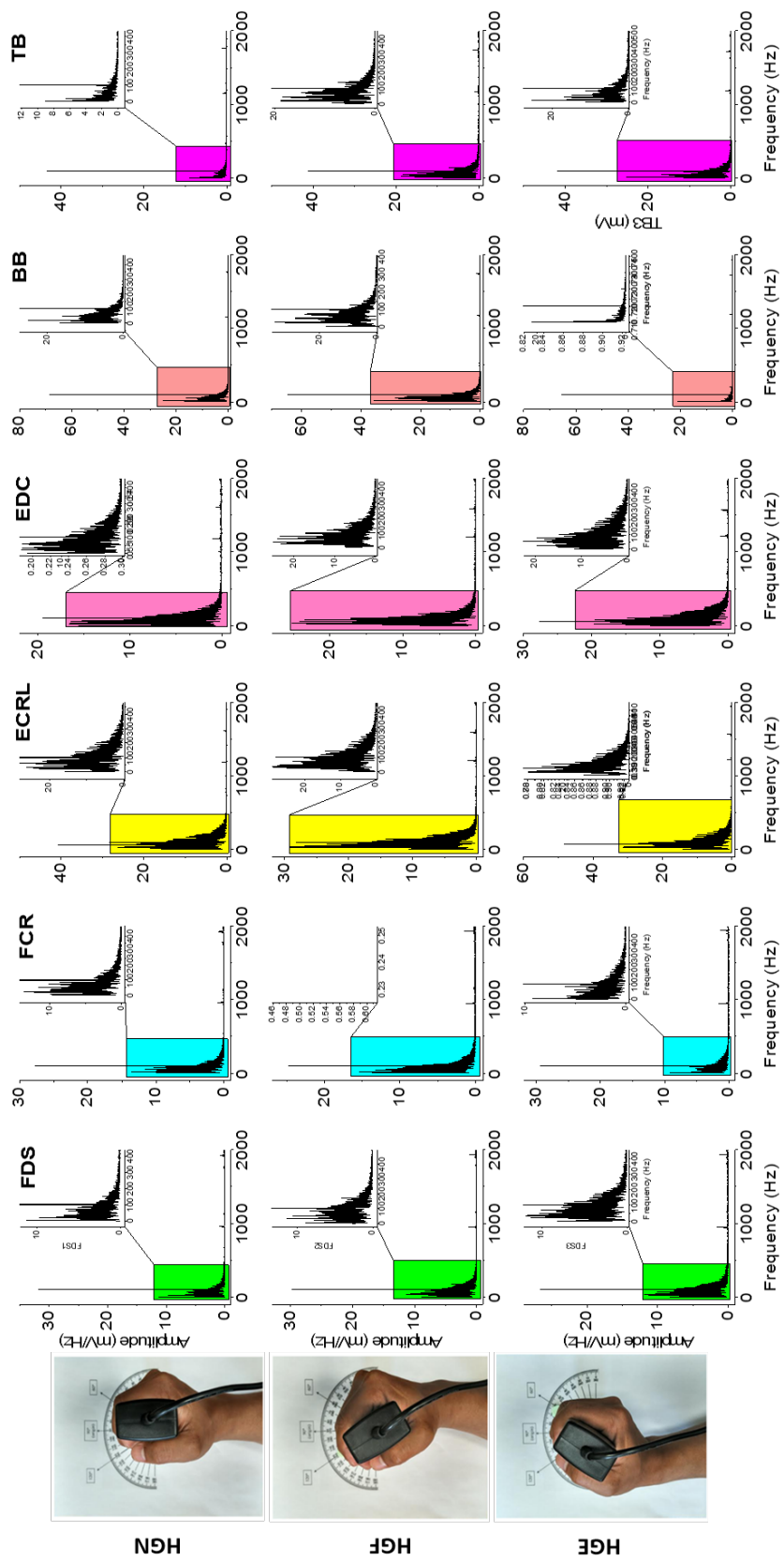


Figure 5.15: Examples of frequency spectrum of EMG signals for hand grip force with respect to Figure 5.14. The frequency shows different characteristic within each hand grip movement. This as shown in zoomed section of each frequency spectrum.

5.3.3 Feature Extraction

In determining the best features correlated with the types of movement set in this study, an analysis and verification is carried out in this section to reveal the real character of TD and FD features. Features are considered as the most valuable criteria in this study, as it will be used as a new representation for the signal movements. It has to be accurately informative and robust enough to react to all the movements.

Feature extraction is considered as the central part of this study. It will give the most compact and informative set of indicators, especially when dealing with the most condensed signal such as EMG. The features were chosen are going to be utilised in this study to associate with EMG based control, achieved maximum class separability, exhibiting robustness in noisy surroundings, and must be computationally low complexity. It is crucially required that the features will work in a real-time environment, and yield better pattern classification performance in EMG.

Features are generally categorised in three domains; time, frequency and time-frequency. Entropy is also considered one type of domain by some in this context. However, the most common features used in EMG study are time and frequency domain.

Therefore, several feature extraction approaches were used to extract useful features and to avoid redundancy. Twelve features from time domain and frequency domain were identified for use in this study. The main reason for having a large number of features is to minimise the computational complexity and time cost. Specifically, the features used were six (6) time domain (TD) features; root mean square (*RMS*), integrated absolute value (*IAV*), zero crossing (*ZC*), waveform length (*WL*), slope sign change (*SSC*), autoregression 6th order (*AR6*), and six (6) frequency domain (FD) features, namely root square zero-order moment (m_0), root square second (m_2) and fourth order moments (m_4), sparseness (*S*), irregularity factor (*IF*), and waveform length ratio (*WLR*). These features have been discussed and used by many researchers, and are listed in Table.

Both TD and FD features were extracted from the raw EMG signals acquired from the subjects. The features that were chosen in this study were generally based on the criterion of reducing the complexity and processing time. Features selected also intended to cover

spatial and temporal information that belong to the signals. Therefore, several key features involved in this study have been proposed in several previous studies as listed in Table 5.2.

5.3.4 Feature reduction technique

The features extracted could show a high degree of commonality in their attributes or dimensionality. Therefore, there is a need for a reduction technique able to minimise the feature dimensionality. In this study, PCA and a variant of LDA (ULDA) are used to assess the performance of the features. These reduction techniques have been chosen for their ability to reduce the redundancy of the features. The detailed explanation of these were given in Chapter 4.

In this study, the features extracted from the TD and FD sets were computed and analysed using MATLAB®R2015b software (Mathworks, USA). The contents of the features were then subjected to the dimensional reduction using PCA and ULDA. The component of feature number (FN) was dimensionally reduced with various sets (from 2 to 24), to investigate the suitability of features with the reduction number. Thus, this will identify which technique is capable of achieving the best FN and higher separability between the movement classes. These will be discussed in the results section.

The reason for the dimensional reduction needed in this study is twofold. Firstly, there are 15 subjects involved with whom to produce useful data for training and testing. Secondly, various numbers of features are used, and these cause the high dimensionality problems impacting on the data processing to be acceptable in ranges. This is important in any classification study.

Features separability

The first phase of analysis constituted inspecting the separability of the chosen features used in this study. The EMG features extracted from different hand movements were plotted using scatter plots showing sample observation of the FCR, FDS, ECRL and EDC muscles of the first subject, their features distribution across seven types of hand movement. The scatter plot figures were displayed to show that different types of muscle features, es-

Table 5.2: Six time domain (TD) features; root mean square (RMS), integrated absolute value (IAV), zero crossing (ZC), waveform length (WL), slope sign change (SSC), auto regression 6th order (AR6), and six (6) frequency domain (FD) features; root square zero order moment (m_0), root square second (m_2) and fourth order moments (m_4), sparseness (S), irregularity factor (IF), and lastly waveform length ratio (WLR). There are 12 features in total and each feature was determined to be used in this study.

Time Domain	Frequency Domain
$RMS = \sqrt{\frac{1}{N} \sum_{i=1}^N x_i^2} \quad (5.1)$	$\overline{m_0} = \sqrt{\sum_{k=0}^{N-1} x[j]^2} \quad (5.2)$
$IAV = \frac{1}{N} \sum_{i=1}^N x_i \quad (5.3)$	$\overline{m_4} = \sqrt{\sum_{k=0}^{N-1} k^4 P[k]} \quad (5.4)$
$ZC = \sqrt{\frac{m_4}{m_0}} \quad (5.5)$	$\overline{m_8} = \sqrt{\sum_{k=0}^{N-1} k^8 P[k]} \quad (5.6)$
$WL = \sum_{i=1}^{N-1} x_{i+1} - x_i \quad (5.7)$	$S = \left \frac{m_0}{\sqrt{m_0 - m_4} \odot \sqrt{m_0 - m_8}} \right $
$SSC = \sum_{i=2}^{N-1} [f[(x_i - x_{i-1})] \dots \times (x_i - x_{i+1})] \quad (5.9)$	$IF = \log \left(\left \frac{m_4}{\sqrt{m_4 m_8}} \right \right) \quad (5.10)$
$AR = \sum_{i=1}^P a(i)x(n-1) + e(n) \quad (5.11)$	$WLR = \log \left(\left(\frac{\sum_{j=0}^{N-1} \Delta^2 x }{\sum_{j=0}^{N-1} \Delta^4 x } \right) \right)$

pecially in time and frequency domains, were exhibiting distinctive classes of separability performance with respect to feature reduction technique applied.

Figures 5.16, 5.18, 5.17, and 5.19 are presented to illustrate the TD and FD features extracted. The scatter plots in these figures were constructed upon the most three discriminant feature components after the dimensionality reduction method using PCA and ULDA, respectively. The class movements are indicated in the variation of colours as labelled in each figure to clarify the seven hand movements involved in this study.

For reasons of comparison in the analysis the plots are shown with PCA on the left side and ULDA on the right side, both with TD and FD. As noted, the TD features had a more substantial variance when ULDA reduction was used as compared to the PCA. PCA gave poor class separability where the features were compact in the same region, especially for the flexor muscle. All muscles performed well when using ULDA, where the distribution appeared to form a precise class of hand movement in TD. Meanwhile, for FD, it was evident that both features had a larger variance when ULDA reduction was used as compared to the PCA. PCA gave poor class separability where the features appeared compact in the same region, especially for flexor muscle. However, all muscles performed well when using ULDA, where the distribution formed a precise class of hand movement.

Meanwhile, it is clear from FD features that the performance of PCA in distributing the feature components was unpredictable. However, ULDA in FD features performed very well. The scatter plot of feature components show a good consistency and looks promising in the class separability, with each muscle showing its characteristic within class variance in each hand movement. FCR and FDS muscles using PCA have shown inconsistencies in their distribution, while ECRL and EDC have formed better class separability. It can be seen that the class separability algorithm used in this study was successful in separating the feature components.

The classification performance of the combinations of the most three prominent TD and FD features were analysed. LDA classifier architecture has been shown to perform the equivalent performance as k-nearest neighbour (kNN) or multilayer perceptron neural network (MLPNN) (Englehart et al. (2001); Geethanjali (2015); Khushaba et al. (2016);

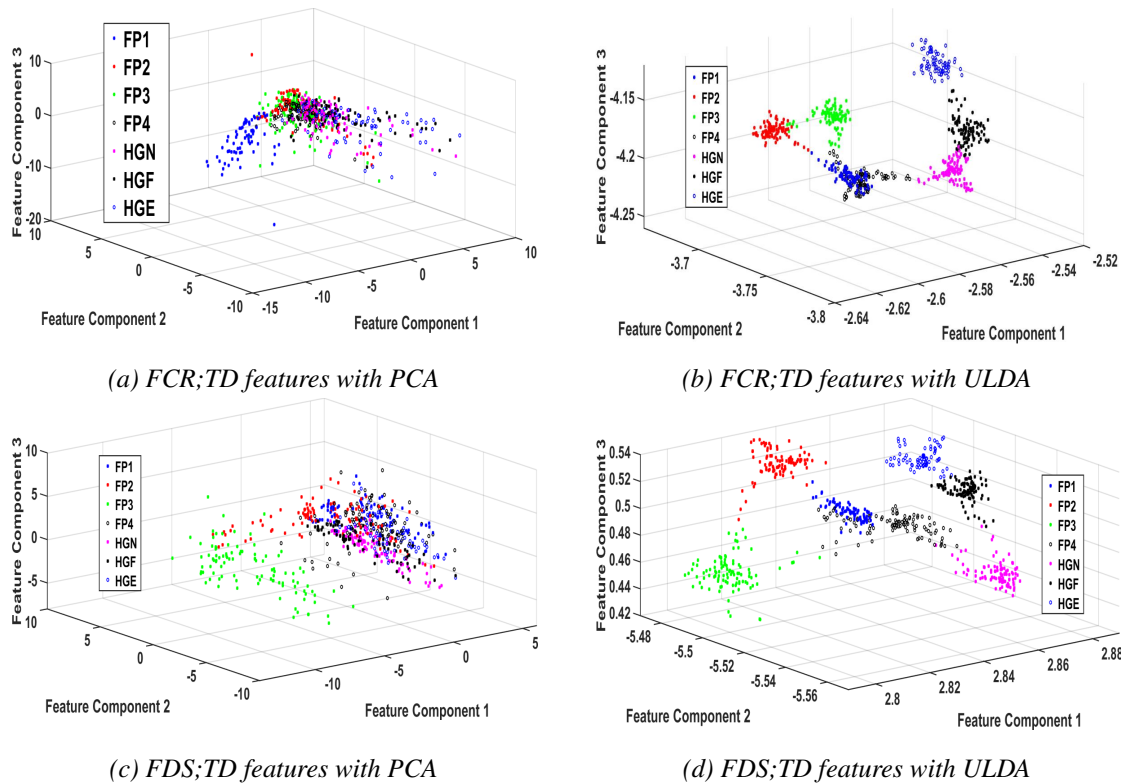


Figure 5.16: Graphical illustration showing TD features and their class of separabilities between two adjacent flexor muscles FCR and FDS concerning the PCA and ULDA. PCA not successful in separating the movement class. This creates new insight into how well PCA adapted to the variations of the feature for different class movements, especially as proposed in this study.

Venugopal et al. (2014)), thus excluded for the further analysis. An analysis of training and testing data for the LDA classifier was performed in this study based on the features extracted from time and frequency domain components. There was high accuracy achieved by both reduction methods. Figure 5.20 shows the error produced in one of the datasets from ECRL muscle. The errors produced were due to the transition moment as the EMG contraction state was undetermined (Winters and Kleweno (1993)).

The example classification sequence for one of the involved muscles shown in Figure 5.20 indicates that the proposed method used in FN reduction on the EMG data set is highly accurate. This technique has been applied to all the datasets available for this study using LDA classifier.

ULDA has shown the top classification performances by giving >98% average for both TD and FD training features. While for PCA, less than 92% average was achieved for both TD and FD training features. The trend appeared almost the same on testing data with

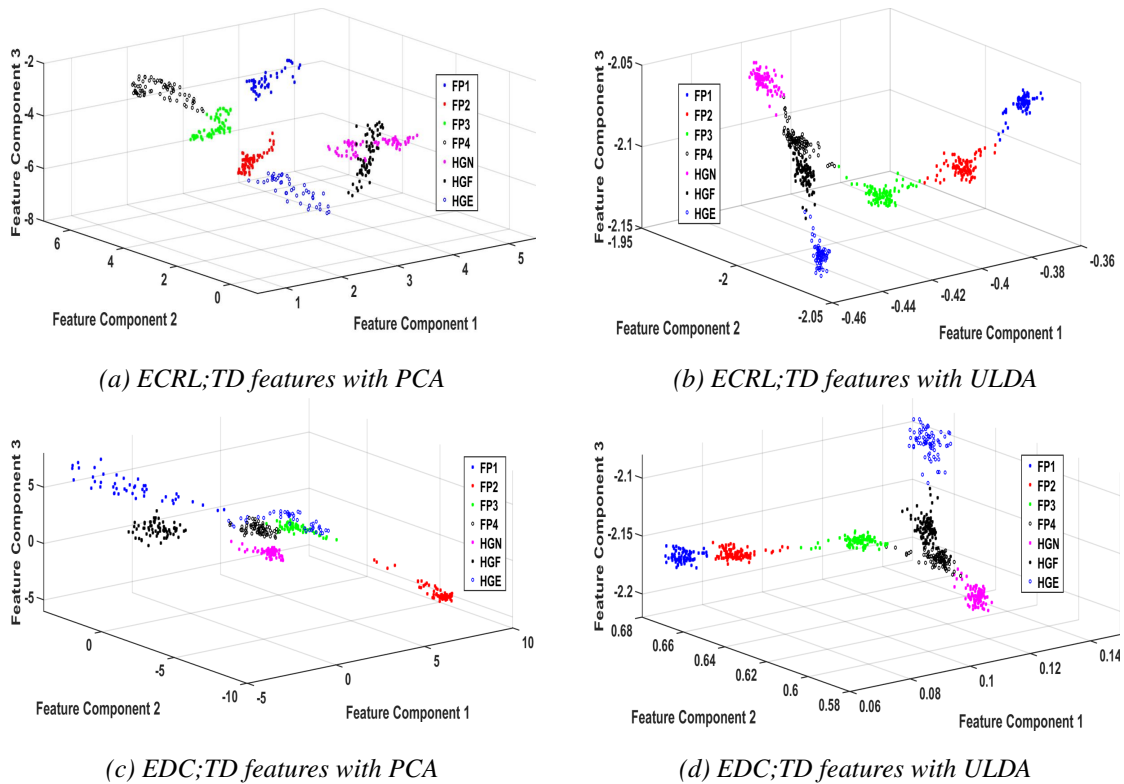


Figure 5.17: Graphical illustration showing TD features and their class of separabilities between two adjacent extensor muscles ECRL and EDC with respect to the PCA and ULDA. Although PCA seems to have good class separability, ULDA proves to be more efficient where all the class movements are compact and within their group boundary. This will result in better classification with ULDA.

ULDA performing much better than PCA (see Table 5.3).

One of the best ways to investigate the performances of adjacent muscles regarding their feature number is based on the concept of correlation of the individual muscle's performance. This can be achieved by estimating the classification rates between those adjacent muscles. High mutuality between nearby muscles with their best-desired classification accuracy, could justify the standard functionality of the muscle. As can be observed in Figure 5.21, there are interesting patterns that appear in the adjacent muscles where different reduction techniques give very likely performances. All the muscles involved in this study tend to perform well with their pairs.

ULDA is outperforming the PCA in terms of achieving high accuracies $>90\%$ at smaller FN, which is by FN of 2 and 4 for (ECRL vs EDC) and (FDS vs FCR) respectively. PCA is believed to require more features to achieve the same results as it works based on reducing the redundancy without considering the features or connectivity of classes. For

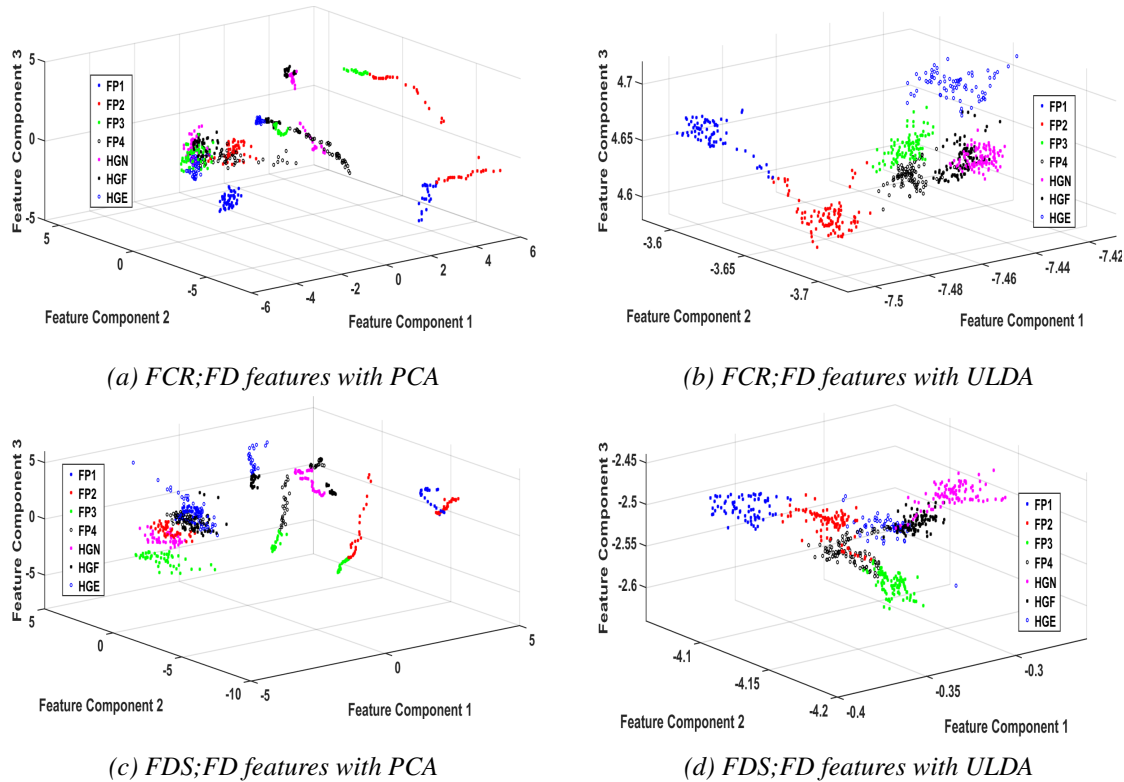


Figure 5.18: Graphical results illustrate FD features and their class of separabilities between two adjacent flexor muscles FCR and FDS with respect to the PCA and ULDA. PCA was unable to separate the movement classes in a good way as all classes were undetermined within their group. This creates unstable classification and might be related to the disability of PCA to reduce the redundancy problems in the FD features.

this case, PCA achieved mutual accuracies $>90\%$ at FN= 12.

As can be seen in Figure 5.21, FDS and FCR performed very similarly when using PCA and ULDA, where they achieved mutual accuracies above 90% at a factor of 12 for FN.

Meanwhile, ECRL and EDC muscles responded very well using both PCA and ULDA. However, this does not affect the objective of the study, where the overall performance between muscles could be the ultimate justification. As can be seen in the Figure B.2 in Appendix B, the similarity performance between both adjacent muscles are high, less than 5% gap for both flexor (FCR and FDS) and extensor (ECRL and EDC) muscles on average. These are applicable to both domains of feature analysis.

On those findings, it is believed that the adjacent muscles perform almost similar in all subjects. Thus, the number of muscles used in the data collection could be reduced as it would make the analysis better. The data arrangement, muscle selection, and feature set

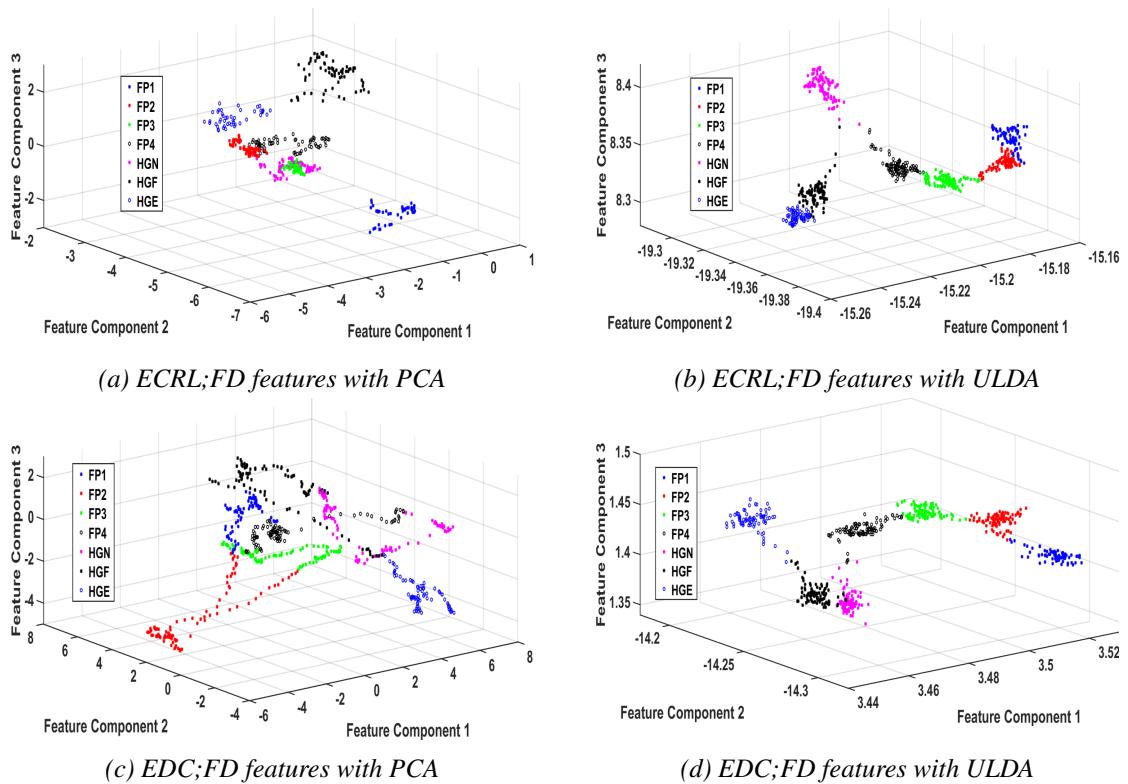


Figure 5.19: Graphical illustration showing FD features and their class of separabilities between two adjacent extensor muscles ECRL and EDC with respect to the PCA and ULDA. ULDA with FD features performed very well as compared to PCA for both muscles (refer Figure 5.19b and 5.19d).

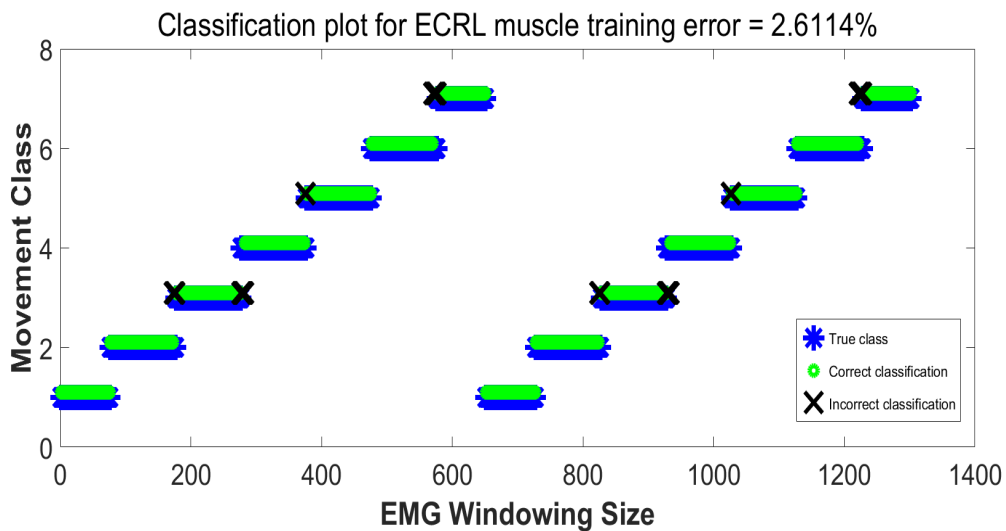


Figure 5.20: Example of classification sequence for FD features of ECRL muscle. The classification time plot is highly successful presenting the actual and estimated class of hand movement with 2.6114% error.

used in the parameter adjustment for an LDA classifier produced better results. LDA can be seen as the most useful classifier, which matches or sometimes exceeds other classifiers in terms of their performance. LDA also performs better in terms of computational efficiency.

Table 5.3: Training and testing data classification accuracies using PCA and ULDA for both time and frequency domain features, FN=10. Training data has excellent performance for both domain and reduction technique. However, performances of testing data are slightly low. This might be due to the variations of the features among subjects.

Analysis Domain	Muscles	Training Data (%)		Testing Data (%)	
		PCA	ULDA	PCA	ULDA
TD	FCR	86.9432	99.5392	85.3403	90.8377
	FDS	85.4071	98.9247	87.8272	92.0157
	ECRL	98.6175	99.6928	93.7173	94.2408
	EDC	97.0814	99.3856	94.3717	99.8691
FD	FCR	91.5515	97.3886	81.4136	87.9581
	FDS	88.0184	98.1567	91.0995	93.9791
	ECRL	97.3886	99.232	80.6283	84.8168
	EDC	94.7773	98.4639	81.6754	76.8325

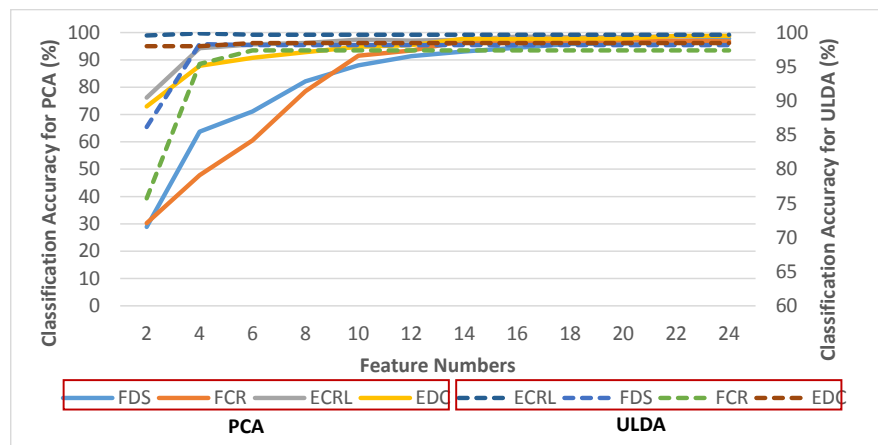


Figure 5.21: The average classification accuracies for all the studied muscles using both the proposed PCA and ULDA reduction techniques with various FN. The adjacent muscles performed similarly in their accuracy for both categories. However, ULDA outperformed the PCA by achieving smaller FN of reduction components, FN=7 to made an accuracy >95%.

This also would help the researchers to be efficient in the time and money spent in the data collection. However, the deservedness of reducing the number of channels or muscles used should reflect the study objectives.

5.3.5 Descriptive statistical strategy

In this study, the overall impact of the EMG signal and its variation on nine (9) TD and FD related statistical features is analysed. Our features created here are solely tied to TD and FD, as is believed that several combinations of features extracted will produce a powerful feature set. Hence, these will be used to identify the most suitable and robust feature sets to deal with the EMG signals. The features selected from this study will also be used in future for comparative analysis.

The analysis of EMG in this study is based on the EMG readings and the features were extracted using descriptive statistical features of TD and FD. The generated features were believed to be at the best component, which will give indication of the highest significant difference between the muscle component and their properties. Thus, it will provide better and useful features for the classification. However, the design of the pattern recognition technique in this study remains challenging. The challenge, as many researchers struggle to deal with this kind of signals, was the issue of robustness and information efficiency for top-notch performance in classification. Therefore, to propose a new approach of analysis, this study attempted to impose a new treatment of EMG signals, their respective muscle and the movement strategy used to compensate for daily human activities.

Nevertheless, in many previous research works, the EMG signals have been acquired from only two or three specific muscle, and the pattern classification is realised based on the different feature extraction methods. Theoretically, there are many differences between the muscle layers and their region of interest. Therefore, for example, the intramuscular muscles are not comparable with the surface muscle, and this cannot guarantee their performances nor effectiveness of the algorithm used. Understanding the nature of EMG signal for hand movements, their characteristics in terms of amplitude and spectrum component are studied. That has been designed and conducted for seven types of hand movement, as

mentioned earlier. For example, Figure 5.13 and Figure 5.14 show the raw EMG signals acquired from six muscles for four finger movements and three hand grip movements.

To better understand the nature of the EMG spectrum for each movement at their specific muscles, the frequency spectrum was plotted using FFT analysis method. These has been shown as in Figure 5.13 and Figure 5.15. The variation of the frequency bandwidth between types of muscle (flexor, extensor and upper arm muscles) may be seen in this figures. For the flexor muscles, the bandwidth was spotted between 1-250Hz, extensor 1-350Hz, and upper arm muscle 1-150Hz. In Figure 5.13 and Figure 5.15, every channel of muscle showed a very distinct peak at roughly around 50Hz, which is probably due to mains power disturbance. This can be seen for all movements. Therefore, there is a need for the use of notch filtering to eliminate the noise.

Table 5.4: The table shows an example correlation coefficient between each feature as proposed in this study. The correlation calculated using Pearson R statistical method. This proves the best linear relationship between each feature at $r > 0.95$. The number indicated in the table was set as a feature and denoted as follows: 1. Mean, 2. Standard deviation, 3. Variance, 4. Skewness, 5. Kurtosis, 6. Mean absolute deviation, 7. Minimum, 8. Medium, and 9. Maximum

	1	2	3	4	5	6	7	8	9
1	–	0.06932	0.0879	0.0188	0.15912	0.04254	0.18599	0.99671	0.32734
2	0.06932	–	0.92887	0.40869	0.3497	0.99639	-0.9282	0.02609	0.91249
3	0.0879	0.92887	–	0.39009	0.37264	0.91285	-0.8601	0.04873	0.89364
4	0.0188	0.40869	0.39009	–	0.7128	0.37124	-0.3283	-0.0416	0.54081
5	0.15912	0.3497	0.37264	0.7128	–	0.2902	-0.3634	0.11724	0.56897
6	0.04254	0.99639	0.91285	0.37124	0.2902	–	-0.9223	0.00207	0.88185
7	0.18599	-0.92821	-0.8601	-0.3283	-0.3634	-0.92229	–	0.22013	-0.8043
8	0.99671	0.02609	0.04873	-0.0416	0.11724	0.00207	0.22013	–	0.27847
9	0.32734	0.91249	0.89364	0.54081	0.56897	0.88185	-0.8043	0.27847	–
MAX	0.99671	0.99639	0.9289	0.7128	0.7128	0.99639	0.2201	0.9967	0.9125
MIN	0.0188	-0.9282	-0.86	-0.328	-0.363	-0.9223	-0.928	-0.042	-0.804

Table 5.5: Linear correlation coefficient using Pearson's R ($r > 0.95$) for finger pinches using TD features at different MVCs; Legend: * Linearly correlated within each paired; * Linearly correlated within each paired; ⊕ Linearly correlated within each paired; ✕ Not linearly correlated

FP	Mean	SD	Var	Skew	Kurt	MAD	Min	Med	Max
1	*	*	✕	✕	✕	*	✕	*	✕
2	*	*⊕	⊕	✕	✕	*	✕	*	✕
3	*	*	✕	✕	✕	*	✕	*	✕
4	*	*	✕	✕	✕	*	✕	*	✕

For finger pinches, the analysis for all subjects involved in this study reveals that sev-



Figure 5.22: Scatter plots of 9 TD features for FP1 at various percentages of MVC. The plots was statistically measured their Pearson's R linear correlation coefficient at $p < 0.05$ confident level.

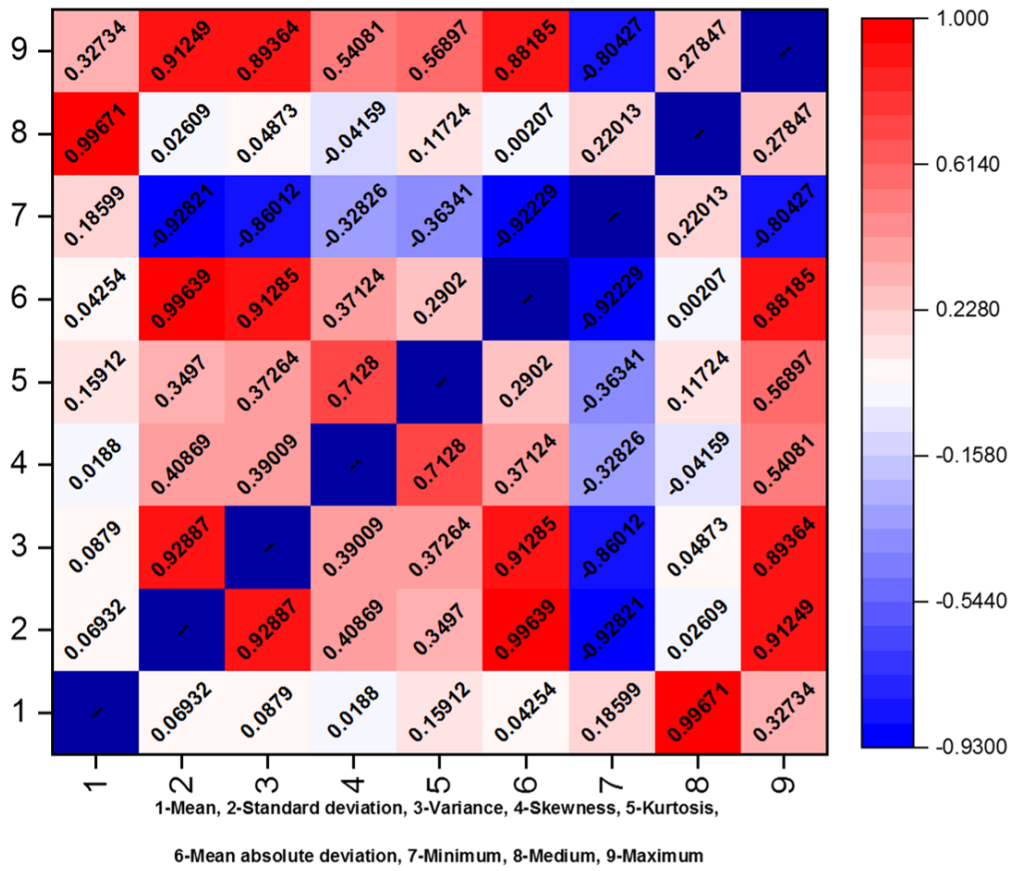


Figure 5.23: Example of confusion matrix Pearson's R correlation coefficient of 9 TD features, at FPI for various percentages of MVC. Results averaged from all subject involved in this study. The highest concentration red box shows the most positive linear correlation $r=0.996$. The acceptable range was set at $r>0.95$.

Table 5.6: Linear correlation coefficient using Pearson's R ($r>0.95$) for finger pinches using FD features at different MVCs

FP	Mean	SD	Var	Skew	Kurt	MAD	Min	Med	Max
1	*	*	✗	✗	✗	*	✗	*	✗
2	*	*⊕	⊕	✗	✗	*	✗	*	✗
3	*	*	✗	✗	✗	*	✗	*	✗
4	*	*	✗	✗	✗	*	✗	*	✗

eral features have been showing strong correlation between each other such as (Mean vs Med, SD vs MAD and SD vs Var). The features were optimised empirically using the pairing system through the measures of their correlation coefficient. The feature at different combinations is calculated using Pearson's correlation coefficient. The chosen features are selected between features with $r > 0.95$ between the pairs.

Table 5.7: Linear correlation coefficient using Pearson's R ($r > 0.95$) for hand grip forces using TD features at different MVCs; Legend: * Linearly correlated within each paired ; ** Linearly correlated within each paired; *** Linearly correlated within each paired; ✕ Not linearly correlated

HG()	Mean	SD	Var	Skew	Kurt	MAD	Min	Med	Max
N	✕	***	✕	✕	✕	*	✕	✕	*
F	✕	***	✕	✕	✕	*	✕	✕	*
E	*	*	✕	✕	✕	*	✕	*	✕

Table 5.8: Linear correlation coefficient using Pearson's R ($r > 0.95$) for hand grip forces using FD features at different MVCs

HG()	Mean	SD	Var	Skew	Kurt	MAD	Min	Med	Max
N	✕	*	✕	✕	✕	*	✕	✕	✕
F	✕	**	✕	✕	✕	*	✕	✕	*
E	*	*	✕	✕	✕	*	✕	*	✕

5.4 Summary

This chapter explored and evaluated the new approaches of data collection and assessing the human upper forearm muscles with force variations, as well as muscle fatigue. It is suggested that the most appropriate use of muscle to establish the inter-relation between two regions of the human upper forearm with the statistical features extracted from the TD and FD domains. It has been shown that there are four statistical features perform very well, and these are mean, standard deviation (SD), mean absolute deviation (MAD) and variance (Var). The analysis results from the data that has been collected, two types of muscle group has been selected for further study. The most highest EMG average power from those tested in this Section was chosen; this has been discussed in Section 5.2.4.

This study offers an opportunity to develop a new feature and classification scheme to enhance the capabilities of disabled people, especially one that may have problems of

weaknesses in muscle contraction or amputated. The current study focuses on paralysed persons or those amputated in the middle region between the forearm and upper arm, where the current single system approach will not be adequate.

This also aimed to minimise the number of EMG channel used, optimise the cost for data collection, and also reduce the complexity in data analysis. Therefore, there is the need to perform this study before proceeding to achieving ultimate objective for the whole study. Consequently, it is necessary to identify all these muscles and their performances with individual hand movement covered in this study. Another potential application that may be applied in this study is the way to distinguish the movement and contraction levels without using all the muscles available in the forearm and upper arm.

Chapter 6

Fuzzy entropy mutual information based on wavelet EMG fusion

6.1 Introduction

The proposed EMG fusion algorithm in the pattern classification for the human UFA are described and presented in this chapter. The fusion modelling covered the forearm and upper arm muscles and their region was discovered. Development of pattern classification with the proposed algorithms for reference to initiating a new approach of concatenating the two regions of muscles as one the application of the pattern classification has been analysed, and the details of the analysis is concluded in this chapter.

It has been proved that the EMG signals exhibit an interconnected function between one another. The basic rule for the muscles, they function independently of one another; however, some parts of the muscle series manifest synchronous potentials. One of the most known terms for this behaviours is synchronisation. This will be the ultimate justification for proposing this idea for the study.

EMG is well known on the problematic situation where it has to deal with the excessive number of inputs. This happened as different input or features extracted from the same region of muscles produces different patterns or properties of the signal. Therefore, by combining or fusing these flexible characteristics, the information gathered is retained while eliminating the redundancy problems. Time-frequency features will be used in this chapter as it is aimed at the real-time application in future work.

A cross-correlation technique based on time-frequency fusion feature was chosen. The

fusion techniques have been popular in the pattern classification study in recent years and well known for its richness properties like EMG signals. Feature fusion typically comprises from three different strategies: pixel-level fusion, feature-level fusion and decision-level fusion.

6.2 Data fusion techniques

The integration of data and information (feature) from various causes have been identified as data fusion. This subchapter summarises the state of the data fusion field and describes the most relevant studies. Generally, the use of knowledge or data fusions can benefit most information or signal that requires any parameter estimation from diverse origins (Castanedo (2013)). The expressions of data/information fusion are known as one meaning; but in some strategies, the data fusion employed for raw data (acquired immediately from sensors) and the feature fusion is used to represent means from pre-processed data.

Hall and Llinas (1997) in their reports stated that data fusion procedures fuse data from many sensors and described information from associated databases to gain upgraded accuracy and more precise results than could be attained by the performance of a single sensor. Feature fusion has been frequently employed in the current interest of pattern classification due to their abundance of quality credentials in the signal database. Feature fusion typically involves three approaches:

- a. Signal or pixel-level : the fusion at the raw/original data layer, or known as data fusion,
- b. Feature-level : utilize fusion at extracted feature from space of different modality profiles, the most important pre-processing step for any classifier,
- c. Decision-level : fuses results from various approaches, algorithms, origins, or classifiers to produce estimations that are of greater quality. This technique also considered as high level fusion.

This technique has been briefly discussed in Luo et al. (2002), which stressed on the

abstraction levels of information/feature fusion. The principal goal of information/feature fusion is to employ entirely appropriate low-level features extracted from the identical or diverse modality outlines of tasks for analysis. Though, the obtained features (or signals) may carry excessive and unnecessary information, which raises the dimensional problems and decreases feature spaces quality.

In this case, standard data integration procedures unable to present a decent understanding. Furthermore, dimensionality problems extend the training execution in the classifiers and thus costs high computation complexity; hence, dimensional reduction strategy using feature projection is necessary.

Feature projection has been popular for the most widely used technique in the feature fusion. It is a technique that described as mapping strategy of original feature space into a new subspace so that the learning criterion or processes optimised.

6.3 Fusion strategy

In this work, two tiers of fusion technique are proposed to improve the usual way of EMG classification scheme. The EMG data acquired, as explained in Chapter 3, and being pre-analysed in Chapter 4 and Chapter 5 were used in this chapter. The effective EMG based with proper EMG channel numbers selected is analysed using fusion techniques. According to the simplified EMG channels concluded in Chapter 4 and 5, the use of the optimised channels with proper classification technique improves the performance.

At first, the raw signals from two regions of muscles are fused together, generating a new whole dataset for the feature extraction. The features using fuzzy mutual information entropy based on wavelet (FEFWC) is extracted. The generalised feature functions based on fuzzy mutual information produced from this method. This approach is believed to works better as multiple fusion strategy will give better resolution on the classification decision. The subject's data from previous works are used in this newly proposed work. It is to make sure that the results gathered from this approach can be compared and the performance of the new proposed idea could be evaluated.

6.4 Wavelet analysis

Fourier is a basic standard of the frequency component, and it is limited to only stationary signals. Fourier working principle is based on the time evolution of a fixed window, following in unpredictable frequency localisation. Fixed window technique is not suitable for human biosignals. Actual human biosignal like EEG, ECG, EMG is not stationary in their natural properties. Intermittencies and uncertainties in their frequency components, notably variable. These type of signals are common with multiscale and transient aspects. Therefore, wavelet was introduced to overcome the problem of frequency localisation in the fixed window as appears in Fourier.

6.4.1 Continuous wavelet transform

The continuous wavelet transform (CWT) is one of the wavelets analysis type. It represent an optimal decomposition of frequency localisation for the time series, $x(t)$, time (t) and frequency or scaling function (a) with a convolution integral:

$$W_f(a, \tau) = \frac{1}{\sqrt{a}} \int_{-\infty}^{+\infty} x(t) \psi^* \left(\frac{t - \tau}{a} \right) dt \quad (6.1)$$

where ψ is refer to the mother wavelet function, a denote the dilation or scale factor, τ translation parameter (time shift) and '*' is a complex conjugate operator. To get this right, it must follow the admissibility condition. Based on admissibility condition as discussed in Section 4.5.2, local wavelet spectrum can be define as:

$$P(k, t) = \frac{1}{2C_\psi k_0} \left| W \left(\frac{k_0}{k}, t \right) \right|^2, k \geq 0, \quad (6.2)$$

where k_0 is the peak frequency of the mother wavelet used in the study. From this

equation, a mean or global wavelet spectrum can be defined as;

$$P(k) = \int_{-\infty}^{+\infty} P(k, t) dt \quad (6.3)$$

which also highly related to the total energy E of the original signal $x(t)$;

Total Energy

$$E = \int_{-\infty}^{+\infty} P(k) dk \quad (6.4)$$

$$P(k, t) = \frac{1}{C_\psi k} \int_0^{+\infty} P_F(\omega) \left| W\left(\frac{k_0}{k}, t\right) \right|^2, \quad (6.5)$$

The square of the FT of shifted wavelet function ψ at frequency k produces the global wavelet spectrum, in their sample average.

Wavelet Cross Correlation

The idea of using wavelet cross-correlation began when we were trying to reach a new adaptation in our study to investigate the correlation between two regions of muscles in the human upper forearm since the muscles in the forearm and upper arm are complexes within its functional and specification. The cross-correlation technique using specific muscles specially chosen from the pre-study highly considered. This methodology is believed to create a new space of information in getting a better and proper analysis of detection or integration of human upper forearm region.

The wavelet fusion strategy is to utilise the wavelet coefficients generated at each fusion signal, to construct new features or variables that can best represent the classes of the task for the hand movement. If the two signals multiplied, and the features extracted from fusion operation will generate the boosted correlation values, while the uncorrelated features will depreciate. The identification of the best bases was a problem that needs to

rectify. The features constructed has to be highly discriminate between each class of the problem tasks.

Let the wavelet transform of two real signals, represents by $f(t)$ and $g(t)$. The wavelet cross-correlation can be define as equation below:

$$W_{fg}(a, \tau) = W_f^*(a, \tau)W_g(a, \tau), \quad (6.6)$$

The symbol for '*' means for complex conjugate operator, and since the analysing wavelet is complex, the $W_{fg}(a, \tau)$ also considered as complex and they can be written in its complexes forms:

$$W_{fg}(a, \tau) = CoW_{fg}(a, \tau) - iQuadW_{fg}(a, \tau), \quad (6.7)$$

If $f(t)$ and $g(t) \in L^2(\mathfrak{R})$, this important relation means:

$$\int_{-\infty}^{+\infty} f(t)g(t)dt = \frac{1}{C_\psi} \int_0^{+\infty} \int_{-\infty}^{+\infty} CoW_{fg}(a, \tau)d\tau da, \quad (6.8)$$

which relates the Co-spectrum to the correlation integral of the signals. Therefore, the local wavelet cross-correlation spectrum is defined by:

$$|W_{fg}(a, \tau)|^2 = |CoW_{fg}(a, \tau)|^2 + |QuadW_{fg}(a, \tau)|^2 \quad (6.9)$$

The integration τ and a of local wavelet equation gives the global wavelet coefficients and correlation energy dispersed by the fusion signal. These equivalent quantities gives better personalisation of features to be used in the classification analysis.

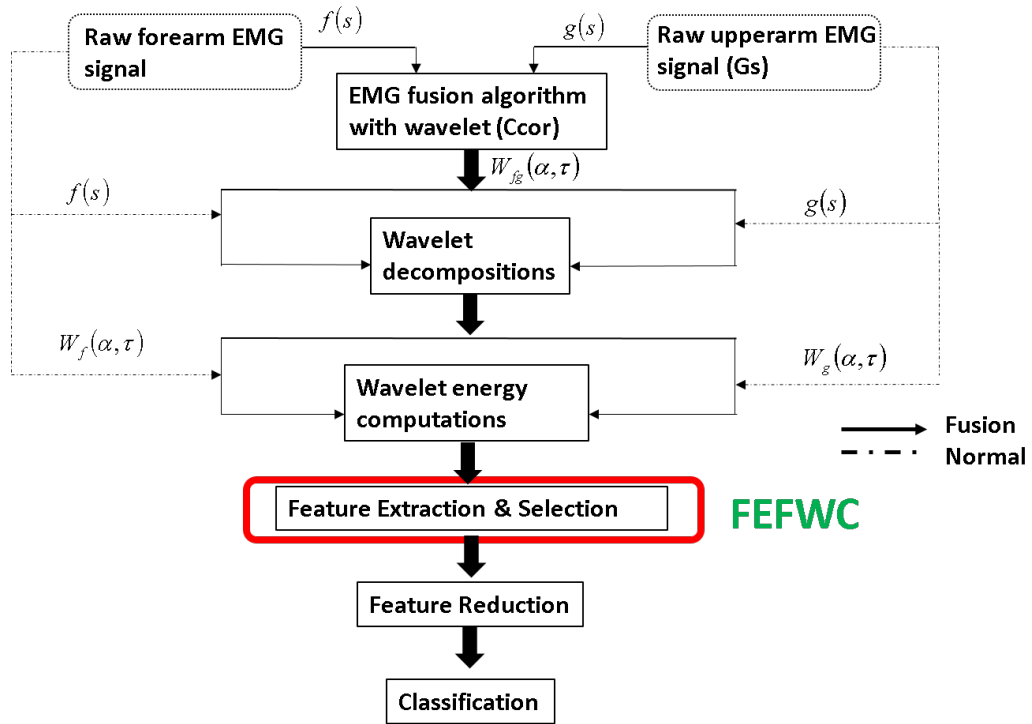


Figure 6.1: The basic fusion strategy introduced for this study.

6.5 Mutual information based on wavelet fusion

Entropy is one types of primary measures that give probabilities of information content for a random variable. Entropy was used by many researchers to estimate the uncertainty of that variable by employing mutual information strategy. This will involves two types of mutual information of variables using a joint probability distribution and a marginal probability distribution (Khushaba et al. (2016)).

The value for the k th vector with class, i th denoted as follow:

$$\mu_{ik} = \mu_i(x_k) \in [0, 1] \quad (6.10)$$

where $X = \{x_1, x_2, x_3, \dots, x_l\}$ are the space pattern, and $k = 1, 2, 3, \dots, l$ is patterns total number. The average sample data of class i th are represented by x_i , while the data radius

r can be found at:

$$r = \max \| \bar{x} - x_k \|_{\sigma} \quad (6.11)$$

Hence, the membership μ_{ik} calculated as:

$$\mu_{ik} = \left(\frac{\| \bar{x} - x_k \|_{\sigma}}{r + \epsilon} \right)^{\frac{-2}{m-1}} \quad (6.12)$$

where m known as fuzzification parameter, and it must be $\epsilon > 0$ to avoid singularity. σ is the distance of the SD, hence the samples membership are individually normalised according to:

$$\sum_{i=1}^c \mu_{ik} = 1 \quad (6.13)$$

Let $X = \{x_1, x_2, \dots, x_n\}$ with n symbols, and the membership degree of x_i to fuzzy set A denoted as $\mu_A(x_i)$, and $F : G(2^X) \rightarrow [0, 1]$ as a set-to-point mapping. The following standard of De Luca–Termini (DLT) axioms are required for the F to be established as a sets of fuzzy entropy:

$$A^c = (1 - \mu_A(x_1), \dots, 1 - \mu_A(x_n)) \quad (6.14)$$

While, Shannon entropy satisfies all the above DLT axioms, and is defined as:

$$H(X) = - \sum_i p(x_i) \log_2 p(x_i) \quad (6.15)$$

The c-fuzzy sets are constructed along with each particular feature using the proposed

membership function. This reflects the membership degrees of the individuals in the problem classes. The fuzzy equivalent to the mutual probability of the practice models that belong to class i is presented as:

$$P(f, c_i) = \frac{\sum_{k \in A_i} \mu_{ik}}{NP} \quad (6.16)$$

while, $P(f, c_i)$ were interpreted as predefined samples class degree that belong to the class i . Meanwhile A_i denoted as the pattern indices for the training data, which NP reflect to the total number of patterns. Therefore, the joint fuzzy entropy of the class i can be stated as:

$$H(f, c_i) = -P_{f, c_i} \log P_{f, c_i} \quad (6.17)$$

The entropy for all c -classes can be calculated by summing along the universal set. This will produce the complete fuzzy entropy set, stated as:

$$H(f, C) = \sum_{i=1}^c H(f, c_i) \quad (6.18)$$

The joint fuzzy entropy did satisfies the four DLT axioms. The associated entropies for each feature can be computed along each features samples. Hence, the marginal entropy for each feature can be produce by adding the estimated membership values of the samples together with the c -fuzzy sets S_i :

$$P(f S_i) = \frac{\sum_k \mu_{ik}}{NP} \quad (6.19)$$

Hence, the feature marginal entropy is denoted as:

$$H(X) = -P_{fS_i} \log P_{fS_i} \quad (6.20)$$

Similarly, for the class marginal entropy can be found by computing the fuzzy class probability $P(c_i)$:

$$P(c_i) = \frac{\sum_{k \in A_i, \forall S} \mu_{ik}}{NP} \quad (6.21)$$

Then,

$$H(Y) = -P_{c_i} \log P_{c_i} \quad (6.22)$$

are referred to as marginal class entropy $H(Y)$.

The fuzzy mutual information (FMI) is then calculated using the equation defined as below:

$$FMI(X, Y) = H(X) + H(Y) - H(X, Y) = H(Y) - H(X|Y) \quad (6.23)$$

where X and Y are two fuzzy variables with respective marginal entropies $H(X)$ and $H(Y)$. $H(X, Y)$ are the fuzzy entropy for X and Y . This will be used to calculate the feature-class FMI and feature-feature FMI. The correlation of a feature generated from feature-class FMI will give a justification of feature with its class label score, and the feature-feature FMI gives the similarity score between two features. The rank of the FMI score can be justified as below:

Handling real data or datasets can get headache as its well known properties such as vagueness or imprecision. These problems may affect model for analysis or study. Fuzzy

Table 6.1: Correlation score for mutual information definition.

Correlation Score (Mutual Information)	Definition
High	Indicators of large reduction in uncertainty
Low	Indicators of small reduction in uncertainty
Zero	Independent variables

was used by many researchers to deal with imprecise data, which estimate the membership value for the specific pattern or variable. The FMI is proposed to gives effective measure for the continuous random variable. The advantages of using mutual information different features for each desired target may produce a better or minimal error in the probabilities function.

6.6 Feature extraction method

The raw dataset for each signal is then was transformed into wavelet to produce a complete tree up to a level of J decomposition. These wavelet signals are fused to generated a new set of cross correlation or decomposition coefficients. As the decomposition coefficients can be considered as a new feature space, each subspaces of $\Omega_{j,k}$ can be constructed using normalised wavelet energy.

Each coefficients subspace are accumulated by squares divided the coefficient numbers. The logarithmic operator is applied for the normalisation of the distributed features, this can be refer as below:

The features from various number of dataset can be use as its normalised variant using the below equation:

$$F_i = \frac{I(C; f_i)}{(H(f_i))} \quad (6.24)$$

Based on the equation (6.24), the criterion for the fuzzy set can be calculated, and will show their classification ability. These normalised features will be ranked and sorted to remove the unnecessary nodes or features. The approaches can be summarised as follows:

Step 1 For each paired signals, perform full continuous wavelet transform. Perform wavelet

cross correlation to get CWT1 and CWT2 of the signals.

Step 2 Apply linear correlation (using Spearman's rank coefficient), resulting in conjugation of scaled wavelet with the subject and signal output.

Step 3 Extract the maximum and minimum correlation scales or location.

Step 4 Extract the individual coefficients at maximum and minimum.

Step 5 Construct elements from 3 and 4 as a set of features and calculate the energy component by accumulating all the features by squares.

Step 6 Calculate the normalised logarithmic energy of the wavelet coefficients of the individual coefficients according to (reflogoperator) .

Step 7 Construct the associated fuzzy sets and compute the fuzzy entropies mutual information based on equation (6.24).

Step 8 In descending order, sort the individual coefficients. The sorted sets is the final FEFWC based decomposition.

The above algorithm is applied for the features selection for each channel, then these features will be concatenated to generate a new vector for the classification purpose.

The aforementioned classification techniques applied in this study has been described as in Chapter 5, which is used in the preliminary studies on determining the best muscles to be used for the whole study objective. The specific objective for this chapter was to verify the significance of the proposed fusion technique using two different muscle region for the hand movement classifications.

6.7 Results

Before the overall scale of proposed analysis can be done, there is the need to investigate few components which is linked closely to the development of the proposed algorithm for the analysis.

6.7.1 Mother wavelet determination

The original concept behind wavelets is to examine signals according to their scale level or decomposition. The wavelet analysis system is to utilise a wavelet prototype function or known as mother wavelet. The mother wavelet are the main key component in wavelet analysis or study. The mother wavelet will determine the suitability of the studies approach. One of the easiest way to choose suitable mother wavelet for the study is referring to the previous article. However, this technique might jeopardize the whole objective of the study if it was wrongly chosen. Therefore, the best way for the wavelet determination is by testing the analysis data with several mother wavelet available in the literatures.

In this study, eight (8) types of mother wavelet has been used to justify the performance of the EMG signals correspond to the level of decompositions. The eight wavelet used in this study are; Daubechies, Gaussian, Symlet, Coiflet, Morlet, Haar, Meyer, and Discrete approximation (Dmeyer), illustrated as in Figure 6.2 . Each wavelet are designed with their own characteristic, such as vanishing moment and scaling function to cope with the analysed raw signal. They will exhibit their own properties, such as frequency component and scaling function of the signal.

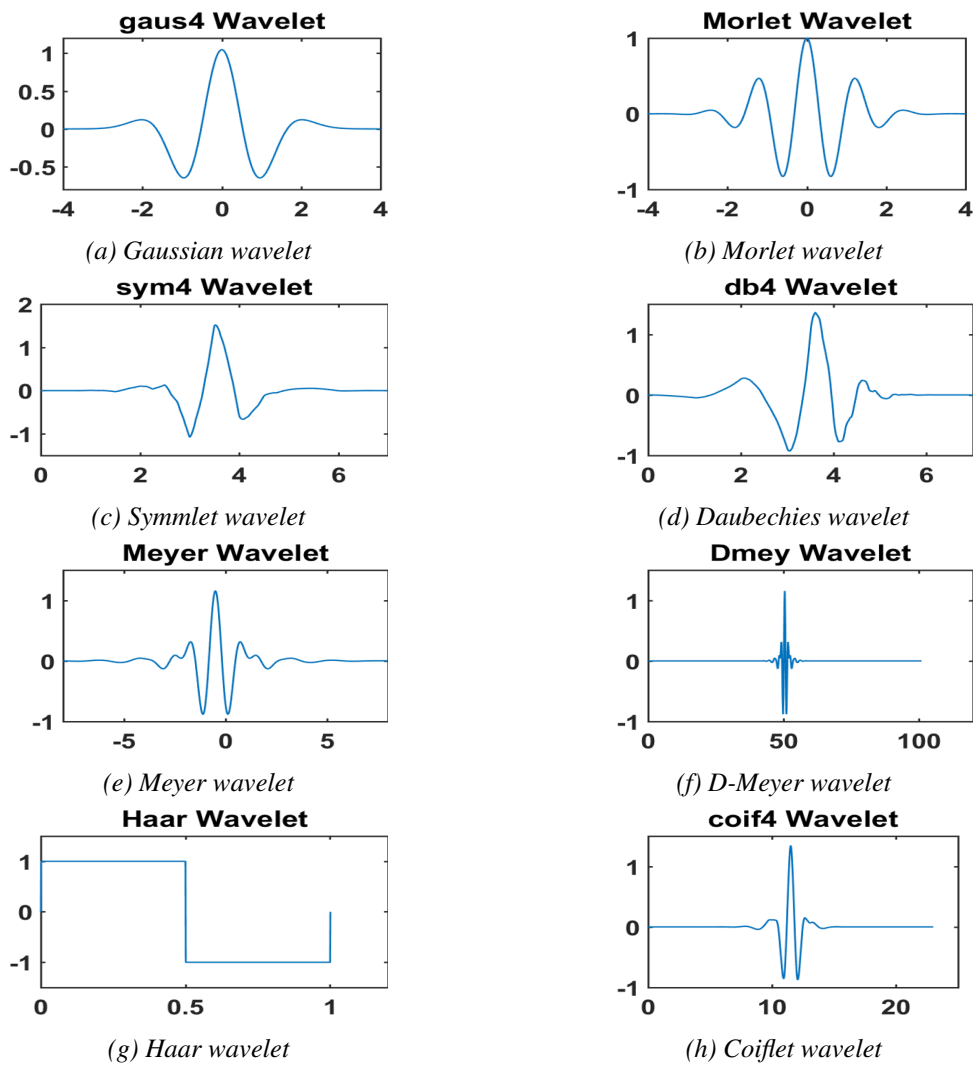


Figure 6.2: The eight (8) mother wavelets used in this topic.

The spectral information found in each of them were analysed. These information will be used to choose which wavelet function give better detection and the features will be extracted based on the chosen one. In general, wavelet analysis works best with selection of a mother wavelet which closely resembles the target oscillation of the original signal.

In this study, the parameter setup for the mother analysis has been develop to generalise the outcome of the study. The parameter setup was fixed as stated below:

Table 6.2: Parameter setup for the mother wavelet analysis

Parameter name	Parameter setup value
Window size	5000 <i>ms</i>
Window increment	256 <i>ms</i>
Sampling frequency	2000 <i>Hz</i>
Level of decomposition	10

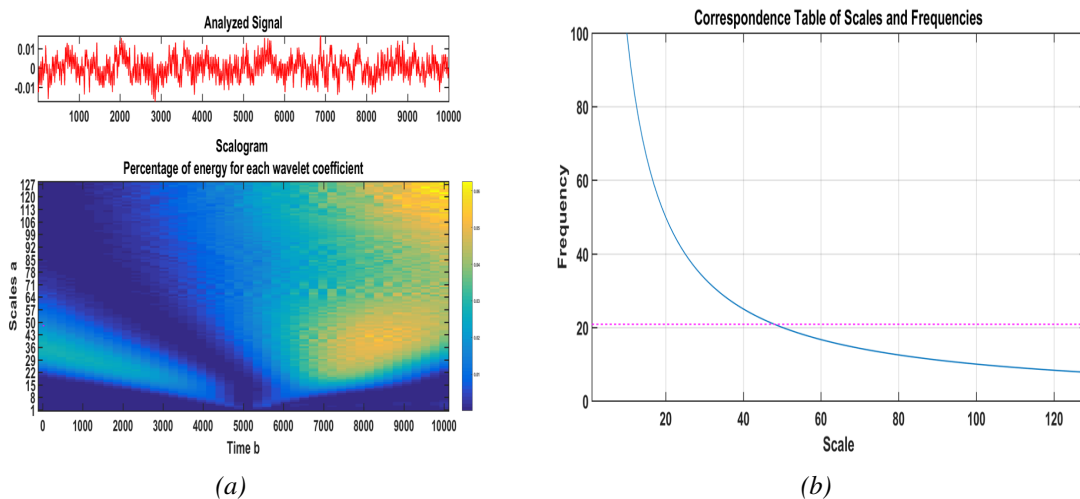


Figure 6.3: (a) Examples of the FP1 raw signals, converted into wavelet scalogram with respect to the Gaussian wavelet; (b) correspondence table of scales and frequencies associated to the analyse wavelet.

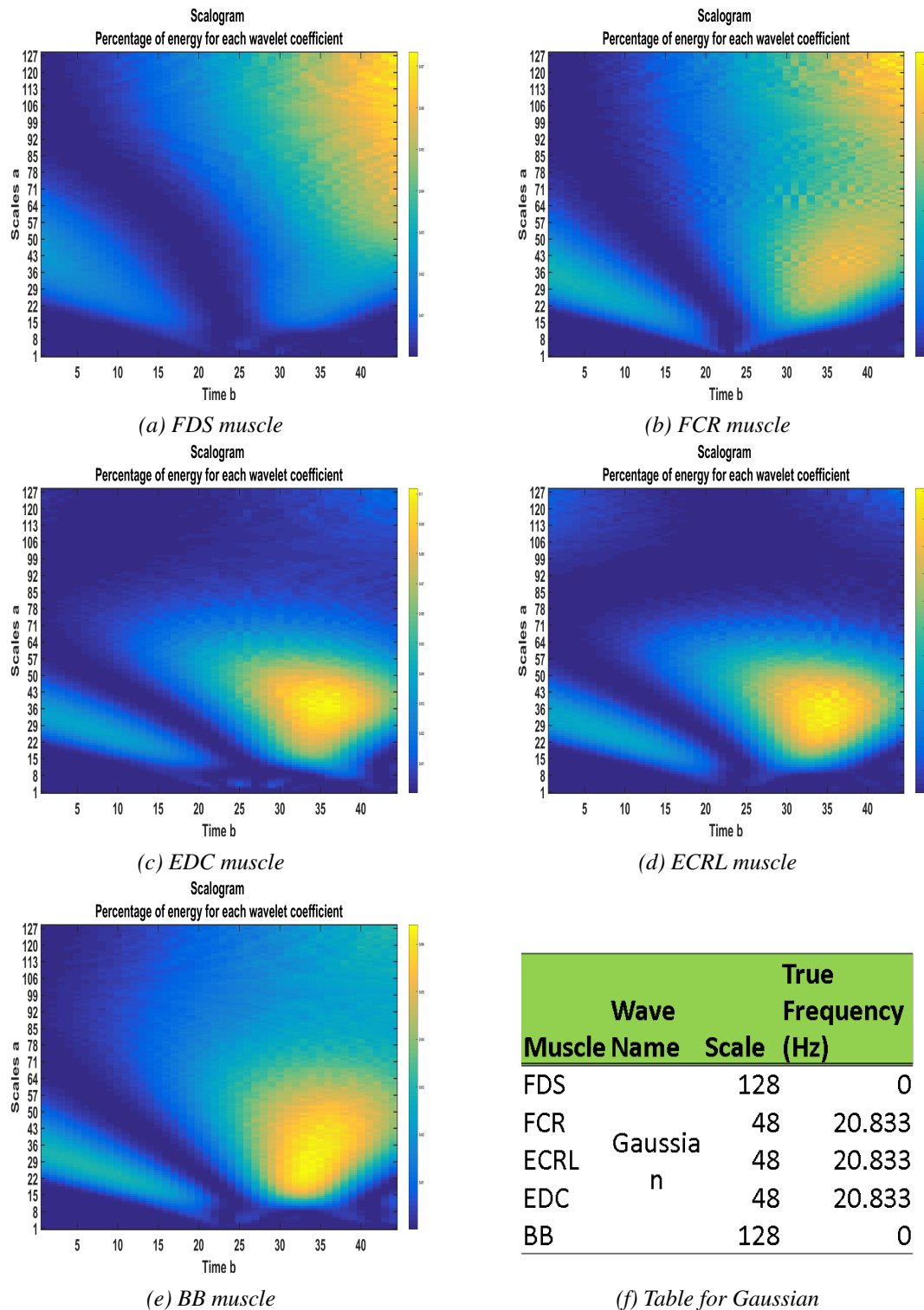


Figure 6.4: The scalogram representation for the FP1 hand movement using Gaussian wavelet at level 4 (gaus4). These shows the variations of coefficient amplitudes at different time and scale for different muscles, even at the same movement.

Table 6.3: Overall eight (8) wavelets performances for subject 1 on finger pinch 1 (FP1). This is just to show the variations may occurs on different wavelet at the different scale and frequency components.

Muscle	Wave Name	Scale	True Frequency (Hz)	Muscle	Wave Name	Scale	True Frequency (Hz)
FDS	Gaussian	128	0	FDS	Meyer	128	0
FCR		48	20.833	FCR		66	20.833
ECRL		48	20.833	ECRL		66	20.833
EDC		48	20.833	EDC		66	20.833
BB		128	0	BB		128	0
FDS	Morlet	128	0	FDS	DMeyer	128	0
FCR		78	20.833	FCR		64	20.833
ECRL		78	20.833	ECRL		64	20.833
EDC		78	20.833	EDC		64	20.833
BB		128	0	BB		128	0
FDS	Symlet	128	0	FDS	Haar	128	0
FCR		69	20.833	FCR		96	20.833
ECRL		69	20.833	ECRL		96	20.833
EDC		69	20.833	EDC		96	20.833
BB		128	0	BB		128	0
FDS	Daubechies	128	0	FDS	Coiflet	128	0
FCR		69	20.833	FCR		67	20.833
ECRL		69	20.833	ECRL		67	20.833
EDC		69	20.833	EDC		67	20.833
BB		128	0	BB		128	0

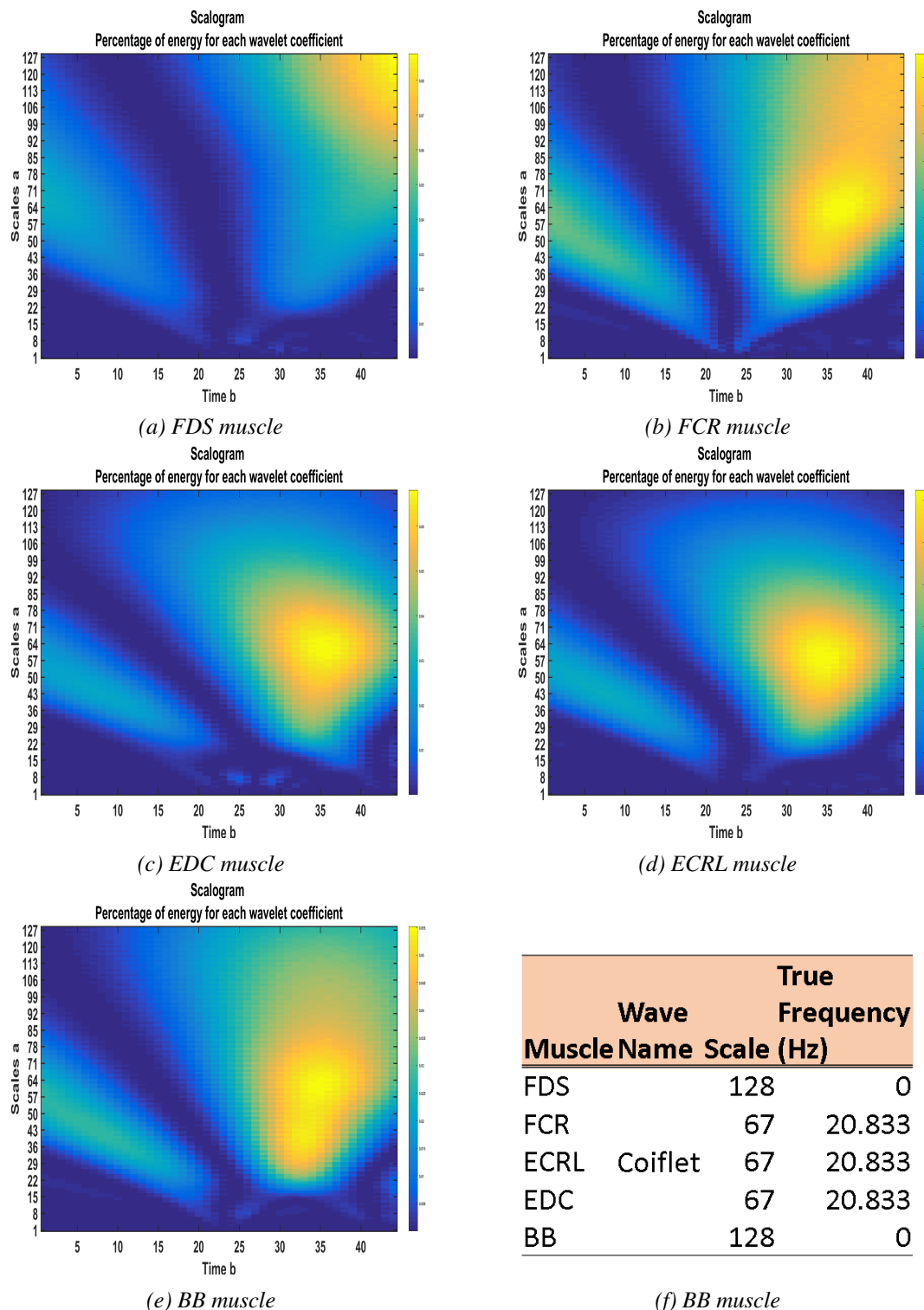


Figure 6.5: The scalogram representation for the FP1 hand movement using Coiflet at level 4 (coif4). These shows the variations of coefficient amplitudes at different time and scale for different muscles, even at the same movement.

Table 6.4: Overall wavelets performance for the finger pinches

Movements	Wavelet Function	Scales	True frequency (Hz)	Movements	Wavelet Function	Scales	True frequency (Hz)
FP1	Gaussian	48	20.833	FP3	Gaussian	48	20.833
	Morlet	78	20.833		Morlet	78	20.833
	Symlet	69	20.833		Symlet	69	20.833
	Daubechies	69	20.833		Daubechies	69	20.833
	Meyer	66	20.833		Meyer	66	20.833
	Dmeyer	64	20.833		Dmeyer	64	20.833
	Haar	96	20.833		Haar	96	20.833
	Coiflet	67	20.833	Coiflet	67	20.833	
FP2	Gaussian	48	20.833	FP4	Gaussian	48	20.833
	Morlet	78	20.833		Morlet	78	20.833
	Symlet	69	20.833		Symlet	69	20.833
	Daubechies	69	20.833		Daubechies	69	20.833
	Meyer	66	20.833		Meyer	66	20.833
	Dmeyer	64	20.833		Dmeyer	64	20.833
	Haar	96	20.833		Haar	96	20.833
	Coiflet	67	20.833	Coiflet	67	20.833	

Table 6.5: Overall wavelets performances for the hand grip movement

Movements	Wavelet Function	Scales	True Frequency (Hz)
HGN	Gaussian	48	20.833
	Morlet	78	20.833
	Symlet	69	20.833
	Daubechies	69	20.833
	Meyer	66	20.833
	Dmeyer	64	20.833
	Haar	96	20.833
	Coiflet	67	20.833
HGF	Gaussian	48	20.833
	Morlet	78	20.833
	Symlet	69	20.833
	Daubechies	69	20.833
	Meyer	66	20.833
	Dmeyer	64	20.833
	Haar	96	20.833
	Coiflet	67	20.833
HGE	Gaussian	24	41.667
	Morlet	39	41.667
	Symlet	34	41.667
	Daubechies	34	41.667
	Meyer	33	41.667
	Dmeyer	32	41.667
	Haar	48	41.667
	Coiflet	33	41.667

The wavelets gives proper detection of the EMG signal each movement, all of it. It shows that the detection on FDS, FCR, ECRL and EDC muscles consistently measured at 20.833 Hz, and different value of scales concerning the all mother wavelet used. It is evident that the analysed data/behaviour have shown pure consistencies for each mother wavelet used in the study. Results indicate a good indicator as the pattern will guide us to understand whether different hands movement could produce different frequency localisation and scales.

6.8 Correlation of EMG fusion with wavelet

The idea of the study prescribed in the Section. It is proved that the cross-correlation analysis revealed the synchronisation between two muscles at the different practice or in this case hand movement. The higher the contraction, the greater sync will be seen due to the existence of synaptic pathways and interaction constitutes pre-condition the process to appear (Person and Mishin (1964)).

The wavelet cross-correlation analysis of the EMG signals between two muscles crucially needed as an EMG data, popular with problems which are intermittent, and it can wax or wane dramatically. Since the technique based on scales concentration, it is indeed a useful tool to study the significance of interrelations between muscles or region of muscles. This analysis allows the researcher to understand at which levels of frequencies and scales correlation between the two muscles involve. If the correlation between these two muscles is high, hence they were having good inter-relations in that specific movement.

Cross-correlation gives valuable information about the dependence of one signal on the other. While wavelet provides better localisation of time resolution at high frequency and proper scale resolution at low frequency, these two combinations will be useful for determining the correlation between two regions of EMG signals at a range of periodicities.

Two muscles at a different region of muscles were paired off simultaneously to create a whole new signal for the analysis. Gaussian (gaus4) wavelet was chosen as this signal closely resembles the original signal. The index number four (4) refers to the number of coefficients. This number of coefficients also represents half of zero moments of vanishing moment for that particular mother wavelet.

The output of wavelet at each scale will be correlated using Spearman (Rs) rank correlation coefficient (Spearman (1904)). The Nyquist criterion in terms of scales selections (1000), scales must be less than half of the signal sampling rate are followed in this study.

The Figure 6.6 shows the example of results of the cross-correlation coefficient for one pair of muscles (FDS and BB) at 1000 scales. The figures show the correlation image generated, which indicating the positions or scales of the two muscles regarding their mutual oscillation. The red colour is showing where the mutual information is present. From

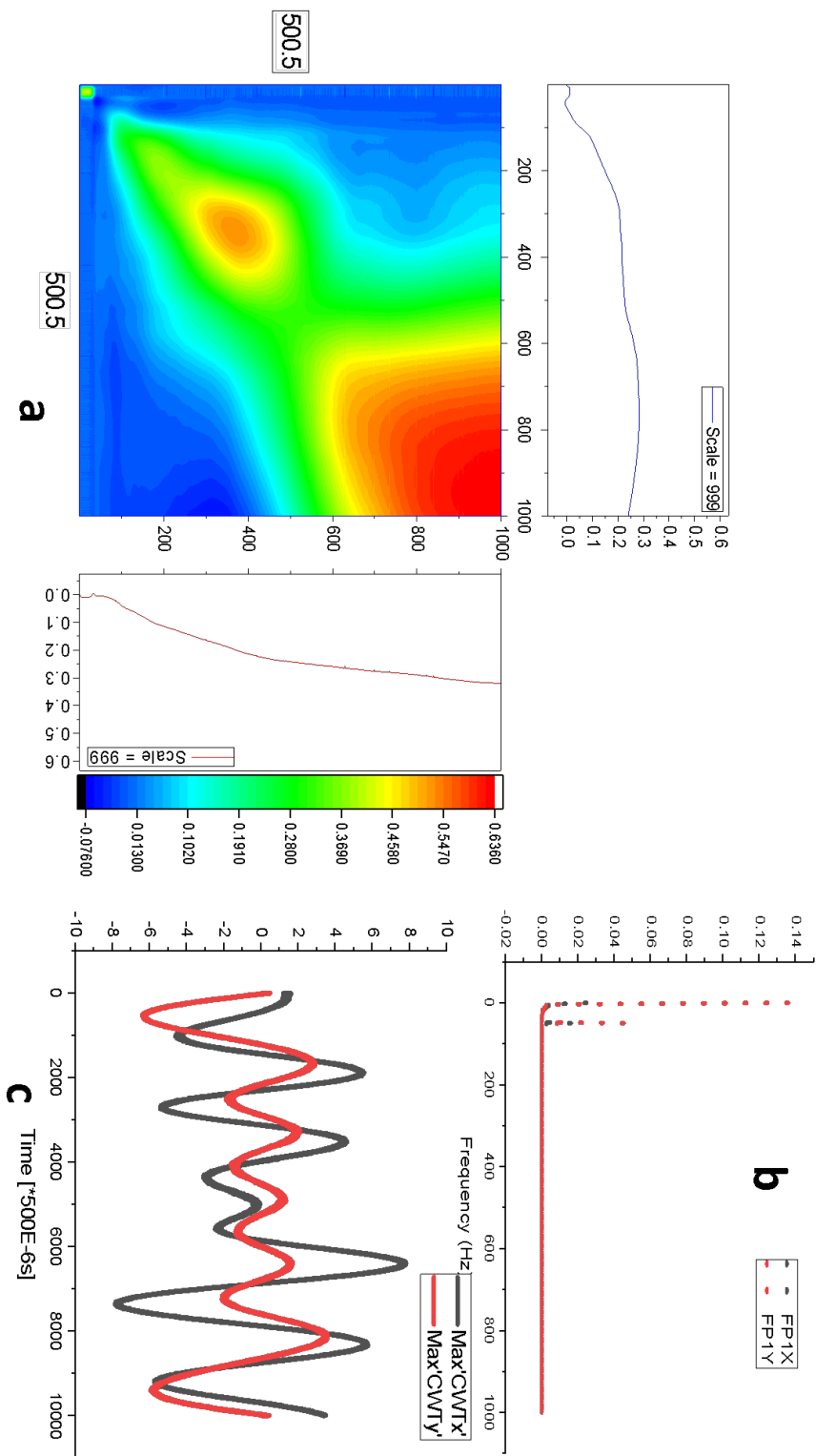


Figure 6.6: Figure (a) shown here to indicates the best correlation between two muscles signal (FDS and BB) for FPI, it is shown that correlation tends to develop over all scales, but it is not quite high until it reaches >500 scales; (b) shown that, these two muscles are sharing the same frequency component which is really good, and (c) is used to understand the phase lag between the max correlation coefficient of these two signals. From there, we could see that they were having a good correlation at scales from 565 to 700. This is a good indicator for us to see whether these signals are out of phase or can be shifted in phase relative to one another.

this, we could know at which scales the mutual oscillations manifest occurred. Each scales represent $0.005s$ in real signal time. At first sight, by using qualitative measures, we can derive some essential features typical for these two correlated EMG signals.

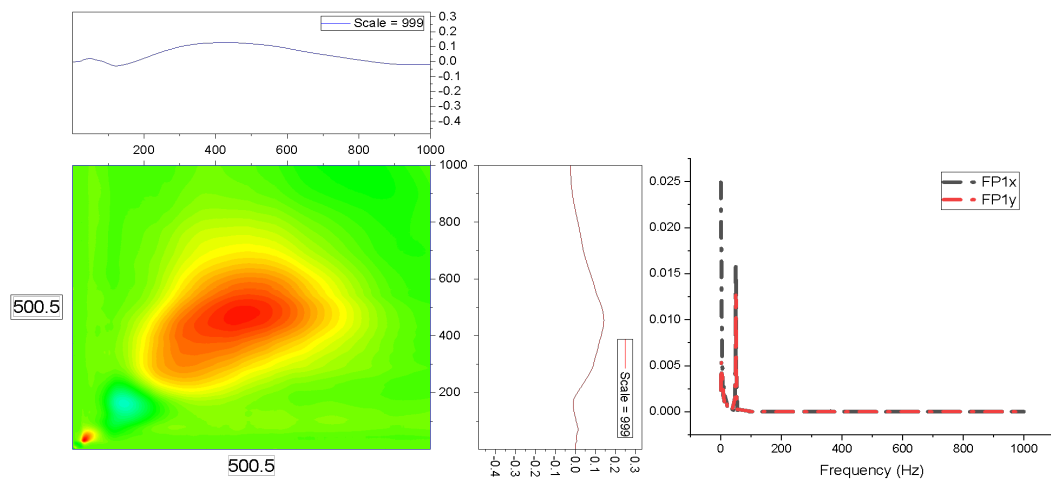
Figure 6.7a shows the example results of the correlation coefficient for a pair of muscles FDS and FCR. It is known that these two muscles are located in adjacent within each other; the association tends to develop a good relationship as it goes over all scales. They also shared the same frequency localisation. The magnitude of FDS muscle is relatively higher than FCR muscle. This is a good indicator as we can say that we will use FDS muscle to be tested with other rest of the muscles in the wavelet correlation analysis.

The correlation coefficient generated from the wavelet analysis shown in Figure 6.7c that these two signals are uncorrelated. Furthermore, we could see some irregular energetic activity occurs at scales 0 to 500. This is related to lower muscle synchronisation and coordination. These also proved by the frequency localisation and their magnitude is showing intermittent features. The unsteady features gain from these two muscles not suitable for our features development. We then further analyse by statistically tabulate the maximum and minimum correlation coefficient and their relative scales. These were done for all subjects and their respected muscles averagely.

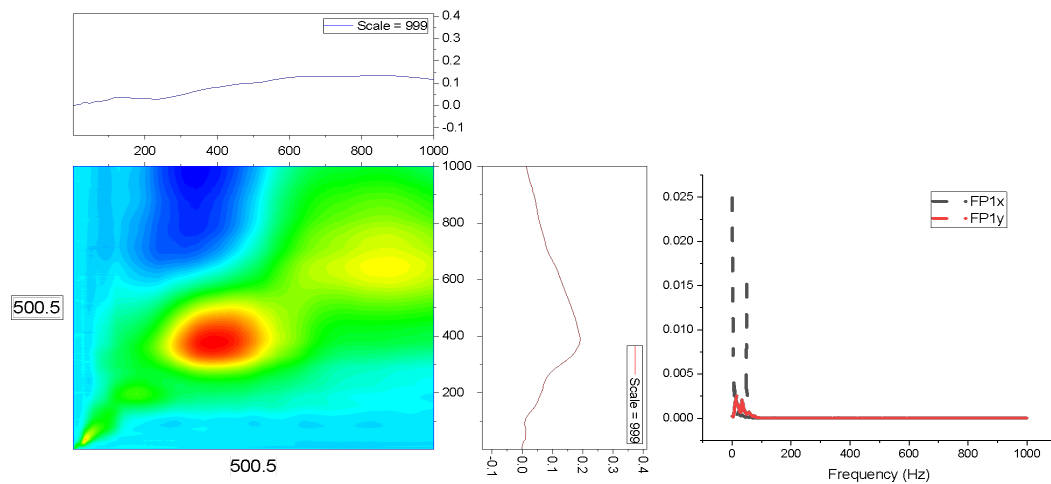
This essential features, which will be used to examine and investigate the correlation behaviour between two muscles, mainly will be focused on two different regions of muscles. As recommended by Cohen (1988), maximum cross-correlation ($MaxCorr$) coefficients between $0.1 \leq MaxCorr \leq 0.3$ were considered small, those $0.3 \leq MaxCorr \leq 0.5$ were deemed to be moderate, and those $0.5 \leq MaxCorr \leq 1.0$ were considered significant.

As the performance of paired muscles has been investigated, the examples of the data tabulated for the investigation are illustrated as in Figure 6.8. Their performances were tabulated and concluded as shown in Table 6.6 and Table 6.7.

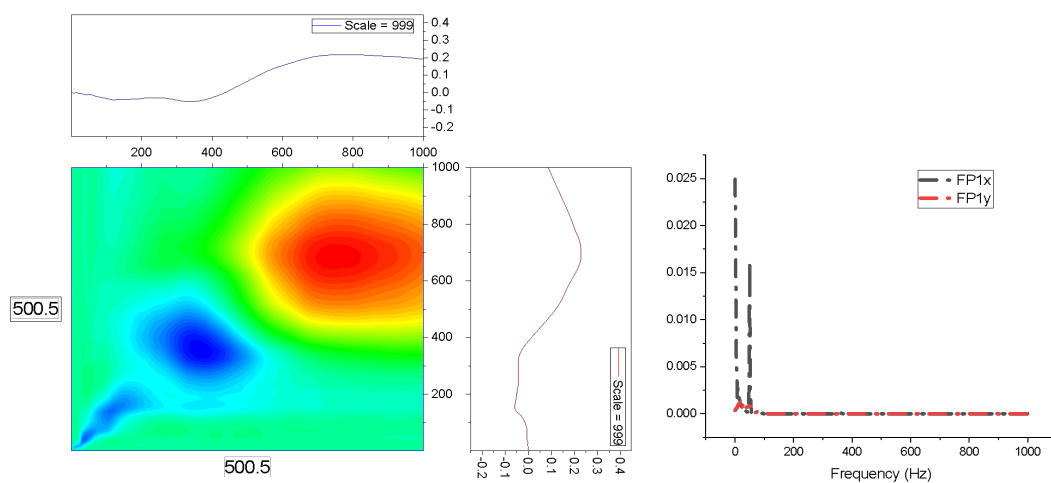
Based on these example performances, it is shown that different pair of muscles generate a different situation in their correlation coefficients. The objective of the study was to look in details about the performance of the pair muscles from two different regions



(a) FDS and FCR muscles



(b) FDS EDC muscles



(c) FDS and ECRL muscles

Figure 6.7: Another examples for FP1 task using the proposed wavelet cross correlation between two muscles, showing certain levels of association between the two muscles at different region of human upper arm. Warmer colouration shows the scales which correlation is manifested by each pair of muscles tested in this study.

	FP1	FP2	FP3	FP4	Muscles
	0.26	0.2846	0.0567	0.1355	FDS_EDC
	0.3606	0.2951	0.5483	0.3474	FDS_BB
	0.5563	0.705	0.5168	0.4971	FDS_ECRL
	0.5183	0.5065	0.352	0.7505	FDS_FCR
	0.4839	0.3459	0.3929	0.0576	FCR_EDC
	0.2663	0.3488	0.3836	0.3835	FCR_ECRL
	0.3072	0.3692	0.6811	0.3641	FCR_BB
	0.3693	0.2636	0.3052	0.3398	EDC_ECRL
	0.0951	0.2509	0.1825	0.3969	EDC_BB
	0.3061	0.3193	0.2892	0.3209	ECRL_BB

	FP1	FP2	FP3	FP4	Muscles
	0.086	0.5494	0.5201	0.238	FDS_EDC
	0.1548	0.3115	0.1152	0.4864	FDS_BB
	0.6919	0.7061	0.6293	0.6605	FDS_ECRL
	0.423	0.2648	0.6079	0.3807	FDS_FCR
	0.2287	0.2798	0.3464	0.2547	FCR_EDC
	0.5091	0.0737	0.1859	0.2257	FCR_ECRL
	0.3936	0.394	0.3541	0.4097	FCR_BB
	0.1561	0.1146	0.0473	0.0743	EDC_ECRL
	0.0566	0.0941	0.0962	0.6251	EDC_BB
	0.6813	0.2468	0.1756	0.3187	ECRL_BB

Figure 6.8: Examples of two subjects data for the correlation coefficients between their respective paired muscles. This approach was done for all the subjects to identified all the correlation coefficients gathered for the study. The variation of maximum correlation coefficients at their own patterns are revealed.

Table 6.6: The five(5) muscles correlation coefficients revealed and tabulated. These includes the scale location for each paired muscles for the finger pinches movement.

Type of Movement	Muscles Correlation	Maximum Correlation	Location Max_Corr	Minimum Correlation	Location Min_Corr
FP1	FDS_EDC	0.4112	380	0.0026	2
	FDS_BB	0.634	970	-0.0615	39
	FDS_ECRL	0.449	2	-0.2496	360
FP2	FDS_FCR	0.3333	34	-0.4847	2
	FDS_EDC	0.587	706	-0.0583	155
	FDS_BB	0.6573	625	-0.039	3
FP3	FDS_ECRL	0.5671	3	-0.2031	712
	FDS_FCR	0.3144	51	-0.5054	3
	FDS_EDC	0.4979	225	-0.5077	108
FP4	FDS_BB	0.3579	449	-0.1896	102
	FDS_ECRL	0.5127	101	-0.2603	198
	FDS_FCR	0.8238	32	-0.35	2
FP4	FDS_EDC	0.4586	528	-0.03	182
	FDS_BB	0.5428	912	-0.0603	34
	FDS_ECRL	0.5023	3	-0.2398	151
FP4	FDS_FCR	0.5327	38	-0.5255	3

Table 6.7: The five(5) muscles correlation coefficients revealed and tabulated. These includes the scale location for each paired muscles for the hand grip force movement.

Type of Movement	Muscles Correlation	Maximum Correlation	Location Max_Corr	Minimum Correlation	Location Min_Corr
HGN	FDS_EDC	0.3872	688	-0.1617	68
	FDS_BB	0.5192	343	-0.0033	3
	FDS_ECRL	0.5547	2	-0.2775	1000
	FDS_FCR	0.6168	34	-0.5443	2
HGF	FDS_EDC	0.1702	113	-0.3882	993
	FDS_BB	0.4745	641	-0.50585	1000
	FDS_ECRL	0.4641	2	-0.0249	14
	FDS_FCR	0.5111	1000	-0.4513	2
HGE	FDS_EDC	0.4045	550	-0.1141	999
	FDS_BB	0.6566	290	-0.0004	33
	FDS_ECRL	0.4756	2	-0.4503	369
	FDS_FCR	0.5225	32	-0.4978	2

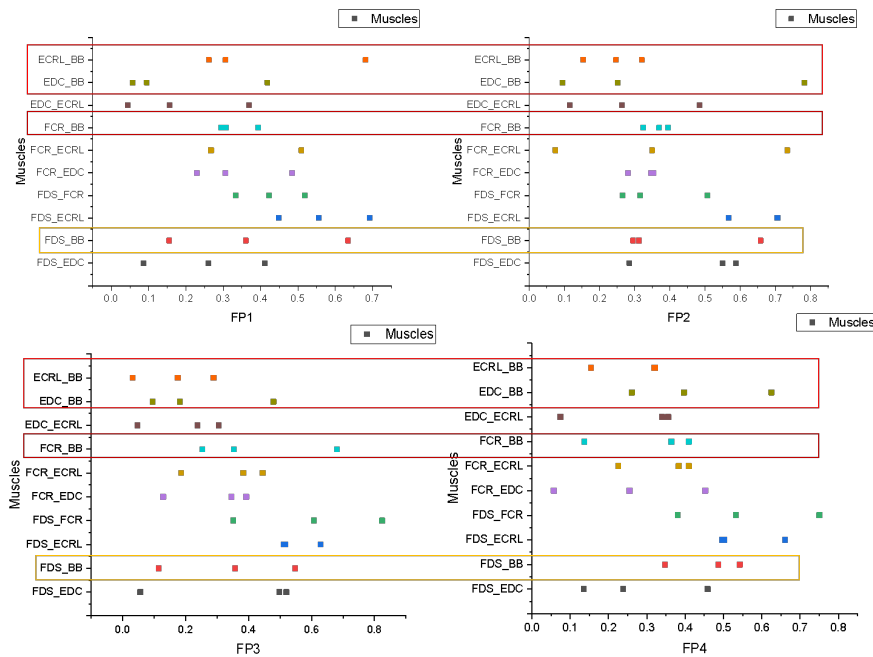
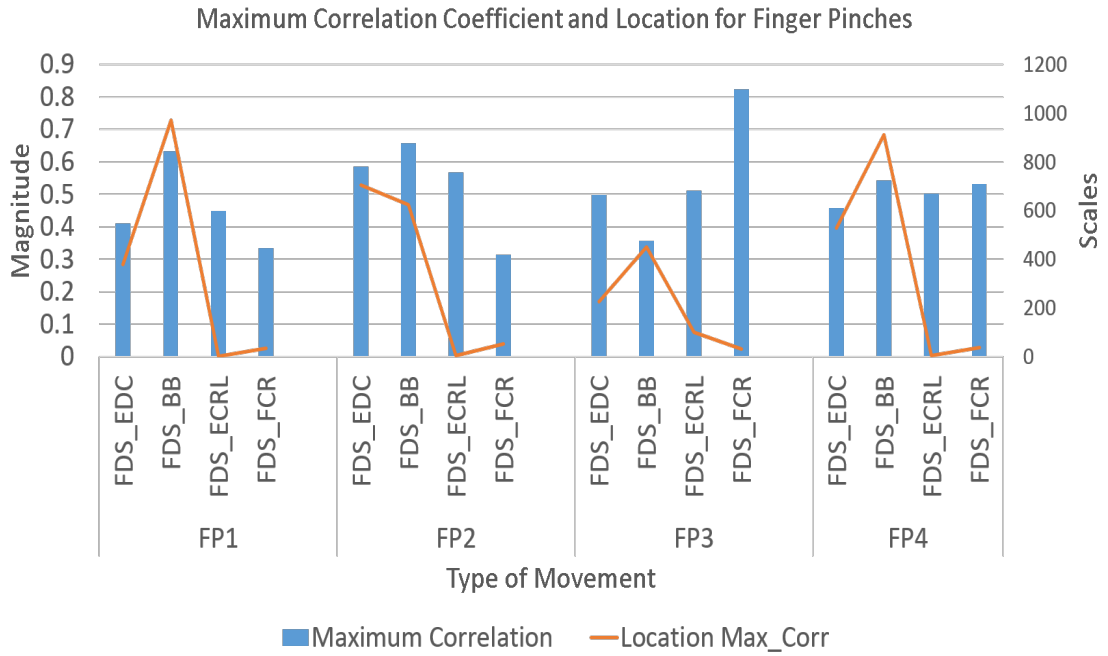


Figure 6.9: The assessment strategy for the muscle chosen used in this study. The highlighted muscles are related to the muscles within the two regions of human upper forearm. This technique will generate a new insight of getting the useful muscles to be use in various application both for normal and amputated people.

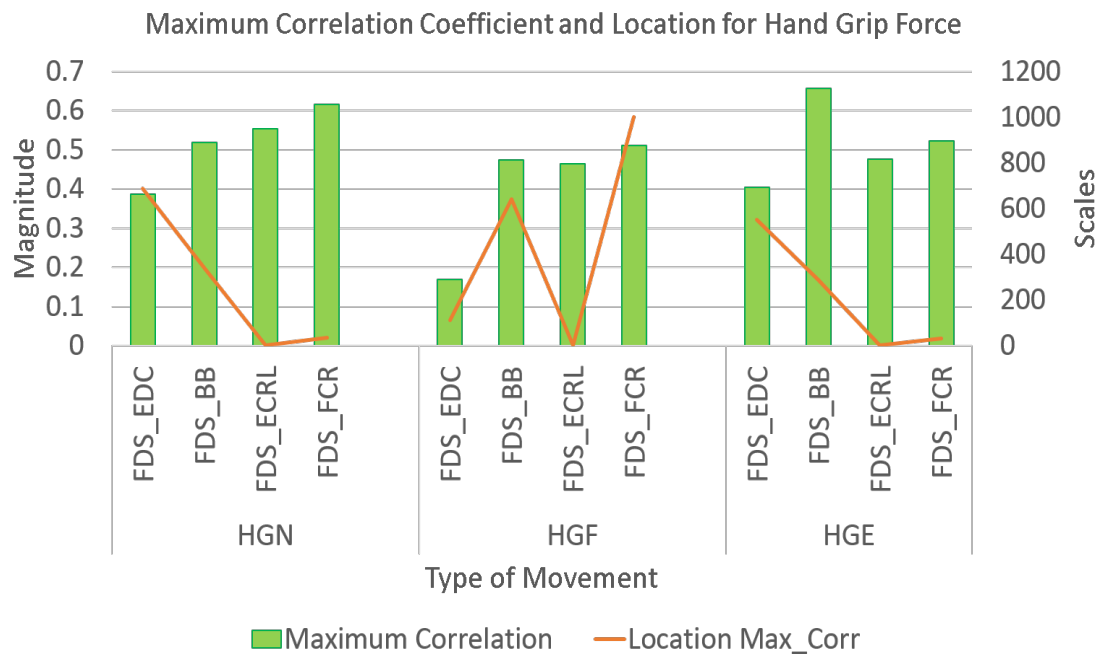
of muscles. This can be referred as forearm muscle (FDS, FCR, ECRL, and EDC) and upper arm muscle (BB and TB), with TB, has been excluded in this study because of its reciprocal property towards the BB. Therefore, the muscle focused in this study is between FDS and BB. This has been concluded in Chapter 5 and supported by the initial findings in this section. We chose the FDS and BB muscles for this final topic as we would like to understand the possibilities of concatenating the two muscles for the generation of the hand movements. The vital energy of EMG signals mainly came from the BB muscles as BB muscles are the most significant fibre muscle available in the human upper forearm and with the extension of other incorporated muscles such as denoted in Chapter 3 and 4.

6.9 Fuzzy mutual information

The fuzzy mutual information analysis starts by computing the feature-class mutual information, to asses the highest mutual information available in each dataset. The feature will be relocated in the subspace as representative for each feature sets.



(a) Finger pinches maximum correlation coefficients and scales location



(b) Hand grip force maximum correlation coefficients and scales location

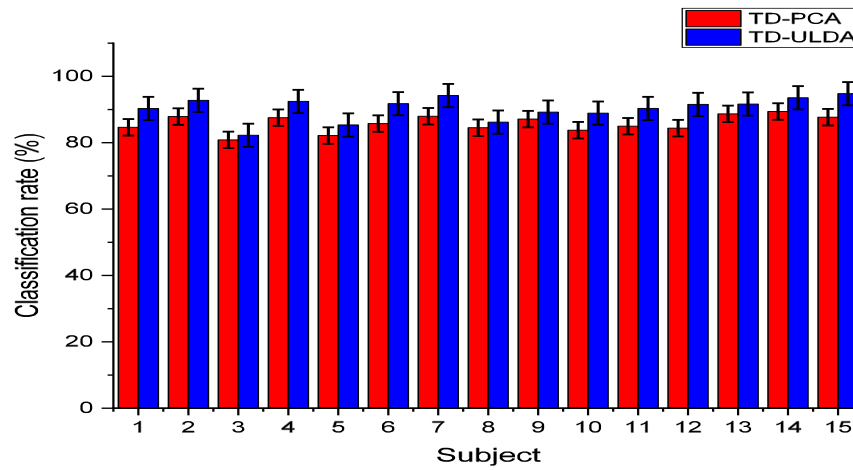
Figure 6.10: The average maximum correlation for the hand movement task as described in (a) and (b).

The dataset from the overall 15 subjects collected has been utilised for this technique. The ultimate goal in this was to acknowledge the significance of using the wavelet cross-correlation as one of the time-frequency domain features, in the classification set. All the aforementioned pre-processing techniques and approaches tested in the previous section applied for this technique.

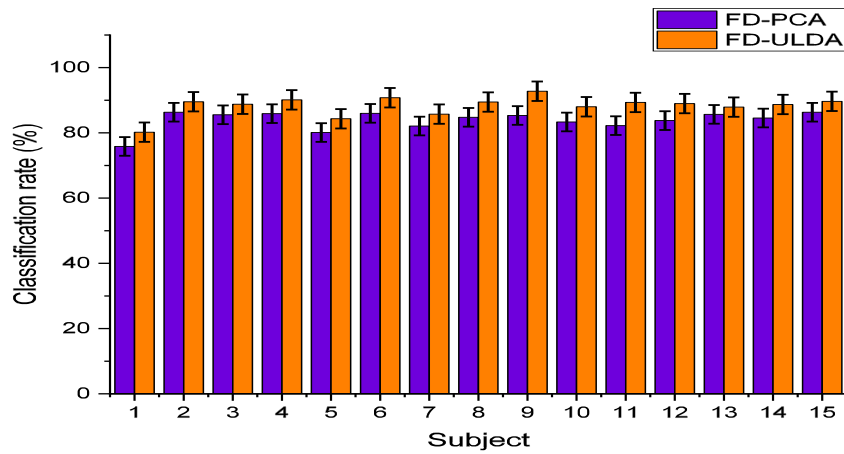
A Gaussian wavelet of order 4 (gaus4) was chosen for this analysis. Since there is a various number of feature domains involved in this study, the implementation of using dimensional reduction technique still needed. Therefore, PCA and ULDA dimensional reduction techniques are used to validate the performance of the new study approach. Their performance has been proven as detailed in Chapter 5, but this time with more subject numbers included.

LDA classifier is used to evaluate the classification performance on several features developed from all the three domains, TD, FD, and TFD proposed in this study. This process was used to validate the new feature developed in the TFD so that their performances are known. Given that from the previous analysis, different hand movements with specific muscle excitation exhibited various performances. The classification accuracies using 50% dataset for the training, and another half for the testing were computed and shown as in Figure 6.11.

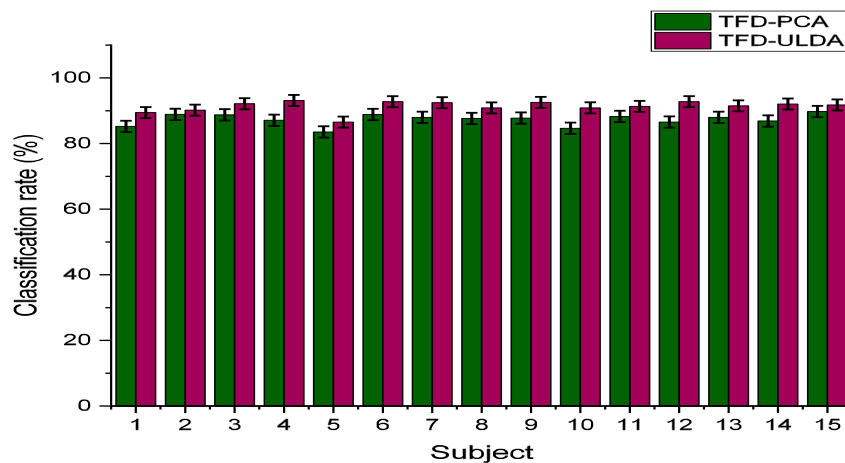
Given data tabulated in Figure 6.11a, 6.11b, and 6.11c that different subjects manifested diverse classification accuracies for each specific domain (TD, FD, TFD) while using different feature reduction methods (PCA, ULDA) with bars expressing the standard errors. Generally, it can be seen that the performances for all the subjects at all types of domains are $> 80\%$, while ULDA improves the classification better than the PCA. The results also show that the performance of the TFD-proposed features performing well compared to the TD and FD domains. The results in Figure 6.12 were plotted to give more details view for the analysis. It is indicated that the proposed features can outperform the TD and FD in both ways of feature reduction strategy where all the components tabulated in their normal distribution graph. The normal distribution graph shows the consistencies of the accuracy towards achieving better performance.



(a) Time domain features



(b) Frequency domain features



(c) Time-frequency domain proposed features- FEFWC

Figure 6.11: The average classification rate for each subject involved in this study with respect to different feature reduction (PCA and ULDA) for three different domains; (a) time domain, (b) frequency domain and (c) time frequency domain-FEFWC.

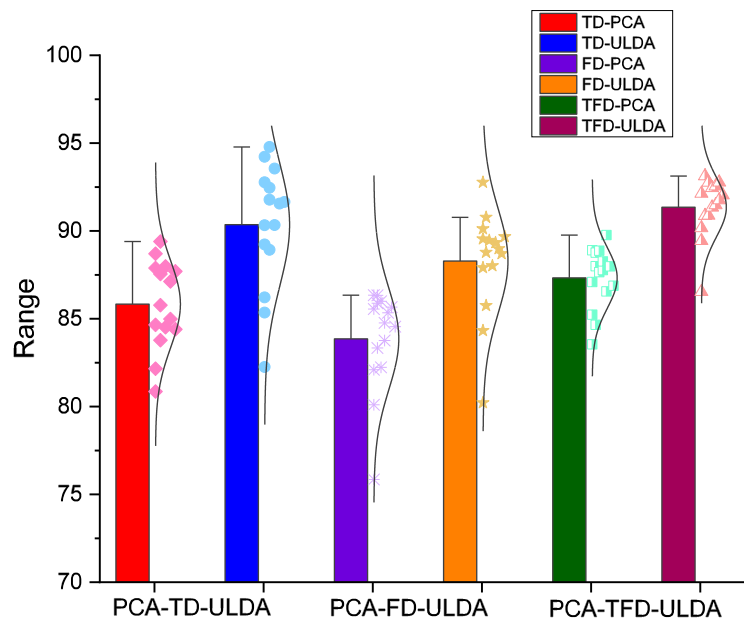


Figure 6.12: Comparison of TD, FD, and TFD performances based on the bar plot with normal distribution measures.

To test the significance of the proposed features and classification accuracies achieved, the analysis of variance (ANOVA) employed in this study. One-way ANOVA and Two-way ANOVA with significance level were set to 0.05 were analysed to make sure the significance of the achieved results. This will measure the results achieved by the proposed features are significant enough and support the findings of the study. The accuracies of proposed features strongly achieved all the significance different from the other two types of features and each of the other two-dimensional reduction technique ($p < 0.05$). The details of the ANOVA analysis can be found in Appendix B.

These results achieved the objective of the study, which is to generate better classification accuracy compared to the other domains. However, it is not suitable to do a basic comparison based on the previous studies performances. Therefore, in this study, the performances comparisons presented are based on the data that was used only in this study. That is why, in this study, the analysis for all TD, FD, and the new features developed in TFD are compared. This will inspire a new approach in realising the real-time performance in the future works.

The final analysis of this study was the processing time required by each method. The average time is calculated (per second) based on the different feature domains and dimensional reduction techniques. This calculation was based on the computer that used to run the analysis for this study, with Intel (i5) 64-bit processor (3.3GHz) and 8 gigabyte of random access memory (RAM). The computational cost for the proposed method outperformed the FD domain and reasonably better than the TD domain. In additions, even though the ULDA processing times slightly higher than PCA ($\pm 0.12s$), it is acceptable as the ULDA methods give superior performance in the classification compared to the others. The results are listed as in Table below:

Table 6.8: Processing time cost comparisons for the all methods used in this study.

Domain	Reduction	Mean	Standard Deviation	Variance	Minimum	Median	Maximum
TD	PCA	1.09108	0.07282	0.0053	1.0021	1.0541	1.2452
	ULDA	1.30056	0.06781	0.0046	1.2004	1.322	1.3982
FD	PCA	1.47919	0.12556	0.01576	1.3289	1.432	1.844
	ULDA	1.57575	0.1734	0.03007	1.3021	1.547	1.855
TFD	PCA	1.20771	0.0801	0.00642	1.0241	1.2001	1.325
	ULDA	1.25248	0.0779	0.00607	1.1014	1.2532	1.3698

6.10 Summary

This study presents an insight into the overall objectives of the study, which ultimately proposed and developed a new features using TFD to distinguish the best classification accuracies for the specific hand movements. This was achieved by analysing the EMG signal from the particular muscles as denoted in the chapters. The new fuzzy mutual information based features (FEFWC) was utilised and analysed using two feature reduction technique, PCA and ULDA. LDA has been chosen as the classifier to compare the classification performances between the new features and other features from TD and FD. The results produced have shown distinctive significant, especially on the proposed features developed. This is supported by the statistical analysis performed using ANOVA.

Chapter 7

Conclusion and future works

7.1 Discussions and conclusions

In the past decades, the development of EMG signal analysis has been exciting, as the importance of EMG has been realised in numerous applications focussing on assisting humans in their daily lives. The EMG signal analysis offers prominent advantages of uplifting the human quality of life. The essential benefit gained from the EMG signal analysis is that it can help people to attain multiple controls of the situation, which outperform the traditional method of EMG based control. Despite the advancement of research in the EMG field, the use of various number of muscles for the analysis of control has produced many challenges for the study. Among these challenges is the lack of intensive research on the significant muscle components based on standard human personalisation. Researchers tend to focus on the unusual case of human to be investigated; hence, their results may be compromised by the ordinary person. That also includes the use of EMG variations of the MVC of the average human. Unlike previous works, this study has focused on the normal human EMG, and has carried out thorough investigation, and the findings have been validated through multiple approaches of analysis.

The methodology designed for this study has involved various number of stages, First, the development of own experimental protocols, by identifying all the muscles involved in a specific designed task. This has produced four types of experimental protocols, investigating the muscles related to the task given and the protocols developed. Inevitably, the investigation requires extensive analyses. The first analysis has involved pre-processing

strategies, which include data arrangement, segmentation, and so on. This is then followed by features extraction strategy, where various domains have been tested, and in light of the literature, 6 TD and FD domains have been chosen for the analysis. This has constituted the main strategy for deciding on suitable EMG muscles and their site selection. Hence, based on these findings, new types of feature extraction with fusion strategy have been proposed.

A comparative assessment with the previous analysis in this study has been carried out to establish the performance of the proposed feature. This constitutes the development of data collection strategy, using several experimental protocols. Four experimental protocols suitable for the study have been developed. The working idea is to develop new approaches of detecting the hand movements based on the two muscle regions in the human upper forearm area. The process begins by implementing the pre-processing strategy in analysis involving signal segmentation, filtering and conditioning. The feature extraction is then tested for performance based on the muscles with specific hand movements. The features are varied from TD, FD, and TFD. The new approach of developing a method of detecting the movements was proposed based on the two regions of muscles, with the implementation of reduced muscle channel to be used in the classification. This was based on pre-analysis of the EMG muscles and proper site selection determination. The proposed idea was then extended to produce a technique of developing new features using the wavelet fusion approach. This technique thus developed was then assessed on a comparative basis and validated to understand the performance of the adopted technique with minimising the number of muscle channels. The study explored and evaluated the new approaches of data collection and assessing the human upper forearm muscles with force variations, as well as muscle fatigue, thus achieving the main objectives of the study. This also suggested the most applicable use of muscle to establish the inter-relation between two regions of human upper forearm. Although the experimental protocols were only implemented for the hand grip movement, the results showed that this could achieve the objective of study. The study thus offers an opportunity to develop new feature extraction and classification scheme to enhance the capabilities of disabled people especially those

that may have problems of weaknesses in the muscle contraction or are amputated.

7.2 Contributions

The main objectives of this study were achieved and contributions to the knowledge are listed below:

- (1) EMG signal and its nature presented for better understanding in the sense of the development of enhanced approaches for detecting, analysing, and classification. The approach adopted has followed certified standards procedure in detecting the EMG signal using muscles coordination, positioning, and electrode placement published by SENIAM.
- (2) New acquisition strategies including EMG acquisition system to be used, subject preferences, sensors selection, and muscle selection protocol. The proposed protocols and experimental procedure have been awarded ethical approval from the Ethical Committee of the University of Sheffield.
- (3) A clear understanding of the state of the art of EMG based analysis, such as classification systems and algorithms including pre and post processing, features extraction, dimensionality reduction and projection, classification strategy and accuracy analysis has been provided.
- (4) Investigation and evaluation of the new approaches of data collection based on the developed protocols and assessing the human upper forearm muscles with force variations, as well as muscle fatigue. These include the basic hand movements such as finger pinches and hand grip force. The strategy developed has given benchmark measures on the standard human capabilities within the scope of the study and justifies the needs of the study objective.
- (5) The work leads to minimisation of the number of EMG channels used, optimises the cost for data collection, and also can reduce the complexity in data analysis.

The necessary and applicable muscles have been identified and their performance with particular hand movement covered in this study. Other findings distinguished the movement and contraction levels without using all the muscles available in the forearm and upper arm.

- (6) Identification of a new feature for best classification scheme to enhance the capabilities of disabled people, especially one that may have weaknesses in muscle contraction or is amputated. This approach will be beneficial in the development of better applications for disabled people who may endure several difficulties in both regions of upper forearm muscles.

7.3 Limitations

It is worth stating that as with any study, there are certain limitations involved. First, the number of muscles used in the study did not cover the overall muscles available in the human upper forearm area. However, the chosen muscles were based on the most significant muscles in their functionality of the hand movement. Secondly, due to the limited datasets for training and testing analysis, the classification accuracies could vary if the number of datasets increased. Therefore, it is suggested for the use of this technique, to consider all the constraints or parameters as set up in this study.

In this study, offline data pre-processing and classification was implemented for the analysis. It is considered that the functional achievement might be lower if real-time analysis is employed due to, possibly transitions periods between movements and rest sessions. This may result in various effects on the EMG signal characteristics, and affect the performance of the classification.

7.4 Suggestions for future works

The suggestions for possible works in the future are stated as below:

- To investigate the proposed technique using online or real-time data from the subject.

The performance of the online system can be evaluated using the offline proposed method. However, to use online data processing, the data acquired must be from an extended period, might be reaching many days, so that the reproducibility of the results confirmed. Therefore, there is the need to develop a new online system which can evaluate the performance of the classification.

- To apply online data analysis, the transition periods or regions between two states of movement need a proper investigation. The areas that have been removed as used in offline processing are not adequate for the online purpose.
- Windowing technique has to be adaptive for the online classification. The adaptive windowing technique is believed can minimise the classification errors. This technique also can shorten the delay time between the processing and classification process. Hence, it improves the computational cost for online recognition.

7.5 Conclusions

This study has presented an insight into the overall objectives of the study, which ultimately has proposed and developed new features using TFD to distinguish the best classification accuracies for specific hand movements. This has been achieved by analysing the EMG signal from the particular muscles identified. New fuzzy mutual information based features (FEFMC) have been utilised and analysed using two feature reduction techniques, namely PCA and ULDA. LDA has been chosen as the classifier to compare the classification performances between the new features and other features from TD and FD. The results produced have shown distinctive significance, especially on the proposed features developed. This is supported by the statistical analysis performed using ANOVA.

The findings have justified the possibilities that only two channel of muscles are capable of achieving a promising result in the hand movements classification. The use of small number of channels will result in far better system error rates, as the minimum number of channels provide brighter information of the actual physiological state of the human upper forearm system. Moreover, minimising the number of channels used in the muscle

study, with proper selection of the domains and their features, give far better error rates and higher classification accuracies with linkage to a suitable dimensional reduction strategy for the features used. Furthermore, the results from this study suggest that the information extracted from the EMG signal using TFD features are more representative than the TD and FD. This, in turn, proves the effectiveness of the proposed features and will support better strategy in developing a real-time analysis rather than using an offline method. Finally, the use of a linear combination in the dimensional reduction and classifier presented in this study has shown that the method achieves high classification rates.

References

- Adam, A. and De Luca, C. J. (2005). Firing rates of motor units in human vastus lateralis muscle during fatiguing isometric contractions. *Journal of Applied Physiology*, 99(1):268–280.
- Ahamed, N. U., Sundaraj, K., Ahmad, B., Rahman, M., Ali, M. A., and Islam, M. A. (2014). Surface electromyographic analysis of the biceps brachii muscle of cricket bowlers during bowling. *Australasian Physical and Engineering Sciences in Medicine*, 37(1):83–95.
- Ahamed, N. U., Sundaraj, K., Ahmad, B., Rahman, M., Islam, A., and Ali, A. (2013). Surface electromyography assessment of the biceps brachii muscle between the end-plate region and distal tendon insertion: Comparison in terms of gender, dominant arm and contraction. *Journal of Physical Therapy Science*, 25(1):3–6.
- Ahamed, N. U., Sundaraj, K., Ahmad, R. B., Rahman, M., and Islam, M. A. (2012). Analysis of right arm biceps brachii muscle activity with varying the electrode placement on three male age groups during isometric contractions using a wireless emg sensor. *Procedia Engineering*, 41:61–67.
- Ahsan, M. R., Ibrahimy, M. I., and Khalifa, O. O. (2011). Electromyography (emg) signal based hand gesture recognition using artificial neural network (ann). pages 1–6. IEEE.
- Akbar, M. A., Ali, A. A. S., Amira, A., Bensaali, F., Benammar, M., Hassan, M., and Bermak, A. (2016). An empirical study for pca-and lda-based feature reduction for gas identification. *IEEE Sensors Journal*, 16(14):5734–5746.
- Al-Angari, H. M., Kanitz, G., and Tarantino, S. and Cipriani, C. (2016). Distance and mutual information methods for emg feature and channel subset selection for classification of hand movements. *Biomedical Signal Processing and Control*, 27:24–31.
- Al-Mulla, M. R., Sepulveda, F., and Al-Bader, B. (2015). Optimal elbow angle for extracting semg signals during fatiguing dynamic contraction. *Computers*, 4(3):251–264.
- Al Omari, F., Hui, J., Mei, C., and Liu, G. (2014). Pattern recognition of eight hand motions using feature extraction of forearm emg signal. *Proceedings of the National Academy of Sciences India Section a-Physical Sciences*, 84(3):473–480.
- Al-Timemy, A., Khushaba, R., Bugmann, G., and Escudero, J. (2015). Improving the performance against force variation of emg controlled multifunctional upper-limb prostheses for transradial amputees. *IEEE Transactions on Neural Systems and Rehabilitation Engineering*, 17(3):1–12.
- Al-Timemy, A. H., Bugmann, G., Escudero, J., and Outram, N. (2013). Classification of finger movements for the dexterous hand prosthesis control with surface electromyography. *IEEE Journal of Biomedical and Health Informatics*, 17(3):608–618.
- Alizadehkhayyat, O., Fisher, A. C., Kemp, G. J., Vishwanathan, K., and Frostick, S. P. (2011). Shoulder muscle activation and fatigue during a controlled forceful hand grip task. *Journal of Electromyography and Kinesiology*, 21(3):478–482.

- Allen, D. G., Lamb, G. D., and Westerblad, H. (2008). Skeletal muscle fatigue: Cellular mechanisms. *Physiological Reviews*, 88(1):287–332.
- Anam, K., Khushaba, R. N., and Al-Jumaily, A. (2013). Two-channel surface electromyography for individual and combined finger movements. pages 4961–4964.
- Anwar, W., Bajwa, I. S., Choudhary, M. A., and Ramzan, S. (2019). An empirical study on forensic analysis of urdu text using lda-based authorship attribution. *IEEE Access*, 7:3224–3234.
- Arendt-Nielsen, L. and Mills, K. R. (1988). Muscle fibre conduction velocity, mean power frequency, mean emg voltage and force during submaximal fatiguing contractions of human quadriceps. *European journal of applied physiology and occupational physiology*, 58(1-2):20–25.
- Arendt-Nielsen, L. and Sinkjær, T. (1991). Quantification of human dynamic muscle fatigue by electromyography and kinematic profiles. *Journal of Electromyography and Kinesiology*, 1(1):1–8.
- Asghari Oskoei, M. and Hu, H. (2007). Myoelectric control systems—a survey. *Biomedical Signal Processing and Control*, 2(4):275–294.
- Bai, D., Chen, S., and Yang, J. (2019). Upper arm motion high-density semg recognition optimization based on spatial and time-frequency domain features. *Journal of Healthcare Engineering*, 2019.
- Bai, F., Lubecki, T. M., Chew, C. M., and Teo, C. L. (2012). Novel time-frequency approach for muscle fatigue detection based on semg. pages 364–367.
- Balakrishnama, S. and Ganapathiraju, A. (1998). Linear discriminant analysis—a brief tutorial. *Institute for Signal and information Processing*, 18:1–8.
- Baspinar, U., Varol, H. S., and Senyurek, V. Y. (2013). Performance comparison of artificial neural network and gaussian mixture model in classifying hand motions by using semg signals. *Biocybernetics and Biomedical Engineering*, 33(1):33–45.
- Beck, T. W., Housh, T. J., Johnson, G. O., Weir, J. P., Cramer, J. T., Coburn, J. W., and Malek, M. H. (2005). The effects of interelectrode distance on electromyographic amplitude and mean power frequency during isokinetic and isometric muscle actions of the biceps brachii. *Journal of Electromyography and Kinesiology*, 15(5):482–495.
- Benjamin, K. B. and Roger, M. E. (2007). The neurobiology of muscle fatigue: 15 years later. *Integrative and Comparative Biology*, 47(4):465–473.
- Bhuiyan, M. S. H., Choudhury, I. A., and Dahari, M. (2014). Development of a control system for artificially rehabilitated limbs: a review. *Biological Cybernetics*, 109(2):141–162.
- Bigland-Ritchie, B., Johansson, R., Lippold, O. C., Smith, S., and Woods, J. J. (1983). Changes in motoneurone firing rates during sustained maximal voluntary contractions. *The Journal of Physiology*, 340(1):335–346.
- Bonato, P., Roy, S. H., Knaflitz, M., and Luca, C. J. d. (2001). Time-frequency parameters of the surface myoelectric signal for assessing muscle fatigue during cyclic dynamic contractions. *IEEE Transactions on Biomedical Engineering*, 48(7):745–753.
- Boostani, R. and Moradi, M. H. (2003). Evaluation of the forearm emg signal features for the control of a prosthetic hand. *Physiological measurement*, 24(2):309.
- Brown, N., Bichler, S., Fiedler, M., and Alt, W. (2016). Fatigue detection in strength training using three-dimensional accelerometry and principal component analysis. *Sports Biomechanics*, 15(2):139–150.
- Bruce, A., Donoho, D., and Gao, H. . (1996). Wavelet analysis [for signal processing]. *IEEE Spectrum*, 33(10):26–35.

- Castanedo, F. (2013). A review of data fusion techniques. *The Scientific World Journal*, 2013.
- Cechetto, A. D., Parker, P. A., and Scott, R. N. (2001). The effects of four time-varying factors on the mean frequency of a myoelectric signal. *Journal of Electromyography and Kinesiology*, 11(5):347–354.
- Chan, A. D. C. and Green, G. C. (2007). Myoelectric control development toolbox. volume 1, pages M0100–1.
- Chen, H., Tong, R., Chen, M., Fang, Y., and Liu, H. (2018). A hybrid cnn-svm classifier for hand gesture recognition with surface emg signals. volume 2, pages 619–624. IEEE.
- Chen, X., Zhang, D., and Zhu, X. (2013). Application of a self-enhancing classification method to electromyography pattern recognition for multifunctional prosthesis control. *Journal of neuroengineering and rehabilitation*, 10(1):44.
- Chowdhury, S. K., Nimbarte, A. D., Jaridi, M., and Creese, R. C. (2013). Discrete wavelet transform analysis of surface electromyography for the fatigue assessment of neck and shoulder muscles. *Journal of Electromyography and Kinesiology*, 23(5):995–1003.
- Cifrek, M., Medved, V., Tonković, S., and Ostojić, S. (2009). Surface emg based muscle fatigue evaluation in biomechanics. *Clinical Biomechanics*, 24(4):327–340.
- Dalton, P. A. and Stokes, M. J. (1993). Frequency of acoustic myography during isometric contraction of fresh and fatigued muscle and during dynamic contractions. *Muscle & Nerve: Official Journal of the American Association of Electrodiagnostic Medicine*, 16(3):255–261.
- Danion, F., Latash, M. L., Li, Z. M., and Zatsiorsky, V. M. (2000). The effect of fatigue on multifinger coordination in force production tasks in humans. *The Journal of Physiology*, 523(2):523–532.
- Daubechies, I. (1990). The wavelet transform, time-frequency localization and signal analysis. *IEEE Transactions on Information Theory*, 36(5):961–1005.
- De Luca, C. J. (1982). Control scheme governing concurrently active human motor units during voluntary contractions. *Journal of Physiology*, 329.
- De Luca, C. J. (1985). Control properties of motor units. *J Exp Biol*, 115.
- De Luca, C. J. (1997). The use of surface electromyography in biomechanics. *Journal of Applied Biomechanics*, 13(2):135–163.
- Dideriksen, J. L., Farina, D., and Enoka, R. M. (2010). Influence of fatigue on the simulated relation between the amplitude of the surface electromyogram and muscle force. *Philosophical Transactions of the Royal Society of London A: Mathematical, Physical and Engineering Sciences*, 368(1920):2765–2781.
- Dimitrova, N. A., Arabadzhiev, T. I., Hogrel, J. Y., and Dimitrov, G. V. (2009). Fatigue analysis of interference emg signals obtained from biceps brachii during isometric voluntary contraction at various force levels. *Journal of Electromyography and Kinesiology*, 19(2):252–258.
- Doerschuk, P. C., Gustafon, D. E., and Willsky, A. S. (1983). Upper extremity limb function discrimination using emg signal analysis. *IEEE Transactions on Biomedical Engineering*, BME-30(1):18–29.
- Doud, J. R. and Walsh, J. M. (1995). Muscle fatigue and muscle length interaction: effect on the emg frequency components. *Electromyography and clinical neurophysiology*, 35(6):331–9.
- Englehart, K., Hudgin, B., and Parker, P. A. (2001). A wavelet-based continuous classifi-

- cation scheme for multifunction myoelectric control. *IEEE Transactions on Biomedical Engineering*, 48(3):302–311.
- Englehart, K. and Hudgins, B. (2003). A robust, real-time control scheme for multifunction myoelectric control. *IEEE Transactions on Biomedical Engineering*, 50(7):848–854.
- Enoka, R. M., Baudry, S., Rudroff, T., Farina, D., Klass, M., and Duchateau, J. (2011). Unraveling the neurophysiology of muscle fatigue. *Journal of Electromyography and Kinesiology*, 21(2):208–219.
- Farina, D., Crosetti, A., and Merletti, R. (2001). A model for the generation of synthetic intramuscular emg signals to test decomposition algorithms. *IEEE Transactions on Biomedical Engineering*, 48(1):66–77.
- Gamet, D. and Maton, B. (1989). The fatigability of two agonistic muscles in human isometric voluntary submaximal contraction: an emg study. *European Journal of Applied Physiology and Occupational Physiology*, 58(4):361–368.
- Gandolla, M., Ferrante, S., Ferrigno, G., Baldassini, D., Molteni, F., Guanziroli, E., Cotti Cottini, M., Seneci, C., and Pedrocchi, A. (2017). Artificial neural network emg classifier for functional hand grasp movements prediction. *Journal of International Medical Research*, 45(6):1831–1847.
- Geethanjali, P. (2015). Comparative study of pca in classification of multichannel emg signals. *Australasian Physical and Engineering Sciences in Medicine*, 38(2):331–343.
- Güler, N. and Koçer, S. (2005). Classification of emg signals using pca and fft. *J Med Syst*, 29(3):241–250.
- Gokgoz, E. and Subasi, A. (2014). Effect of multiscale pca de-noising on emg signal classification for diagnosis of neuromuscular disorders. *J Med Syst*, 38(4):1–10.
- González-Izal, M., Malanda, A., Gorostiaga, E., and Izquierdo, M. (2012). Electromyographic models to assess muscle fatigue. *Journal of Electromyography and Kinesiology*, 22(4):501–512.
- Guersoy, M. I. and Subasi, A. (2008). *A comparison of PCA, ICA and LDA in EEG signal classification using SVM*. 2008 Ieee 16th Signal Processing, Communication and Applications Conference, Vols 1 and 2. Elsevier.
- Hagan, M. T. and Menhaj, M. B. (1994). Training feedforward networks with the marquardt algorithm. *IEEE transactions on Neural Networks*, 5(6):989–993.
- Hall, D. L. and Llinas, J. (1997). An introduction to multisensor data fusion. *Proceedings of the IEEE*, 85(1):6–23.
- Hargrove, L. J., Englehart, K., and Hudgins, B. (2007). A comparison of surface and intramuscular myoelectric signal classification. *IEEE Transactions on Biomedical Engineering*, 54(5):847–853.
- Hudgins, B., Parker, P., and Scott, R. N. (1993). A new strategy for multifunction myoelectric control. *IEEE Transactions on Biomedical Engineering*, 40(1):82–94.
- Ibrahimy, M. I., Ahsan, R., and Khalifa, O. O. (2013). Design and optimization of levenberg-marquardt based neural network classifier for emg signals to identify hand motions. *Measurement Science Review*, 13(3):142–151.
- Jahani Fariman, H., Ahmad, S. A., Hamiruce Marhaban, M., Ali Jan Ghasab, M., and Chappell, P. H. (2015). Simple and computationally efficient movement classification approach for emg-controlled prosthetic hand: Anfis vs. artificial neural network. *Intelligent Automation and Soft Computing*, 21(4):559–573.
- Jieping, Y., Tao, L., Tao, X., and Janardan, R. (2004). Using uncorrelated discriminant analysis for tissue classification with gene expression data. *IEEE/ACM Transactions*

- on *Computational Biology and Bioinformatics*, 1(4):181–190.
- Jin, Z., Yang, J.-Y., Hu, Z.-S., and Lou, Z. (2001). Face recognition based on the uncorrelated discriminant transformation. *Pattern Recognition*, 34(7):1405–1416.
- Jordanic, M. and Magjarevic, R. (2012). Estimation of muscle fatigue during dynamic contractions based on surface electromyography and accelerometry. pages 201–205.
- Kamen, G. and Caldwell, G. E. (1996). Physiology and interpretation of the electromyogram. *Journal of Clinical Neurophysiology*, 13(5).
- Karlik, B., Osman Tokhi, M., and Alci, M. (2003). A fuzzy clustering neural network architecture for multifunction upper-limb prosthesis. *IEEE Transactions on Biomedical Engineering*, 50(11):1255–1261.
- Karlik, B., Tokhi, M. O., and Alci, M. (2003). A fuzzy clustering neural network architecture for multifunction upper-limb prosthesis. *IEEE Transactions on Biomedical Engineering*, 50(11):1255–1261.
- Khezri, M. and Jahed, M. (2009). An exploratory study to design a novel hand movement identification system. *Computers in Biology and Medicine*, 39(5):433–442.
- Khushaba, R. N., Al-Ani, A., and Al-Jumaily, A. (2010). Orthogonal fuzzy neighborhood discriminant analysis for multifunction myoelectric hand control. *Biomedical Engineering, IEEE Transactions on*, 57(6):1410–1419.
- Khushaba, R. N., Al-Ani, A., Al-Jumaily, A., and Nguyen, H. T. (2008). A hybrid nonlinear-discriminant analysis feature projection technique. pages 544–550. Springer Berlin Heidelberg.
- Khushaba, R. N., Al-Ani, A., Al-Timemy, A., and Al-Jumaily, A. (2016). A fusion of time-domain descriptors for improved myoelectric hand control. pages 1–6.
- Khushaba, R. N., Al-Jumaily, A., and Al-Ani, A. (2009). Evolutionary fuzzy discriminant analysis feature projection technique in myoelectric control. *Pattern Recognition Letters*, 30(7):699–707.
- Khushaba, R. N. and Kodagoda, S. (2012). Electromyogram (emg) feature reduction using mutual components analysis for multifunction prosthetic fingers control. pages 1534–1539.
- Khushaba, R. N., Kodagoda, S., Takruri, M., and Dissanayake, G. (2012). Toward improved control of prosthetic fingers using surface electromyogram (emg) signals. *Expert Systems With Applications*, 39(12):10731–10738.
- Khushaba, R. N., Takruri, M., Miro, J. V., and Kodagoda, S. (2014). Towards limb position invariant myoelectric pattern recognition using time-dependent spectral features. *Neural Networks*, 55:42–58.
- Krogh-Lund, C. and Jørgensen, K. (1991). Changes in conduction velocity, median frequency, and root mean square-amplitude of the electromyogram during 25% maximal voluntary contraction of the triceps brachii muscle, to limit of endurance. *European Journal of Applied Physiology and Occupational Physiology*, 63(1):60–69.
- Krogh-Lund, C. and Jørgensen, K. (1992). Modification of myo-electric power spectrum in fatigue from 15% maximal voluntary contraction of human elbow flexor muscles, to limit of endurance: reflection of conduction velocity variation and/or centrally mediated mechanisms? *European Journal of Applied Physiology and Occupational Physiology*, 64(4):359–370.
- Krogh-Lund, C. and Jørgensen, K. (1993). Myo-electric fatigue manifestations revisited: power spectrum, conduction velocity, and amplitude of human elbow flexor muscles during isolated and repetitive endurance contractions at 30% maximal voluntary contraction. *European Journal of Applied Physiology and Occupational Physiology*,

- 66(2):161–173.
- Kukulka, C. G. and Clamann, H. P. (1981). Comparison of the recruitment and discharge properties of motor units in human brachial biceps and adductor pollicis during isometric contractions. *Brain Research*, 219(1):45–55.
- Lalitharatne, T. D., Teramoto, K., Hayashi, Y., Nanayakkara, T., and Kiguchi, K. (2013). Evaluation of fuzzy-neuro modifiers for compensation of the effects of muscle fatigue on emg-based control to be used in upper-limb power-assist exoskeletons. *Journal of Advanced Mechanical Design Systems and Manufacturing*, 7(4):736–751.
- Liu, Y.-H., Huang, H.-P., and Weng, C.-H. (2007). Recognition of electromyographic signals using cascaded kernel learning machine. *IEEE/ASME Transactions on Mechatronics*, 12(3):253–264.
- Luca, C. J. D. (1979). Physiology and mathematics of myoelectric signals. *IEEE Transactions on Biomedical Engineering*, BME-26(6):313–325.
- Luo, R. C., Yih, C.-C., and Su, K. L. (2002). Multisensor fusion and integration: approaches, applications, and future research directions. *IEEE Sensors journal*, 2(2):107–119.
- Ma, L., Chablat, D., Bennis, F., Zhang, W., Hu, B., and Guillaume, F. (2011). A novel approach for determining fatigue resistances of different muscle groups in static cases. *International Journal of Industrial Ergonomics*, 41(1):10–18.
- MacIsaac, D. T., Parker, P. A., Englehart, K. B., and Rogers, D. R. (2006). Fatigue estimation with a multivariable myoelectric mapping function. *IEEE Transactions on Biomedical Engineering*, 53(4):694–700.
- Mamaghani, N. K., Shimomura, Y., Iwanaga, K., and Katsuura, T. (2002). Mechanomyogram and electromyogram responses of upper limb during sustained isometric fatigue with varying shoulder and elbow postures. *Journal of Physiological Anthropology and Applied Human Science*, 21(1):29–43.
- Mamaghani, N. K., Shimomura, Y., and Iwanaga, K. and Katsuura, T. (2001). Changes in surface emg and acoustic myogram parameters during static fatiguing contractions until exhaustion: Influence of elbow joint angles. *Journal of Physiological Anthropology and Applied Human Science*, 20(2):131–140.
- McGill, K. C. (2004). Surface electromyogram signal modelling. *Medical and Biological Engineering and Computing*, 42(4):446–454.
- Merletti, R. (1999). Standards for reporting emg data. *J Electromyogr Kinesiol*, 9(1):3–4.
- Merletti, R. (2000). Surface electromyography: The seniam project. *Europa Medicophysics*, 36(4):167–169.
- Merletti, R. and Hermens, H. (2000). Introduction to the special issue on the seniam european concerted action. *Journal of Electromyography and Kinesiology*, 10(5):283–286.
- Merletti, R. and Parker, P. (2004). *Electromyography [electronic resource] : physiology, engineering, and noninvasive applications*. Piscataway, NJ : IEEE Press ; Hoboken, N.J. : Wiley-Interscience, c2004, Piscataway, NJ : Hoboken, N.J.
- Miyoshi, T., Takahashi, Y., Lee, H., Yamaguchi, M., and Komeda, T. (2009). Methodological consideration for the recruitment of upper limb muscles during two joint arm movements. pages 442–446.
- Mobasser, F. and Hashtrudi-Zaad, K. (2012). A comparative approach to hand force estimation using artificial neural networks. *Biomedical engineering and computational biology*, 4:BECEB–S9335.
- Monjo, F. (2015). Muscle fatigue as an investigative tool in motor control: A review

- with new insights on internal models and posture-movement coordination. *Human Movement Science*, 44:225–233.
- Mukaka, M. M. (2012). Statistics corner: A guide to appropriate use of correlation coefficient in medical research. *Malawi medical journal : the journal of Medical Association of Malawi*, 24(3):69–71.
- Noor, K., Jan, T., Basher, M., Ali, A., Khalil, R. A., Zafar, M. H., Ashraf, M., Babar, M. I., and Shah, S. W. (2018). Performances enhancement of fingerprint recognition system using classifiers. *IEEE Access*.
- Parsaei, H. and Stashuk, D. W. (2012). Svm-based validation of motor unit potential trains extracted by emg signal decomposition. *IEEE transactions on biomedical engineering*, 59(1):183–191.
- Parson, S. H. (2009). Clinically oriented anatomy, 6th edn. *Journal of Anatomy*, 215(4):474–474.
- Person, R. and Mishin, L. (1964). Auto-and cross-correlation analysis of the electrical activity of muscles. *Medical electronics and biological engineering*, 2(2):155–159.
- Petrofsky, J. S. and Lind, A. R. (1980). Frequency analysis of the surface electromyogram during sustained isometric contractions. *European Journal of Applied Physiology and Occupational Physiology*, 43(2):173–182.
- Phillips, C. L., Parr, J. M., and Riskin, E. A. (2003). *Signals, systems, and transforms*. Prentice Hall Upper Saddle River.
- Phinyomark, A., Hu, H., Phukpattaranont, P., and Limsakul, C. (2012a). Application of linear discriminant analysis in dimensionality reduction for hand motion classification. *Measurement Science Review*, 12(3):82–89.
- Phinyomark, A., Limsakul, C., and Phukpattaranont, P. (2009). A novel feature extraction for robust EMG pattern recognition. *Journal of Computing*, 1(1):71–79.
- Phinyomark, A., Phukpattaranont, P., and Limsakul, C. (2012b). Feature reduction and selection for emg signal classification. *Expert Systems with Applications*, 39(8):7420–7431.
- Raez, M. B. I., Hussain, M. S., and Mohd Yasin, F. (2006). Techniques of emg signal analysis: detection, processing, classification and applications. *Biological Procedures Online*, 8:11–35.
- Ravier, P., Buttelli, O., Jennane, R., and Couratier, P. (2005). An emg fractal indicator having different sensitivities to changes in force and muscle fatigue during voluntary static muscle contractions. *Journal of Electromyography and Kinesiology*, 15(2):210–221.
- Resnik, L., Huang, H. H., Winslow, A., Crouch, D. L., Zhang, F., and Wolk, N. (2018). Evaluation of emg pattern recognition for upper limb prosthesis control: a case study in comparison with direct myoelectric control. *Journal of neuroengineering and rehabilitation*, 15(1):23.
- Riley, N. A. and Bilodeau, M. (2002). Changes in upper limb joint torque patterns and emg signals with fatigue following a stroke. *Disability and Rehabilitation*, 24(18):961–969.
- Rogers, D. R. and MacIsaac, D. T. (2011). Emg-based muscle fatigue assessment during dynamic contractions using principal component analysis. *Journal of Electromyography and Kinesiology*, 21(5):811–818.
- Rojas, R. (1996). The backpropagation algorithm in neural networks. pages 149–182. Springer.
- Rojas-Martinez, M. and Mananas, M. A. (2014). Changes of hd-semg maps of the upper

- limb during isometric endurance contractions. *Conference proceedings : ... Annual International Conference of the IEEE Engineering in Medicine and Biology Society. IEEE Engineering in Medicine and Biology Society. Annual Conference*, 2014:3570–3.
- Roman-Liu, D., Tokarski, T., and Wójcik, K. (2004). Quantitative assessment of upper limb muscle fatigue depending on the conditions of repetitive task load. *Journal of Electromyography and Kinesiology*, 14(6):671–682.
- Sang-Hui, P. and Seok-Pil, L. (1998). Emg pattern recognition based on artificial intelligence techniques. *IEEE Transactions on Rehabilitation Engineering*, 6(4):400–405.
- Santos, J., Baptista, J. S., Monteiro, P. R. R., Miguel, A. S., Santos, R., and Vaz, M. A. P. (2016). The influence of task design on upper limb muscles fatigue during low-load repetitive work: A systematic review. *International Journal of Industrial Ergonomics*, 52:78–91.
- Scheme, E. J., Englehart, K. B., and Hudgins, B. S. (2011). Selective classification for improved robustness of myoelectric control under nonideal conditions. *IEEE Transactions on Biomedical Engineering*, 58(6):1698–1705.
- Schober, P., Boer, C., and Schwarte, L. A. (2018). Correlation coefficients: Appropriate use and interpretation. *Anesthesia and Analgesia*, 126(5).
- Sijiang, D. and Vuskovic, M. (2004). Temporal vs. spectral approach to feature extraction from prehensile emg signals. pages 344–350.
- Song, J. H., Jung, J. W., and Bien, Z. (2006). *Robust EMG Pattern Recognition to Muscular Fatigue Effect for Human-Machine Interaction*, pages 1190–1199. Springer Berlin Heidelberg, Berlin, Heidelberg.
- Soylu, A. R. and Arpinar-Avsar, P. (2010). Detection of surface electromyography recording time interval without muscle fatigue effect for biceps brachii muscle during maximum voluntary contraction. *Journal of Electromyography and Kinesiology*, 20(4):773–776.
- Sparto, P. J., Parnianpour, M., Barria, E. A., and Jagadeesh, J. M. (2000). Wavelet and short-time fourier transform analysis of electromyography for detection of back muscle fatigue. *IEEE Transactions on Rehabilitation Engineering*, 8(3):433–436.
- Spearman, C. (1904). The proof and measurement of association between two things. *American journal of Psychology*, 15(1):72–101.
- Spiestersbach, A., Röhrig, B., du Prel, J.-B., Gerhold-Ay, A., and Blettner, M. (2009). Descriptive statistics: the specification of statistical measures and their presentation in tables and graphs. part 7 of a series on evaluation of scientific publications. *Deutsches Arzteblatt international*, 106(36):578–583.
- Stein, R. B. and Milner-Brown, H. S. (1973). *Contractile and Electrical Properties of Normal and Modified Human Motor Units in Control of Posture and Locomotion*, pages 73–86. Springer, Boston, MA.
- Subasi, A. (2012). Classification of emg signals using combined features and soft computing techniques. *Applied Soft Computing*, 12(8):2188–2198.
- Subasi, A. and Gursoy, M. I. (2010). Eeg signal classification using pca, ica, lda and support vector machines. *Expert Systems with Applications*, 37(12):8659–8666.
- Subasi, A. and Kiymik, M. K. (2010). Muscle fatigue detection in emg using time-frequency methods, ica and neural networks. *Journal of Medical Systems*, 34(4):777–785.
- Takahashi, C. D., Nemet, D., Rose-Gottron, C. M., Larson, J. K., Cooper, D. M., and Reinkensmeyer, D. J. (2006). Effect of muscle fatigue on internal model forma-

- tion and retention during reaching with the arm. *Journal of Applied Physiology*, 100(2):695–706.
- Tenore, F. V. G., Ramos, A., Fahmy, A., Acharya, S., Etienne-Cummings, R., and Thakor, N. V. (2009). Decoding of individuated finger movements using surface electromyography. *IEEE Transactions on Biomedical Engineering*, 56(5):1427–1434.
- Thongpanja, S., Phinyomark, A., Phukpattaranont, P., and Limsakul, C. (2012a). A feasibility study of fatigue and muscle contraction indices based on emg time-dependent spectral analysis. *Procedia Engineering*, 32:239–245.
- Thongpanja, S., Phinyomark, A., Phukpattaranont, P., and Limsakul, C. (2012b). A feasibility study of fatigue and muscle contraction indices based on emg time dependent spectral analysis. *Procedia Engineering*, 32:239–245.
- Thrasher, A., Graham, G. M., and Popovic, M. R. (2005). Reducing muscle fatigue due to functional electrical stimulation using random modulation of stimulation parameters. *Artificial Organs*, 29(6):453–458.
- Tkach, D., Huang, H., and Kuiken, T. A. (2010). Study of stability of time-domain features for electromyographic pattern recognition. *Journal of NeuroEngineering and Rehabilitation*, 7(1):1–13.
- Venugopal, G., Navaneethakrishna, M., and Ramakrishnan, S. (2014). Extraction and analysis of multiple time window features associated with muscle fatigue conditions using semg signals. *Expert Systems with Applications*, 41(6):2652–2659.
- Vernier Software Technology, . (2019a). Ekg sensor and cable. <https://www.vernier.com/manuals/ekg-bta/>. Accessed: 2019-01-16.
- Vernier Software Technology, . (2019b). Hand dynamometer. <https://www.vernier.com/manuals/hd-bta/>. Accessed: 2019-01-16.
- Vernier Software Technology, . (2019c). Labquest mini. <https://www.vernier.com/products/interfaces/lq-mini/>. Accessed: 2019-01-16.
- Vøllestad, N. K. (1997). Measurement of human muscle fatigue. *Journal of Neuroscience Methods*, 74(2):219–227.
- Wang, L. and Buchanan, T. S. (2002). Prediction of joint moments using a neural network model of muscle activations from emg signals. *IEEE Transactions on Neural Systems and Rehabilitation Engineering*, 10(1):30–37.
- Westerblad, H., Lee, J. A., Lannergren, J., and Allen, D. G. (1991). Cellular mechanisms of fatigue in skeletal-muscle. *American Journal of Physiology*, 261(2):C195–C209.
- Winters, J. M. and Kleweno, D. G. (1993). Effect of initial upper-limb alignment on muscle contributions to isometric strength curves. *Journal of Biomechanics*, 26(2):143–153.
- Yan, Z. and Liu, Z. (2013). The study on feature selection strategy in emg signal recognition. pages 711–716.
- Yang, W., Dai, D., and Yan, H. (2008). Feature extraction and uncorrelated discriminant analysis for high-dimensional data. *IEEE Transactions on Knowledge and Data Engineering*, 20(5):601–614.
- Yao, B., Zhang, X., Li, S., Li, X., Chen, X., Klein, C. S., and Zhou, P. (2015). Analysis of linear electrode array emg for assessment of hemiparetic biceps brachii muscles. *Frontiers in Human Neuroscience*, 9.
- Yoon, T., De-Lap, B. S., Griffith, E. E., and Hunter, S. K. (2008). Age-related muscle fatigue after a low-force fatiguing contraction is explained by central fatigue. *Muscle and Nerve*, 37(4):457–466.
- Yuan, D., Liang, Y., Yi, L., Xu, Q., and Kvalheim, O. M. (2008). Uncorrelated linear discriminant analysis (ulda): A powerful tool for exploration of metabolomics data.

- Chemometrics and Intelligent Laboratory Systems*, 93(1):70–79.
- Zardoshti-Kermani, M., Wheeler, B. C., Badie, K., and Hashemi, R. M. (1995). Emg feature evaluation for movement control of upper extremity prostheses. *IEEE Transactions on Rehabilitation Engineering*, 3(4):324–333.
- Zhou, Q., Chen, Y., Ma, C., and Zheng, X. (2011). Evaluation of upper limb muscle fatigue based on surface electromyography. *Science China Life Sciences*, 54(10):939–944.
- Zivanovic, M. (2014). Time-varying multicomponent signal modeling for analysis of surface emg data. *IEEE Signal Processing Letters*, 21(6):692–696.

Appendix A

Ethical Approval



Downloaded: 16/12/2016
Approved: 15/12/2016

Wan Mohd Bukhari Bin Wan Daud
Registration number: 150234724
Automatic Control and Systems Engineering
Programme: PhD

Dear Wan Mohd Bukhari

PROJECT TITLE: EMG Signal Data Collection Involving Human Forearm and Upper Arm Muscles
APPLICATION: Reference Number 008393

On behalf of the University ethics reviewers who reviewed your project, I am pleased to inform you that on 15/12/2016 the above-named project was **approved** on ethics grounds, on the basis that you will adhere to the following documentation that you submitted for ethics review:

- University research ethics application form 008393 (dated 14/11/2016).
- Participant information sheet 1025040 version 1 (14/11/2016).
- Participant consent form 1025041 version 1 (14/11/2016).

The following optional amendments were suggested:

You are wasting Ethical Reviewers' time by not addressing their comments fully. This does not engender confidence in the manner in which this study will be carried out

If during the course of the project you need to [deviate significantly from the above-approved documentation](#) please inform me since written approval will be required.

Yours sincerely

Matthew Ham
Ethics Administrator
Automatic Control and Systems Engineering

Figure A.1: Official approval letter from the Ethical Review Committee The University Of Sheffield.



The
University
Of
Sheffield.

Automatic
Control &
Systems
Engineering.

Head of Department
Professor Daniel Coca

Mappin Street
Sheffield S1 3JD
United Kingdom

27 January 2017

Telephone: +44 (0) 114 222 5250
Fax: +44 (0) 114 222 5661
Email: acse@sheffield.ac.uk
Website: <http://www.sheffield.ac.uk/acse/>

To Whom it May Concern:

Ethics Application 008393

This is to confirm that Ms Norafizah Binti Abas (student registration number 140263978) was an additional researcher on the Ethics Application 008393. This Ethics application was submitted by the ACSE PhD student, Mr Wan Mohd Bukhari Bin Wan Daud (student registration number 150234724).

Mr Bin Wan Daud has confirmed that he is happy for Ms Binti Abas to be named as an additional researcher on the Ethics application. As the Department's Ethics Administrator I asked for approval to this request from the three academic staff who reviewed the Ethics application and they all gave their consent.

The application was approved on ethics grounds on 15 December 2016, on the basis that the applicants adhere to the comments made by the reviewers about the documentation supplied.

Yours faithfully

Matthew Ham
Ethics Administrator
Department of Automatic Control and Systems Engineering
University of Sheffield

Tel: 0114 222 5641
Email: m.ham@sheffield.ac.uk

Professor M A Balikhin, Space Science and Instrumentation
Professor T J Dodd, Autonomous Systems Engineering
Professor P J Fleming, Industrial Systems and Control
Professor R F Harrison, Computational Data Modelling
Professor V Kadiramanathan, Signal and Information Processing

Professor Z-Q Lang, Complex Systems Analysis and Design
Professor M Mahfouf, Intelligent Systems Engineering
Professor L S Mihaylova, Signal Processing and Control
Professor S Veres, Autonomous Control Systems



THE QUEEN'S
ANNIVERSARY PRIZES
FOR HIGHER AND FURTHER EDUCATION
1998 2000 2002

Figure A.2: Additional researcher added on the approval letter



Department of Automatic Control and Systems Engineering
Amy Johnson Building
The University of Sheffield
Portobello Street
Sheffield S1 3JD

11 November 2016

Dear participants

As part of the research requirements for doctoral program at The University of Sheffield (TUOS), I am conducting a research for the purpose of investigating the inter-relation between forearm electromyogram (EMG) signals hand grip force and wrist angles. This will feed into design of assistive exoskeleton hand control. The electromyogram is extracted from forearm muscles using surface electrodes thus non-invasive.

I would welcome participants either male or female aged between 20 to 50 years old. Your participation is entirely voluntary, and you may withdraw from this study at any time. The promise of strict confidentiality is assured in both the collection and reporting of the data. Any findings obtained in connection with this study will be presented in such a way that no individual will be identifiable. By completing the attached consent form, you will be granting me permission to publish aggregated results in my dissertation, in peer reviewed journals, and at professional conferences.

Hopefully, the results from this research will enhance the technology in communication between human and machine and assist the control development of exoskeleton hand in ways that would benefit and assist stroke survivors and others. Should you have any questions about this study, please contact us at nabas1@sheffield.ac.uk / wmbbinwandaud1@sheffield.ac.uk. Thank you in advance for your time and willingness to participate in this study.

Sincerely,

Norafizah Abas & Wan Mohd Bukhari
PhD Candidate
E-mail: nabas1@sheffield.ac.uk / wmbbinwandaud1@sheffield.ac.uk

Figure A.3: Letter of Consent

Department of Automatic Control and Systems Engineering, The University of Sheffield

Participant Information Sheet (Amended Version)

Date: 31th May 2018

1. *Research Project Title:*

EMG Signal Data Collection Involving Human Forearm and Upper Arm Muscles

2. *Invitation paragraph*

You have been invited to participate in this project. It is essential for you to understand the purpose of this research and what is involved before you decide to take part. Please take time to read the following information carefully. Ask us if any clarification or further information is needed. Thank you for reading this.

3. *What is the project's purpose?*

This data collection relates to several PhD projects together under supervision of Dr Osman Tokhi in the Department of Automatic Control and System Engineering (ACSE). The research students are Norafizah Abas and Wan Mohd Bukhari Wan Daud. The purpose of this data collection is to investigate the inter-relation between forearm and upper arm electromyogram (EMG) signals hand grip force, wrist angles, and curl exercises. This will be used for signal processing and analysis, and fed into design of assistive exoskeleton hand control. The EMG signals are extracted from forearm and upper arm muscles using surface electrodes thus non-invasive. There are four experiments incorporated in this data collection: i) extraction of EMG signals from forearm muscles contributing to the finger(s) pinching at various wrist movements, ii) extraction of EMG signals from forearm and upper arm muscles contributing to hand grasping, wrist movements, and curl exercises, iii) extraction of EMG signals from forearm and upper arm muscles contributing to pronation and supination of hand with curl exercises, vi) extraction of EMG signals from upper arm muscles contributing to curl exercises alone.

Figure A.4: Participant information sheet page 1-amended version in 2018 due to the ethical policy changes

Department of Automatic Control and Systems Engineering, The University of Sheffield

4. *Duration of project*

The duration for this project is one year, from 1st December 2016 to 30th November 2018.

4. *Why have I been chosen?*

Participants are normally limbed adults without any neuro-muscular problems, aged between 20-50 years old, chosen on a voluntary basis, and the number of participants will be approximately 10 people.

5. *Do I have to take part?*

Deciding to take part in this research is up to you. If you wish to participate, this information sheet will be given for you to keep. You will be asked to sign a consent form. You can withdraw from this research at any time if you wish to, and you are not required to provide a reason for your withdrawal.

6. *What will happen to me if I take part?*

When you agree to take part in a research study, the information about your health and care may be provided to researchers running other research studies in this organisation and in other organisations. These organisations may be universities, NHS organisations or companies involved in health and care research in this country or abroad. Your information will only be used by organisations and researchers to conduct research in accordance with the UK Policy Framework for Health and Social Care Research.

The principle researcher will contact you to arrange a suitable date and time to conduct the experiment. During the course of the experiment, your weight, height, and hand length will be measured. You will be asked to sit on an armchair in an upright position with your forearm (dominant hand) supported and fixed at one position. In this experiment, surface EMG electrode is used to detect the EMG signal. It is non-invasive technology that allows user to easily place EMG electrodes with stickers to the skin.

Figure A.5: Participant information sheet page 2-amended version in 2018 due to the ethical policy changes

Department of Automatic Control and Systems Engineering, The University of Sheffield

The skin (area is based on the respective muscle) is scrubbed with a paper towel to remove skin oil and moisture. You will then have six electrode patches placed on the skin around your forearm and upper arm. (Please refer to Figures 1(a) and 1(b) for the electrode patch placement)

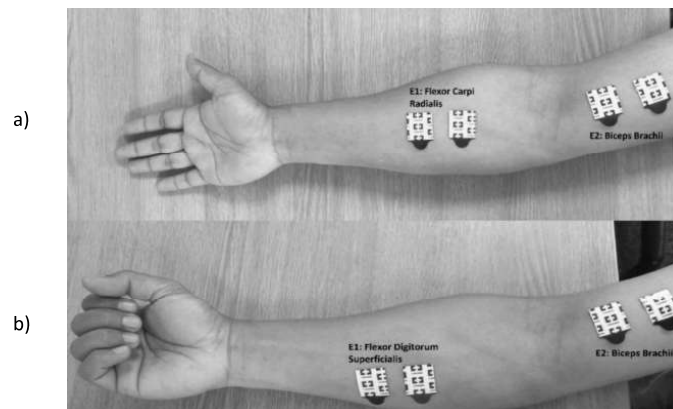


Figure 1 Example of electrode placement for a) forearm and b) upper arm muscles.

A cable is attached to each electrode to connect the electrodes with the LabQuest mini data acquisition. You are then asked to grasp/pinch the hand dynamometer at certain strength at various wrist angles. A protractor is used to measure the wrist angle. (Please refer to Figure 2 for the experiment set up)

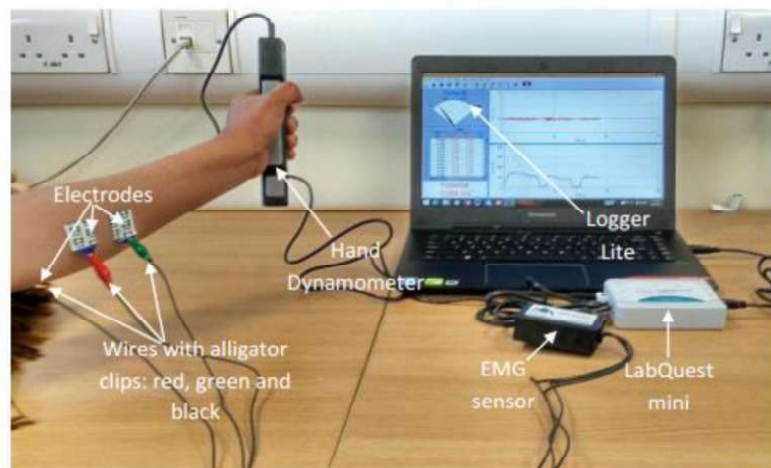


Figure 2: Experimental set-up.

Department of Automatic Control and Systems Engineering, The University of Sheffield

You can ask for complete experimental procedures for detail information.

7. *How will this affect me?*

There will be no restriction or change in your normal lifestyle as a result from participating in this research.

8. *What are the possible disadvantages and risks of taking part?*

You might feel a little muscle stiffness and fatigue due to continuous hand/finger grasping. However this will not be painful in any way. Rest sessions (for 5 seconds) are incorporated within the experiments to prevent muscle fatigue. Multiple published work is available which uses this similar approach.

9. *What are the possible benefits of taking part?*

Whilst there are no immediate benefits for participants, your contribution is essential to this research as we are optimistic that development of upper-limb exoskeleton will assist stroke survivors/amputee to regain their hand strength and functionality, and improve their quality of life.

10. *What happens if the research study stops earlier than expected?*

We will duly inform participants of any changes in circumstances that will affect participants in any way.

11. *What if something goes wrong?*

All equipment used are tested for safety using the university's PAT testing protocol. Risk assessment for the equipment have also been conducted and approved by the department's safety officer. If you have any dissatisfaction towards the way researchers are conducting the activity, you are advised to issue a complaint to the researcher's

Department of Automatic Control and Systems Engineering, The University of Sheffield

supervisor who is listed at the end of this information sheet. Your complaint will be escalated through the appropriate channels.

12. *About your data? Will my taking part in this project be kept confidential?*

We will be using information from you in order to undertake this study and will act as the data controller for this study. This means that we are responsible for looking after your information and using it properly. We will keep identifiable information about you and will keep it confidential.

Your rights to access, change or move your information are limited, as we need to manage your information in specific ways in order for the research to be reliable and accurate. If you withdraw from the study, we will keep the information about you that we have already obtained. To safeguard your rights, we will use the minimum personally-identifiable information possible.

You can find out more about how we use your information by contacting us as stated at the end of this document.

As any information that we collect about you during this research will be kept confidential. You will not be identified in any reports or publications.

13. *What type of information will be sought from me and why is the collection of this information relevant for achieving the research project's objectives?*

We will only require information of you age, height, weight, gender and the measurements of hand length. This is required as part of the data used in this research.

14. *What will happen to the results of the research project? Where data is intended to or likely to be used for future research*

It is expected that results of this research will be published within two years in reputable publications. We will ensure that your identity is anonymous in all of the publications. You can contact the person listed at the end of this information sheet to get further information on how to obtain published reports. It is also very likely that data collected

Department of Automatic Control and Systems Engineering, The University of Sheffield

in this work will be of interest and useful for future research activities. We will ask for your consent for your data to be shared, and if you agree to do so, we will ensure that the data collected about you is untraceable back to you before allowing others to use it. This information will not identify you and will not be combined with other information in a way that could identify you. The information will only be used for the purpose of health and care research, and cannot be used to contact you or to affect your care. It will not be used to make decisions about future services available to you, such as insurance.

15. *Who has ethically reviewed the project?*

This project have been ethically approved by the department of automatic control and systems engineering's ethics review procedure.

16. *Contact for further information*

Principle Researcher:

Norafizah Abas & Wan Mohd Bukhari Wan Daud

Department of Automatic Control and Systems Engineering, the University of Sheffield, Mappin Street, S1 3JD, Sheffield, United Kingdom

Email: nabas1@sheffield.ac.uk / wmbbinwandaud1@sheffield.ac.uk

Telephone: 0114 222 5659

Research Supervisor:

Professor Mahdi Mahfouf / Dr Osman Tokhi

Department of Automatic Control and Systems Engineering, the University of Sheffield, Mappin Street, S1 3JD, Sheffield, United Kingdom

Email: m.mahfouf@sheffield.ac.uk / o.tokhi@sheffield.ac.uk

Note: Participants will be given a copy of the information sheet and signed consent form.

Appendix B

Tables












Muscle	20% MVC	40% MVC	60% MVC	80% MVC	Trend
FDS	0.00040558	0.00082706	0.001066885	0.0019442	
FCR	0.00044452	0.00045446	0.000468684	0.00049107	
FCU	0.00044452	2.01E-06	0.000494938	0.00138734	
FPL	0.00044452	2.03E-05	0.000685173	0.00087808	
PT	0.00044452	6.07E-05	7.30E-05	0.00011918	
PQ	0.00044452	0.00047074	0.000511775	0.00065962	
ECRL	0.00012274	0.00018636	0.000367729	0.00091714	
ECU	0.00052343	0.00054911	0.000640165	0.00082068	
EDC	4.02E-05	9.20E-05	0.000280567	0.00069902	
BB	7.53E-05	7.13E-05	6.64E-05	6.16E-05	
TB	0.00038031	0.0004032	0.000416722	0.00042659	

Figure B.1: Average power for each muscles.

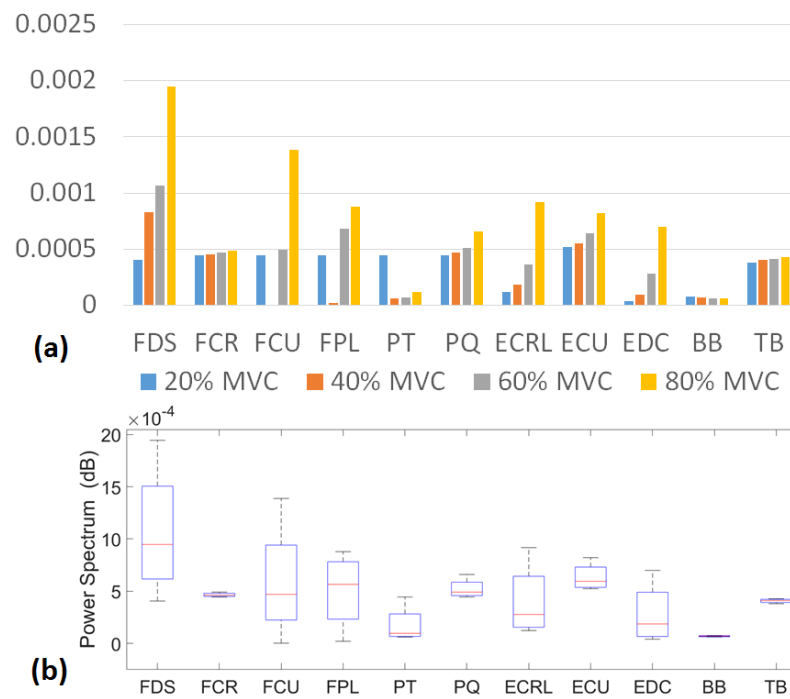


Figure B.2: (a) Bar, and (b) box plot; comparisons study for the muscle average power performances.

Table B.1: An example of statistical values of 4 subjects for handgrip force

Subject	Muscle	%MVC	Movements									
			Mean	SD	Variance	Skewness	Kurtosis	MAD	Minimum	Median	Maximum	
1	FDS	20	-0.0115	0.0102	1.04E-04	-0.1279	0.17029	0.00813	-0.0523	-0.0111	0.02525	
		40	-0.0114	0.01354	1.83E-04	-0.0168	0.44536	0.01063	-0.0633	-0.0111	0.04951	
		60	-0.0111	0.01846	3.41E-04	-0.1575	0.83362	0.01402	-0.0851	-0.0111	0.05432	
		80	-0.0097	0.0351	0.00123	0.39524	1.95573	0.02573	-0.1421	-0.0099	0.18044	
		100	-0.0101	0.03231	0.00104	0.05789	1.86266	0.02363	-0.1797	-0.0099	0.13191	
		20	-0.0123	0.00659	4.34E-05	0.00185	-0.3617	0.00535	-0.0337	-0.0131	0.00748	
		40	-0.0125	0.00715	5.12E-05	0.16225	-0.1907	0.00578	-0.0337	-0.0131	0.0135	
		60	-0.0127	0.00788	6.21E-05	0.1021	-0.0312	0.00635	-0.0411	-0.0131	0.01595	
		80	-0.0124	0.00954	9.11E-05	0.06749	0.25746	0.00753	-0.0507	-0.0131	0.02441	
		100	-0.0127	0.01291	1.67E-04	-0.1745	2.60105	0.00941	-0.0774	-0.0131	0.05112	
2	FDS	20	-0.0115	0.00532	2.83E-05	0.06159	-0.0784	0.00429	-0.0267	-0.0114	0.00562	
		40	-0.0114	0.00776	6.01E-05	-0.119	0.13312	0.0061	-0.0364	-0.0111	0.01267	
		60	-0.0111	0.01024	1.05E-04	-0.2341	0.23352	0.00804	-0.0509	-0.0108	0.01839	
		80	-0.0096	0.01742	3.03E-04	0.06146	0.42944	0.01347	-0.0745	-0.0101	0.05949	
		100	-0.0101	0.01662	2.76E-04	0.16399	0.6883	0.01261	-0.0737	-0.0101	0.05083	
		20	-0.0123	0.00407	1.66E-05	-0.2346	-0.5154	0.00336	-0.0242	-0.012	-0.0031	
		40	-0.0125	0.00404	1.63E-05	0.09905	-0.1425	0.00324	-0.0237	-0.0125	-1.19E-04	
		60	-0.0127	0.00417	1.74E-05	0.11329	-0.0918	0.00334	-0.0231	-0.0128	0.00236	
		80	-0.0124	0.0048	2.30E-05	0.14942	-0.2742	0.00392	-0.0257	-0.0126	0.00197	
		100	-0.0127	0.00665	4.42E-05	-0.0286	0.57916	0.00518	-0.0346	-0.0127	0.01393	
3	FDS	20	-0.0123	0.00407	1.66E-05	-0.2346	-0.5154	0.00336	-0.0242	-0.012	-0.0031	
		40	-0.0125	0.00404	1.63E-05	0.09905	-0.1425	0.00324	-0.0237	-0.0125	-1.19E-04	
		60	-0.0127	0.00417	1.74E-05	0.11329	-0.0918	0.00334	-0.0231	-0.0128	0.00236	
		80	-0.0124	0.0048	2.30E-05	0.14942	-0.2742	0.00392	-0.0257	-0.0126	0.00197	
		100	-0.0127	0.00665	4.42E-05	-0.0286	0.57916	0.00518	-0.0346	-0.0127	0.01393	
		20	-0.0115	0.00532	2.83E-05	0.06159	-0.0784	0.00429	-0.0267	-0.0114	0.00562	
		40	-0.0114	0.00776	6.01E-05	-0.119	0.13312	0.0061	-0.0364	-0.0111	0.01267	
		60	-0.0111	0.01024	1.05E-04	-0.2341	0.23352	0.00804	-0.0509	-0.0108	0.01839	
		80	-0.0096	0.01742	3.03E-04	0.06146	0.42944	0.01347	-0.0745	-0.0101	0.05949	
		100	-0.0101	0.01662	2.76E-04	0.16399	0.6883	0.01261	-0.0737	-0.0101	0.05083	
4	FDS	20	-0.0123	0.00407	1.66E-05	-0.2346	-0.5154	0.00336	-0.0242	-0.012	-0.0031	
		40	-0.0125	0.00404	1.63E-05	0.09905	-0.1425	0.00324	-0.0237	-0.0125	-1.19E-04	
		60	-0.0127	0.00417	1.74E-05	0.11329	-0.0918	0.00334	-0.0231	-0.0128	0.00236	
		80	-0.0124	0.0048	2.30E-05	0.14942	-0.2742	0.00392	-0.0257	-0.0126	0.00197	
		100	-0.0127	0.00665	4.42E-05	-0.0286	0.57916	0.00518	-0.0346	-0.0127	0.01393	
		20	-0.0115	0.00532	2.83E-05	0.06159	-0.0784	0.00429	-0.0267	-0.0114	0.00562	
		40	-0.0114	0.00776	6.01E-05	-0.119	0.13312	0.0061	-0.0364	-0.0111	0.01267	
		60	-0.0111	0.01024	1.05E-04	-0.2341	0.23352	0.00804	-0.0509	-0.0108	0.01839	
		80	-0.0096	0.01742	3.03E-04	0.06146	0.42944	0.01347	-0.0745	-0.0101	0.05949	
		100	-0.0101	0.01662	2.76E-04	0.16399	0.6883	0.01261	-0.0737	-0.0101	0.05083	

Table B.2: An example of statistical values of 4 subjects for finger pinch

Subject	Muscle	%MVC	Movements												
			FP1 Stats										Minimum	Median	Maximum
			Mean	SD	Variance	Skewness	Kurtosis	MAD	Minimum	Median	Maximum				
1	FDS	20	-0.01107	0.01336	1.78E-04	8.75E-01	2.21361	0.01053	-0.04753	-0.01236	0.06279				
		40	-0.0109	0.01723	2.97E-04	7.78E-01	2.10289	0.01336	-0.06088	-0.01236	0.10643				
		60	-0.01031	0.02323	5.39E-04	8.76E-01	2.13677	0.0176	-0.07416	-0.01236	0.12947				
		80	-0.01032	0.02683	7.20E-04	6.88E-01	1.37434	0.02067	-0.08995	-0.01236	0.121				
		100	-0.00853	0.04493	0.00202	1.10E+00	3.44372	0.03249	-0.16632	-0.01236	0.25192				
2	FDS	20	0.01158	0.01204	1.45E-04	0.03717	-1.03776	0.01042	-0.01642	0.01143	0.04301				
		40	0.01151	0.01252	1.57E-04	0.06121	-0.87318	0.01065	-0.01886	0.01143	0.04782				
		60	0.01121	0.01161	1.35E-04	0.02113	-1.10044	0.01011	-0.01642	0.01143	0.03935				
		80	0.01183	0.01204	1.45E-04	0.06141	-1.04211	0.01043	-0.01642	0.01143	0.04538				
		100	0.01116	0.01231	1.51E-04	0.1045	-0.91055	0.01055	-0.02252	0.01143	0.04301				
3	FDS	20	-0.01106	0.00564	3.18E-05	5.58E-01	0.57836	0.00442	-0.02616	-0.01167	0.01333				
		40	0.00636	0.00771	5.95E-05	7.39E-02	-0.2684	0.00632	-0.01793	0.00633	0.0354				
		60	-0.0103	0.01036	1.07E-04	5.15E-01	0.39269	0.00815	-0.03328	-0.01134	0.03192				
		80	-0.01021	0.01199	1.44E-04	3.95E-01	0.58584	0.00929	-0.04212	-0.01072	0.03679				
		100	-0.00838	0.01994	3.98E-04	3.07E-01	0.48636	0.01552	-0.0631	-0.00986	0.07433				
4	FDS	20	0.01155	0.00411	1.69E-05	0.0576	0.03461	0.00329	-0.00159	0.01157	0.02549				
		40	0.01155	0.00459	2.10E-05	0.09761	-0.29344	0.00371	-0.00195	0.01157	0.02514				
		60	0.01122	0.00367	1.34E-05	-0.05449	-0.00334	0.0029	-5.50E-04	0.01127	0.02191				
		80	0.01182	0.00379	1.43E-05	0.22317	0.3599	0.00301	-5.25E-05	0.01165	0.02765				
		100	0.01117	0.00421	1.77E-05	0.07249	-0.37724	0.00343	-3.75E-04	0.01107	0.02241				

Table B.3: Average wavelet scales and their true frequency based on mother wavelet

Muscle	Wave Name	Scale	True Frequency (Hz)	Muscles	Wave Name	Scale	True Frequency (Hz)
FDS	Gaussian	128	0	FDS	Meyer	128	0
FCR		48	20.833	FCR		66	20.833
ECRL		48	20.833	ECRL		66	20.833
EDC		48	20.833	EDC		66	20.833
BB		128	0	BB		128	0
FDS	Morlet	128	0	FDS	DMeyer	128	0
FCR		78	20.833	FCR		64	20.833
ECRL		78	20.833	ECRL		64	20.833
EDC		78	20.833	EDC		64	20.833
BB		128	0	BB		128	0
FDS	Symlet	128	0	FDS	Haar	128	0
FCR		69	20.833	FCR		96	20.833
ECRL		69	20.833	ECRL		96	20.833
EDC		69	20.833	EDC		96	20.833
BB		128	0	BB		128	0
FDS	Daubechies	128	0	FDS	Coiflet	128	0
FCR		69	20.833	FCR		67	20.833
ECRL		69	20.833	ECRL		67	20.833
EDC		69	20.833	EDC		67	20.833
BB		128	0	BB		128	0

Table B.4: Average cross-correlation values and their respective locations.

Type of Movement	Muscles Pair	Max Corr	Location Max_Corr	Min Corr	Location Min_Corr	Muscles Pair	Max Corr	Location Max_Corr	Min Corr	Location Min_Corr
FP1	FDS_EDC	0.4112	380	0.0026	2	FDS_EDC	0.3872	688	-0.1617	68
	FDS_BB	0.634	970	-0.0615	39	FDS_BB	0.5192	343	-0.0033	3
	FDS_ECRL	0.449	2	-0.2496	360	FDS_ECRL	0.5547	2	-0.2775	1000
	FDS_FCR	0.3333	34	-0.4847	2	FDS_FCR	0.6168	34	-0.5443	2
FP2	FDS_EDC	0.587	706	-0.0583	155	FDS_EDC	0.1702	113	-0.3882	993
	FDS_BB	0.6573	625	-0.039	3	FDS_BB	0.4745	641	-0.50585	1000
	FDS_ECRL	0.5671	3	-0.2031	712	FDS_ECRL	0.4641	2	-0.0249	14
	FDS_FCR	0.3144	51	-0.5054	3	FDS_FCR	0.5111	1000	-0.4513	2
FP3	FDS_EDC	0.4979	225	-0.5077	108	FDS_EDC	0.4045	550	-0.1141	999
	FDS_BB	0.3579	449	-0.1896	102	FDS_BB	0.6566	290	-0.0004	33
	FDS_ECRL	0.5127	101	-0.2603	198	FDS_ECRL	0.4756	2	-0.4503	369
	FDS_FCR	0.8238	32	-0.35	2	FDS_FCR	0.5225	32	-0.4978	2
FP4	FDS_EDC	0.4586	528	-0.03	182	FDS_EDC	0.4045	550	-0.1141	999
	FDS_BB	0.5428	912	-0.0603	34	FDS_BB	0.6566	290	-0.0004	33
	FDS_ECRL	0.5023	3	-0.2398	151	FDS_ECRL	0.4756	2	-0.4503	369
	FDS_FCR	0.5327	38	-0.5255	3	FDS_FCR	0.5225	32	-0.4978	2

Table B.5: Subjects compilation classification and processing time based on their average from 3 trials

Subject	Domain	Classification rate		Time (s)	
		PCA	ULDA	PCA	ULDA
1	TD	89.55	91.76	1.0021	1.2355
2	TD	88.9	92.43	1.2001	1.3652
3	TD	87.65	93.65	1.1002	1.3982
4	TD	87.89	92.77	1.032	1.2541
5	TD	86.98	91.22	1.1004	1.2852
6	TD	87.55	92.45	1.165	1.3254
7	TD	84.56	93.54	1.0251	1.2552
8	TD	85.77	91.77	1.124	1.322
9	TD	87.98	94.22	1.0322	1.214
10	TD	88.53	93.12	1.0541	1.322
11	TD	87.12	92.12	1.054	1.3963
12	TD	85.78	92.34	1.054	1.2004
13	TD	87.98	94.33	1.1542	1.225
14	TD	88.4	91.55	1.0236	1.3224
15	TD	88.7	91.65	1.2452	1.3875
1	FD	88.15	90.24	1.4226	1.855
2	FD	86.34	89.54	1.3885	1.6254
3	FD	85.55	88.78	1.4203	1.855
4	FD	85.88	90.12	1.4001	1.547
5	FD	84.63	89.76	1.6332	1.6225
6	FD	85.99	90.77	1.5224	1.322
7	FD	85.76	91.54	1.844	1.6241
8	FD	84.76	89.454	1.411	1.5332
9	FD	85.34	92.77	1.3289	1.5221
10	FD	86.34	91.45	1.4884	1.3021
11	FD	85.23	90.33	1.523	1.4223
12	FD	84.76	90.98	1.432	1.8233
13	FD	85.66	92.9	1.3952	1.6325
14	FD	84.55	88.7	1.522	1.5241
15	FD	86.33	89.67	1.4562	1.4257
1	TFD	90.23	91.44	1.2001	1.3552
2	TFD	88.9	90.17	1.3002	1.2582
3	TFD	88.76	92.13	1.1925	1.3147
4	TFD	87.09	93.12	1.2445	1.2514
5	TFD	87.54	92.17	1.1092	1.3698
6	TFD	88.87	92.76	1.1924	1.274
7	TFD	87.99	92.45	1.325	1.1014
8	TFD	87.65	90.87	1.2001	1.235
9	TFD	87.77	92.55	1.1547	1.1654
10	TFD	84.65	92.98	1.3223	1.2014
11	TFD	88.26	91.34	1.0241	1.1458
12	TFD	86.55	92.77	1.2011	1.2532
13	TFD	87.98	91.48	1.2365	1.3258
14	TFD	86.88	92.04	1.1548	1.2145
15	TFD	89.76	91.76	1.2582	1.3214

Table B.6: Average statistical classification performance based on different domain and feature reductions.

Domain	Reduction	Mean	Standard Deviation	Variance	Minimum	Median	Maximum
TD	PCA	85.83067	2.48163	6.15851	80.86	85.77	89.4
	ULDA	90.35667	3.498	12.23601	82.25	91.55	94.78
FD	PCA	83.852	2.86323	8.19806	75.85	84.76	86.34
	ULDA	88.28693	2.97713	8.86333	80.21	88.98	92.77
TFD	PCA	87.32533	1.7244	2.97357	83.54	87.77	89.76
	ULDA	91.35333	1.68363	2.83462	86.54	91.76	93.12

Table B.7: One-way ANOVA analysis for classification performances

	DF	Sum of Squares	Mean Square	F Value	Prob>F
Model	6	82531.1489	13755.19	1571.66003	4.96E-95
Error	98	857.69743	8.75201		
Total	104	83388.8463			

Null Hypothesis: The means of all levels are equal.

Alternative Hypothesis: The means of one or more levels are different.

At the 0.05 level, the population means are significantly different.

Table B.8: Two-way ANOVA analysis for classification performances

	DF	Sum of Squares	Mean Square	F Value	P Value
Factor A	1	25080.8629	25080.86	60.03541	1.80E-10
Factor B	1	22158.2003	22158.2	53.03951	1.07E-09
Model	2	47239.0632	23619.53	56.53746	2.95E-14
Error	57	23812.7656	417.7678	–	–
Corrected Total	59	71051.8287	–	–	–

At the 0.05 level, the population means of Factor A are significantly different.

At the 0.05 level, the population means of Factor B are significantly different.

Table B.9: Average statistical processing time performance based on different domain and feature reductions.

Domain	Reduction	Mean	Standard Deviation	Variance	Minimum	Median	Maximum
TD	PCA	1.09108	0.07282	0.0053	1.0021	1.0541	1.2452
	ULDA	1.30056	0.06781	0.0046	1.2004	1.322	1.3982
FD	PCA	1.47919	0.12556	0.01576	1.3289	1.432	1.844
	ULDA	1.57575	0.1734	0.03007	1.3021	1.547	1.855
TFD	PCA	1.20771	0.0801	0.00642	1.0241	1.2001	1.325
	ULDA	1.25248	0.0779	0.00607	1.1014	1.2532	1.3698

Table B.10: One-way ANOVA analysis for processing time performances

	DF	Sum of Squares	Mean Square	F Value	Prob \leq F
Model	6	576.5053	96.08422	33.51516	1.06E-21
Error	98	280.9551	2.86689		
Total	104	857.4604			

Null Hypothesis: The means of all levels are equal.

Alternative Hypothesis: The means of one or more levels are different.

At the 0.05 level, the population means are significantly different.